

HYPHENATED TECHNOLOGY



HYPHENATED TECHNOLOGY

The Best Answers Happen When Great Technologies Connect

PerkinElmer's hyphenated solutions couple two or more instruments to greatly increase the power of analyses and save precious time by acquiring more information from a single run.

PerkinElmer TGA 8000™ and STA systems coupled with FT-IR, MS, and/or GC/MS instruments represent the industry's most complete and advanced line of hyphenated platforms for materials characterization in polymers, pharmaceuticals, chemicals, petroleum, rubber, and food. Its applications include identifying harmful chemicals in soil, quantitating components in polymers, determining leachables that may contaminate a product's packaging, and identifying phthalates in PVC samples.

We understand the unique and varied needs of the customers and markets we serve and we are the only company in the industry capable of making, supporting, and servicing combined systems that streamline and simplify the entire process from sample handling and analysis to the communication of test results.

Hyphenation with PerkinElmer will provide your lab with new pathways for innovation and scientific understanding.

**The More You Know,
The More Your Laboratory Can Achieve.**

Table of Contents

Introduction

Polymers Analysis

TG-IR Analysis of Layers of a Cable Used in the Automotive Industry.....	3
Confirmation of the Presence of Styrene Butadiene Resin (SBR) Polymer in Drywall Primer	7
Polymer Crystallinity Studies by DSC Raman Spectroscopy	13
Qualitative Analysis of Evolved Gases by TG-GC/MS.....	16
The Analysis of Ethylene Vinyl Acetate by TG-MS.....	20
The Analysis of PVC with Different Phthalate Content by TG-MS and TG-GC/MS.....	22
UV-DSC Study on New Double Furnace DSC	25
Plasticizer Characterization by TG-IR	29
Analysis of Unknown Aqueous Samples TG-IR-GC/MS.....	32
Analysis of Light Cured Acrylics by UV-DSC	35
Curing of an Optical Adhesives by UV Irradiation in the DSC 8000.....	41
<i>In-situ</i> Evolved Gas Analysis During the 3D Printing Procedure	43
Detection of Additive Used in Gloves by TG-GC/MS Hyphenation System	46

Pharmaceutical Analysis

Evolved Gas Analysis: a High Sensitivity Study of a Solvent of Recrystallization in a Pharmaceutical	51
Polymorphism in Acetaminophen Studied by Simultaneous DSC and Raman Spectroscopy	53
Evolved Gas Analysis: Residual Solvent Contamination Measured by TG-MS.....	56
Study of the Decomposition of Calcium Oxalate Monohydrate by TG-IR.....	59

Food and Beverage Analysis

TG-GC/MS Technology - Enabling the Analysis of Complex Matrices in Coffee Beans	62
---	----

Nanomaterials Analysis

A Study of Aged Carbon Nanotubes by Thermogravimetric Analysis.....	65
Characterizing Interaction of Nanoparticles with Organic Pollutants Using TG-GC/MS ...	70

Environmental Analysis

Characterization of Soil Pollution by TG-IR Analysis	74
--	----

Thermal Analysis

Author

Maria Garavaglia
PerkinElmer Italia
Via Tiepolo 24
Monza, Italy 20052

TG-IR Analysis of Layers of a Cable Used in the Automotive Industry

identification by infrared spectroscopy was not applicable. Thus we decided to use the TG-IR technique, as it allows the identification of a material through its decomposition products. Such analysis is completely free from interferences due to the presence of carbon.

TG-IR Analysis – Sample Preparation

There is no particular sample preparation needed for TG-IR analysis. A sharp scalpel is used to remove a small part of the external rubber sheath (about 26 mg).

As general rule, in order to be able to identify gas released in limited quantities, the mass of a sample for TG-IR analysis must range between 10 and 30 mg. A too small sample can prevent a correct analysis, while a too large sample can lead to incomplete combustion (or pyrolysis) of that part of the sample not undergoing the gas flow.

Introduction

PerkinElmer was given a sample of a cable used in the automotive industry. The purpose was the identification of the polymer used to form the external sheath of the cable.

The cable is composed of five concentric layers disposed in the following sequence: rubber, fabric, rubber, fabric, rubber.

As the polymeric material of the cable is carbon black filled, its

TG-IR Analysis – Experimental

While under nitrogen flow (100 mL/min), the sample is heated at a rate of 20 °C/min.

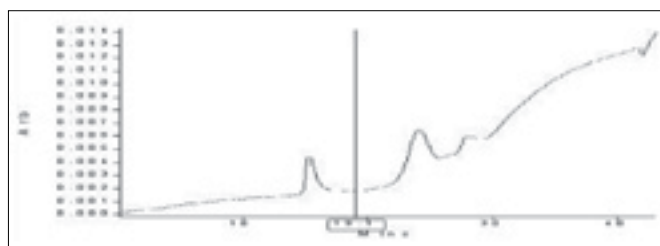
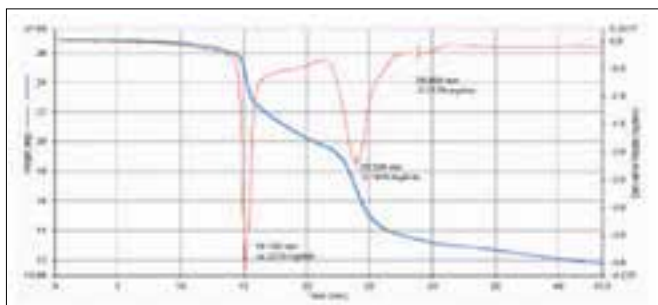
During the TGA analysis process, spectra of the gas released by the sample are acquired at a sampling frequency of one spectrum every 4 seconds, and with a spectral resolution of 4 cm⁻¹.

TG-IR Analysis – Discussion of the Results

The TGA analysis and the intensity profile of the gases released by the sample are discussed. Three main weight losses are seen: the first around minute 15, the second around minute 24, and the third around minute 29. Together with the weight loss, three TG-IR peaks are detected: hence the sample degrades while releasing gas.

Let us now analyse the details of the acquired spectra, and then proceed to the identification of the released gases.

Ten minutes after start up of the analysis (T = 200 °C) there is a slight decline in the derived curve: from this point onward the spectra show the stretching band of the –CH₂ and –CH₃ (peak A) groups; a limited CO₂ generation reaching a maximum at minute 15 (Figures 1 and 2) is also observed.



TGA has 3 weight losses; IR detects 3 peaks as the sample degrades.

The carbon dioxide peak probably derives from the CO₂ loss of the vinyl-acetic group of the polymer; the peak related to the organic part could originate from the evaporation of an additive or an early decomposition of the polymeric matrix. This last hypothesis would also appear to be supported by the fact that immediately after, a marked generation of HCl occurs. See the following graphs: In Figure 3 the intensity profiles related to hydrochloric acid and A peak are compared; Figure 4 shows the HCl spectrum superimposed on the A peak as it appears before data processing. Figure 5 shows the HCl band after the subtraction of peak A.

Hydrochloric acid emission during the analysis confirms the presence of chlorine in the sample.

Let us now pass to the analysis of the gases released during the second important weight loss, occurring around minute 24 (about 500 °C). At this temperature, the polymer decomposes markedly, giving off different gases due to chain fragmentation: the presence of methane, ethylene and medium-short alkyl chain fragments can be noted. Obviously, the spectra of these gases are partially overlapping. To identify the chemical species, please see the following graphs: (6) shows the spectra of the spectra atlas, and the spectrum recorded at minute 24.4, (7) shows the profiles relative to each of the gases.

Once the generation of these gases is over, from 27 minutes onwards and until the end of the analysis, emission of CO₂ and traces of CO can be detected.

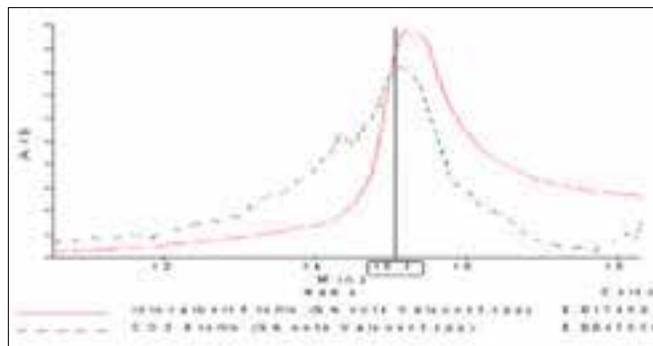


Figure 1. Released gases.

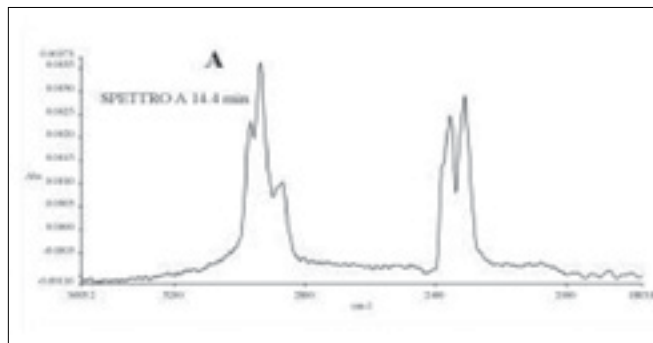


Figure 2. Peak A shows the stretching of –CH₂ and –CH₃ groups; and CO₂ peak.

These experiments were performed using the Pyris™ 1 TGA. PerkinElmer offers both Thermal Analysis and IR for better and more complete sample characterization from a single supplier.

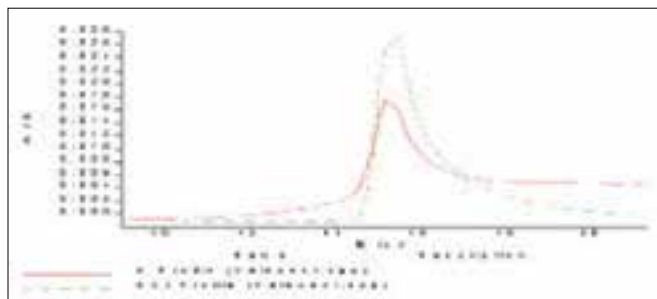


Figure 3. Intensity profiles of released gases.

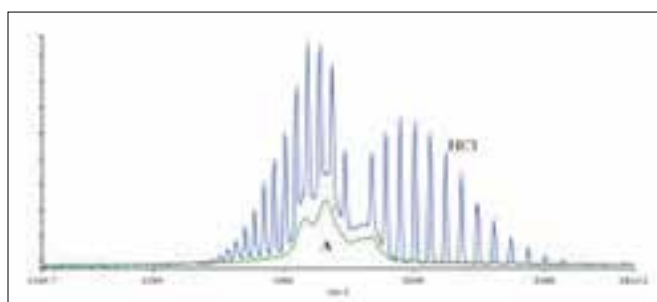


Figure 4. HCl spectrum superimposed on Peak A.

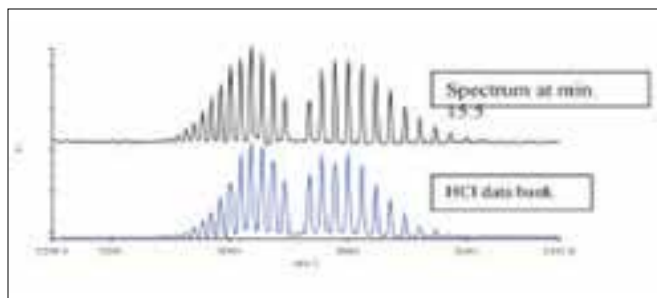


Figure 5. HCl band after Peak A subtracted.

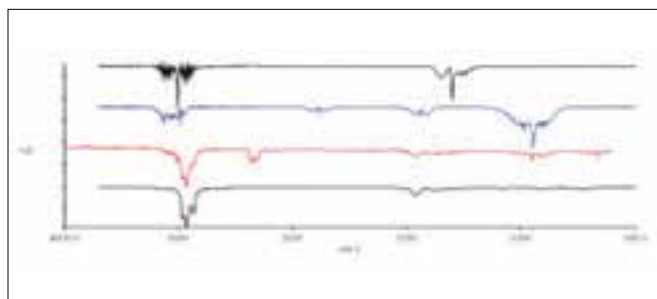


Figure 6. Atlas of spectra.

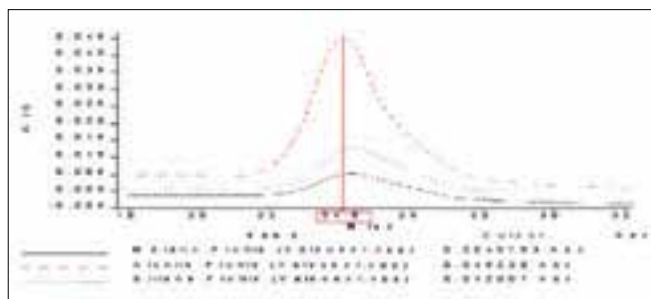


Figure 7. Gas profiles superimposed.

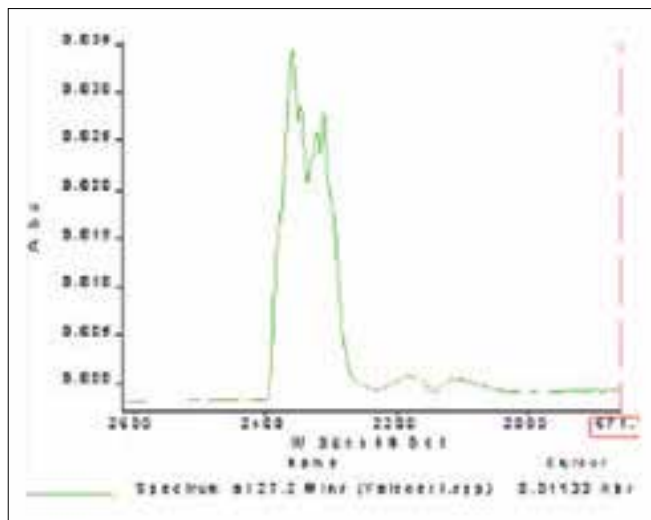


Figure 8. CO₂ profile.

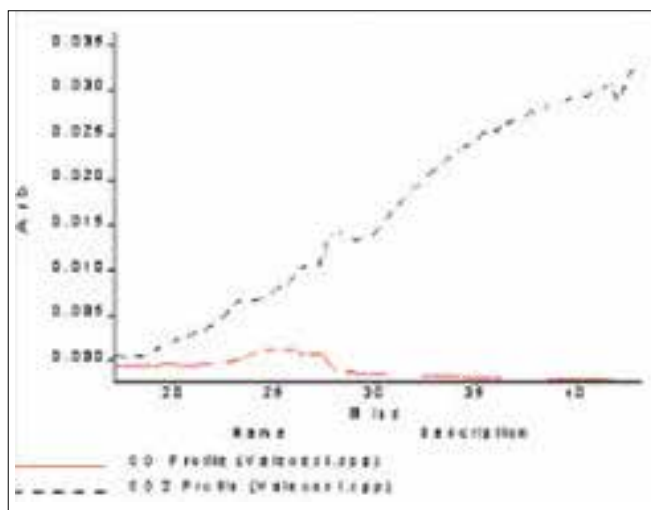
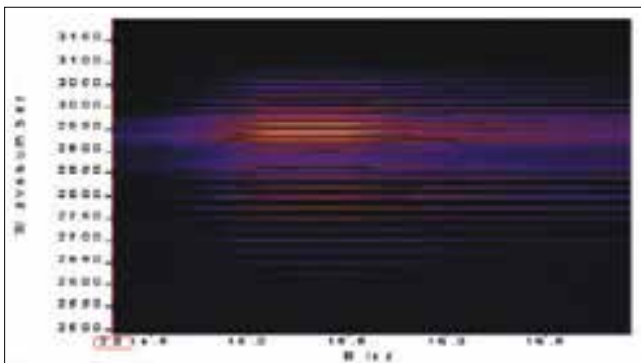


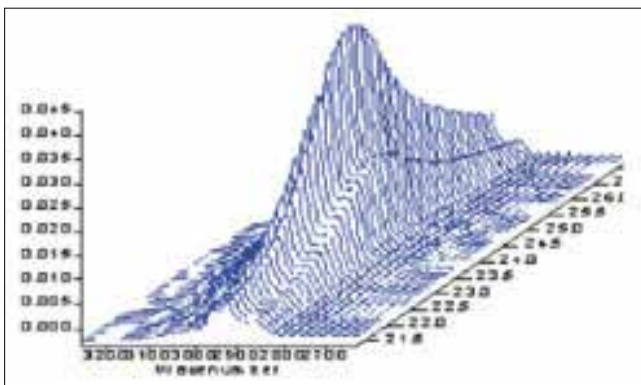
Figure 9. Gas profiles of CO₂ and traces of CO.

Appendix

The appendix shows several graphical representations of the analyses that for space saving reasons were not presented on the previous pages.



False color map relative to the generation of hydrochloric acid.



Stack plot centered on the band at 2950 cm⁻¹, between 21.5 and 28.0.

FT-IR Spectroscopy and
Thermogravimetric Analysis

Authors

Dale C. Mann, BS

Keith G. Cline, PE

MDE, Inc
700 S. Industrial Way
Seattle, WA 98108

Confirmation of the Presence of Styrene Butadiene Resin (SBR) Polymer in Drywall Primer Applications.

A combination of Fourier Transform Infrared (FT-IR) Spectrometry and Thermogravimetric Analysis (TGA) was used to distinguish and identify styrene butadiene from polyvinyl acrylic resin-based interior latex primers and paints. A wide range of standard mixtures of the two resins were analyzed and the relative percentages of the two accurately estimated using the two methods. The isolation techniques and analytical methods of analysis were developed to verify the composition of primer/texture/paint applications used on interior condominium walls.

Introduction

Over the past several years, architects and developers of condominium housing projects in western Washington have begun to utilize the Washington State's Energy Code¹ allowing a rated vapor barrier primer/paint to replace the traditional polyethylene plastic sheeting or Kraft-backed insulation bats historically used in the construction to achieve the required water vapor perm rating of 1.0 or less. Building specifications for the interior wall finish called for the application of a vapor barrier rated primer followed by the normal decorative paint/top coat.

A literature review of many major paint distributors of interior vapor barrier primers shows the resin in the vapor barrier primers is a styrene butadiene rubber (SBR) formulation. This formulation is quite different from the normal drywall primer, polyvinyl acrylic (PVA). Litigation involving the perceived lack of a SBR primer on interior drywall surfaces soon led MDE Forensic Laboratories to develop methods to positively identify the presence/absence of an SBR primer after a PVA top coat had been applied to the walls.

Laboratory Methods

Cross sections of the texture, primer and paint applied to the interior of the drywall were prepared by mounting specimens in acrylic and polishing. Examination of these samples showed the presence of a primer layer applied to the drywall, followed by a texture and finally the decorative top coat paint. The primer layer exhibited an average dry film thickness that met all manufacturers' specifications, regardless of the potential resin formulation of the primer.

Fourier Transform Infrared Spectrometry

The decorative top coat and texture were physically separated from the primer layer. The primer layer and uppermost layer of drywall paper were peeled off and ultrasonically extracted using a 50/50 mixture of tetrahydrofuran/methylene chloride solvent. The solvent was evaporated to dryness and the isolated primer resin analyzed using FT-IR^{2,3}.

FT-IR results for pure SBR and PVA resins are shown in Figure 1. The predominant absorbances for an SBR resin, resulting from the styrene content, are at 700 and 730 cm^{-1} . Figure 2 illustrates some typical results from the extracted condominium primer layers. Many of these did not yield pure SBR spectra, however absorbances typically due to styrene were readily detected in all extractions. The primary absorbances in these spectra appeared to be due to the co-extracted presence of a quantity of PVA resin. Note that a PVA resin decorative top coat was originally present on each sample.

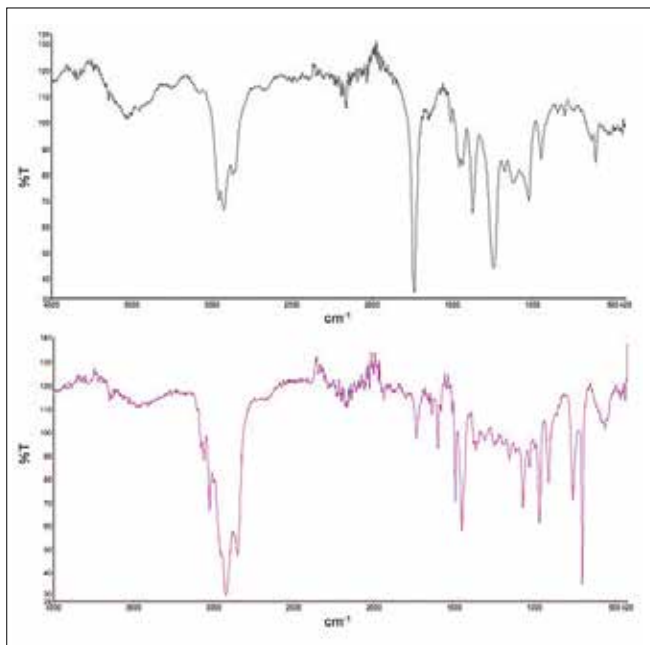


Figure 1. FT-IR comparison of a pure PVA resin (top) and a pure SBR resin (bottom).

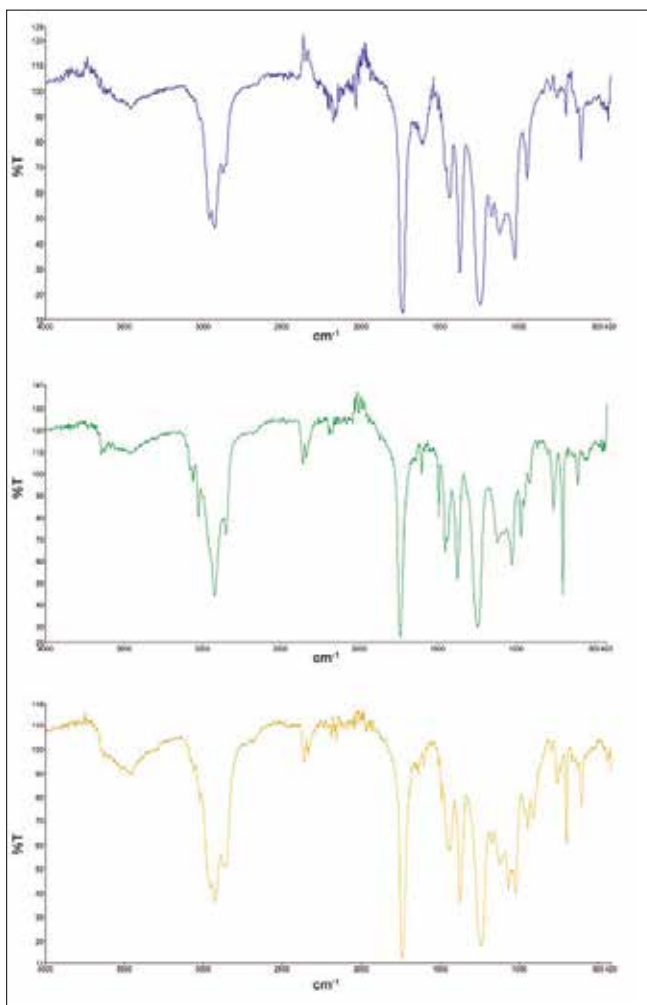


Figure 2. Examples of three "typical" FT-IR results from the solvent extraction of isolated primer layers from three separate condominium units. Note the lack of a definitive SBR spectra but the presence of a styrene absorption at 700 cm^{-1} .

Thermogravimetric Analysis

Resins extracted from both PVA and SBR formulated paints were analyzed using TGA^{4,5,6}. The samples were analyzed using nitrogen gas and a temperature program of 25-600 $^{\circ}\text{C}$ with a 20 $^{\circ}\text{C}/\text{min}$ ramp. This temperature program caused the complete pyrolysis of the paint resin samples. Evaluation of the data showed distinctly different slopes in the weight loss versus temperature curves. The first derivative of these curves was used to identify the inflection points. The temperatures of these inflection points were found to be 350 $^{\circ}\text{C}$ for the PVA resin and 425 $^{\circ}\text{C}$ for the SBR resin. Figure 3 illustrates the first order weight loss curve and the first derivative of that curve for both pure SBR and PVA resins.

Pyrolysis Gas Chromatography/Mass Spectrometry

Pyrolysis GC/MS methodology was also investigated as a means of verifying the presence of SBR by using the presence of styrene. However, it was found that small amounts of styrene were produced during the pyrolysis of PVA resin. This artifact and the desire to use available instrumentation led us to not pursue this methodology.

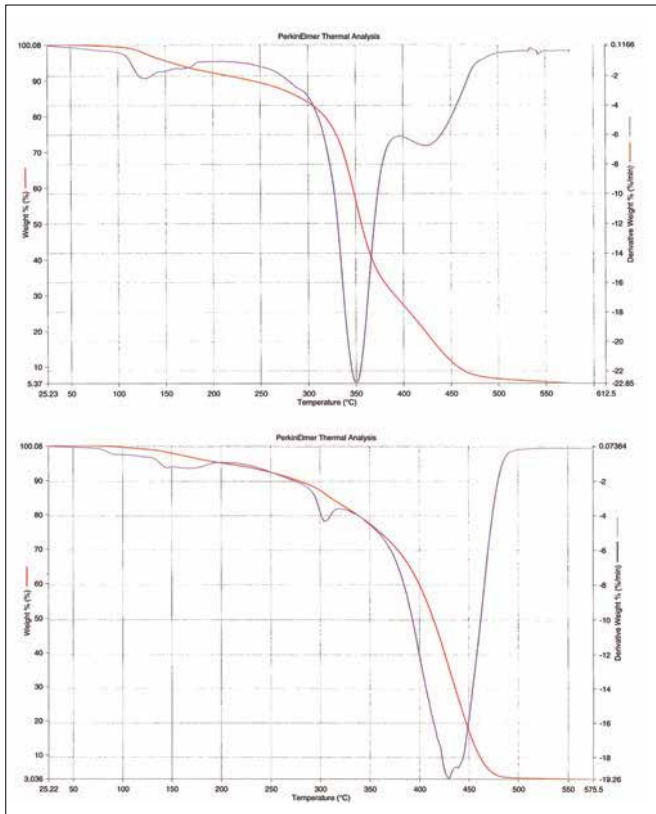


Figure 3. TGA comparison of a pure PVA resin (top) and a pure SBR resin (bottom). The weight loss vs. temperature is shown in blue and the 1st derivative of that curve is shown in red.

Analysis of Standard Mixtures

Pure SBR and PVA resins were extracted from exemplar primer and paint products. The purity of the resulting evaporated extracts was evaluated using FT-IR and TGA. Mixtures of the two were made by adding a weighed amount of each resin, dissolving in solvent to homogenize and drying for analysis.

The standard mixtures were 0%, 10%, 30%, 50%, 70%, 90% and 100% of SBR resin in PVA. These mixtures were analyzed using both FT-IR and TGA. The ratio of the peak height at 700 cm^{-1} (the styrene absorption for the SBR) to the 1740 cm^{-1} (the carbonyl adsorption for the PVA) was used to estimate the relative amounts of the two resins. Figure 4 illustrates typical FT-IR results and Figure 5 depicts the resulting calibration curve.

The standard mixtures were likewise analyzed using TGA. The ratio of the peak heights of the second derivative plots at 425 $^{\circ}\text{C}$ (for the SBR) to the 350 $^{\circ}\text{C}$ (for the PVA) was used to estimate the relative amounts of the two resins in the mixture. Figure 6 illustrates typical TGA 1st derivative plots and Figure 7 depicts the resulting calibration curve using the log of the ratio of the peak heights of these curves.

Subject Samples

Samples isolated for the several condominium projects evaluated during the course of the investigations yielded a wide range of FT-IR and TGA results. In some instances, a SBR was easily and cleanly confirmed by both analytical methods. In other condominium projects evidence of SBR was much less pronounced. Figures 2 and 8 depict the range of FT-IR and TGA results for some of these investigations

Some "contamination" of the physically isolated primer layer by the overlying PVA paint was expected due to the difficulty of mechanically separating the coating layers during sample preparation. This was particularly true when the primer and paint had been applied without an intervening layer of texture. For some projects only low relative concentrations of SBR were calculated, even when it was thought a "clean" isolation of the primer layer was performed.

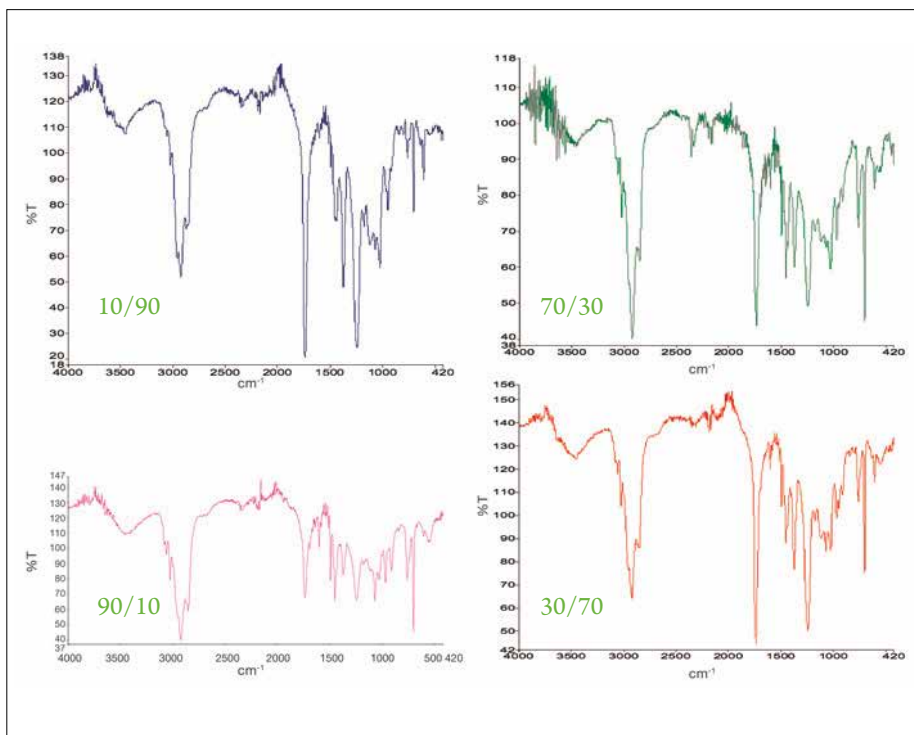


Figure 4. FT-IR comparison of standard mixtures of SBR and PVA resins. The SBR/PVA ratios are 10/90 (blue), 90/10 (red), 70/30 (green), and 30/70 (brown).

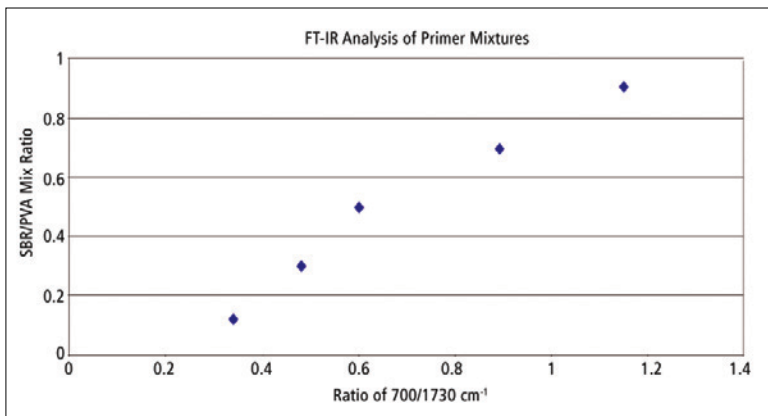


Figure 5. Calibration curve for the FT-IR analysis of standard mixtures of SBR and PVA. Peak height ratios are the SBR/styrene absorbance at 700 cm⁻¹ divided by the PVA/carbonyl absorbance at 1732 cm⁻¹.

As laboratory work progressed during these investigations, many of the locally available drywall primers (both vapor barrier products and traditional drywall primers) were analyzed. Though not clearly specified on product labels or in the product technical data sheets, it became apparent during the laboratory analysis that many primers labeled as vapor barrier products were actually a blend of SBR and PVA resins. At least one manufacturer alluded to this in their product information. Figures 9 and 10 depict the FT-IR and TGA results for a variety of exemplar vapor barrier primers.

Calculation of the relative amount of SBR to PVA in the analyzed exemplar primers showed a range from 100% SBR to 20% SBR. In one condominium project, the calculated SBR in the isolated primer layer never exceeded 20%. The primer that was later confirmed to have been used as the vapor barrier was a blended resin containing only 20% SBR. This information was only confirmed after the laboratory results were used as motivation to persuade the manufacturer to release their formulation.

Summary

The combination of FT-IR and TGA analysis of vapor barrier primers is a powerful analytical method useful for confirming the presence/absence of a styrene butadiene resin in the primer. A semi-quantitative estimate of the relative amount of the SBR compared to the more traditionally used PVA resin is possible.

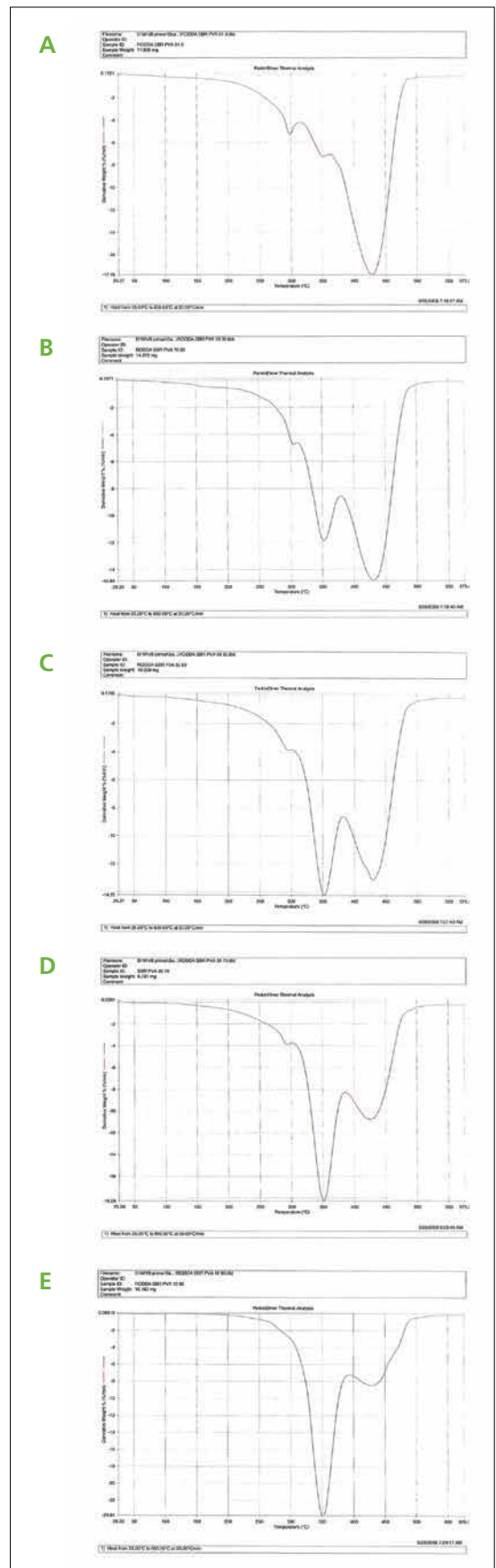


Figure 6. TGA comparison (using 1st derivative of weight loss curve) of standard mixtures of SBR and PVA resins. From top to bottom, the SBR/PVA ratios are 90/10 (A), 70/30 (B), 50/50 (C),

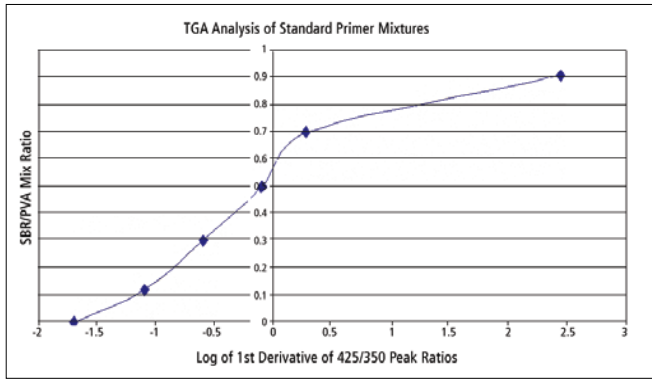


Figure 7. Calibration curve for the TGA analysis of standard mixtures of SBR and PVA. Calculated ratios are the SBR/1st derivative peak height at 425 °C divided by the PVA/1st derivative peak height at 350 °C.

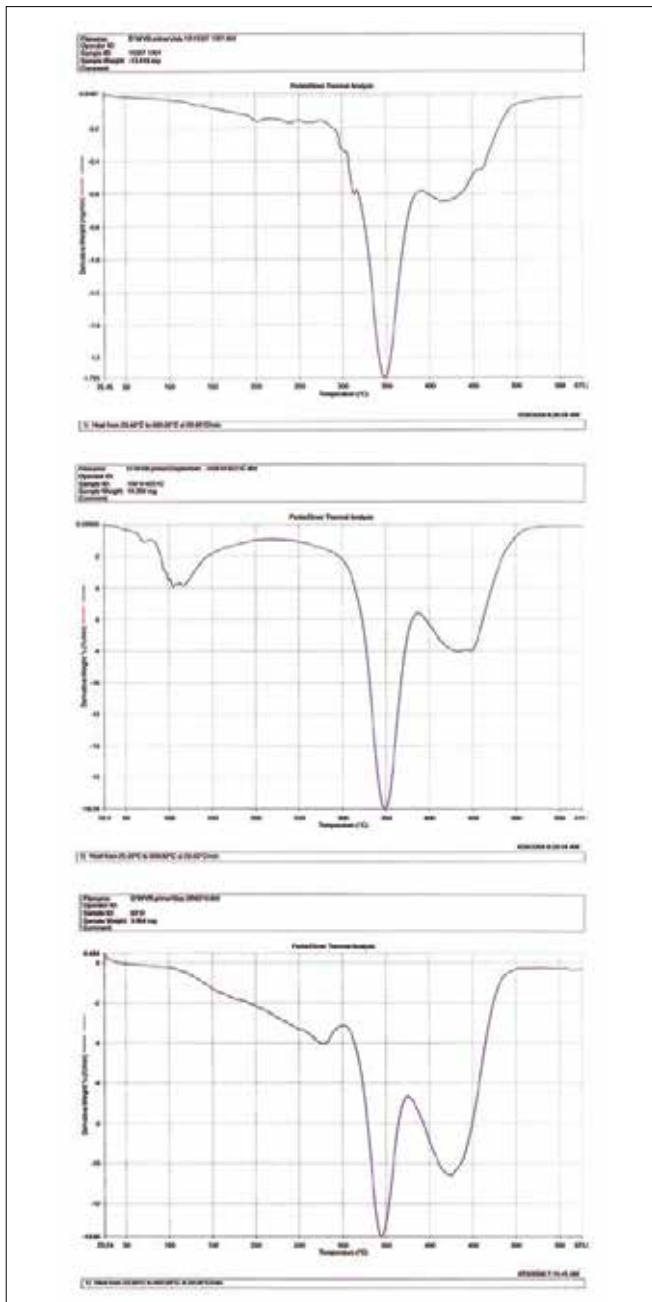


Figure 8. Examples of three "typical" TGA 1st derivative results from the solvent extraction of isolated primer layers from three separate condominium units.

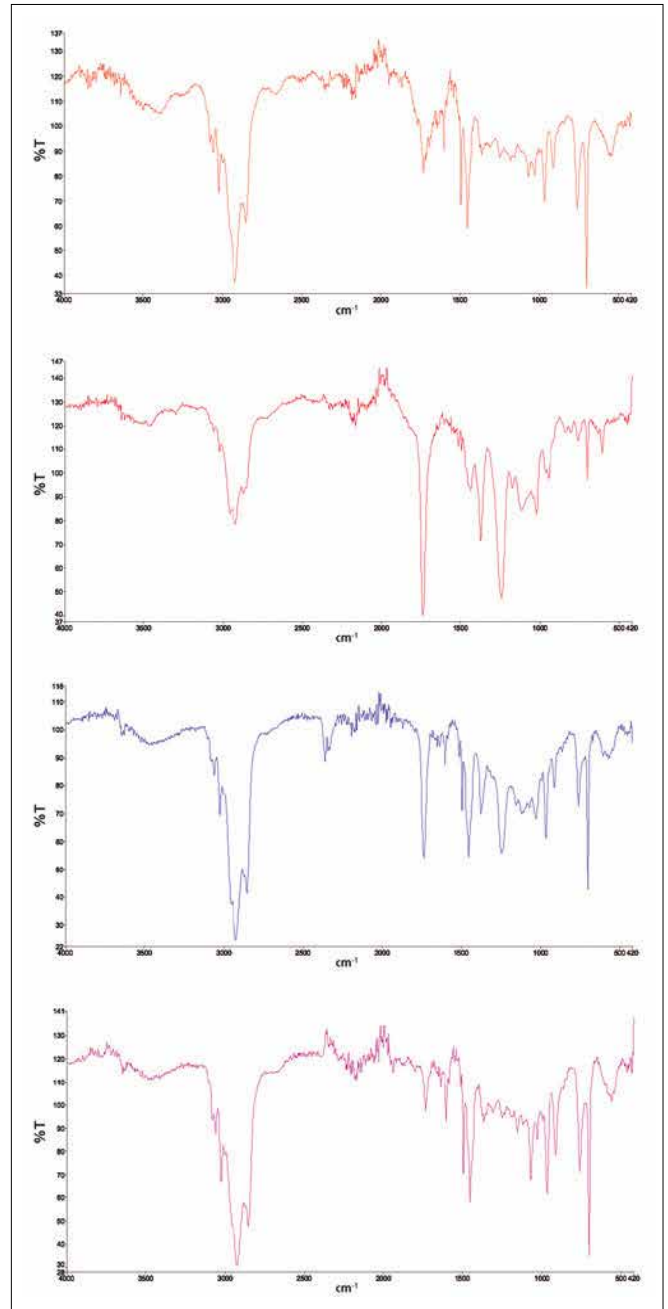


Figure 9. FT-IR spectra of four different brands of vapor barrier primer. Each is a mixture of SBR and PVA resins.

References

1. Washington State Energy Code, 502.1.6.1-4, 1994.
2. ASTM® D3168-85 (2005) Standard Practice for Qualitative Identification of Polymers in Emulsion Paints, 2005.
3. Kolske, Joseph V. Paint and Coating Testing Manual, Chapter 75:850-852, 1995.
4. Earnst, C.M, Ed. The Compositional Analysis by Thermogravimetry, STP 977, ASTM®, 1988.
5. ASTM® E1131-03 Standard Test Method for Compositional Analysis by Thermogravimetry, 2003.
6. ASTM® E2008-06 Standard Test Method for Volatility Rate by Thermogravimetry, 2006.

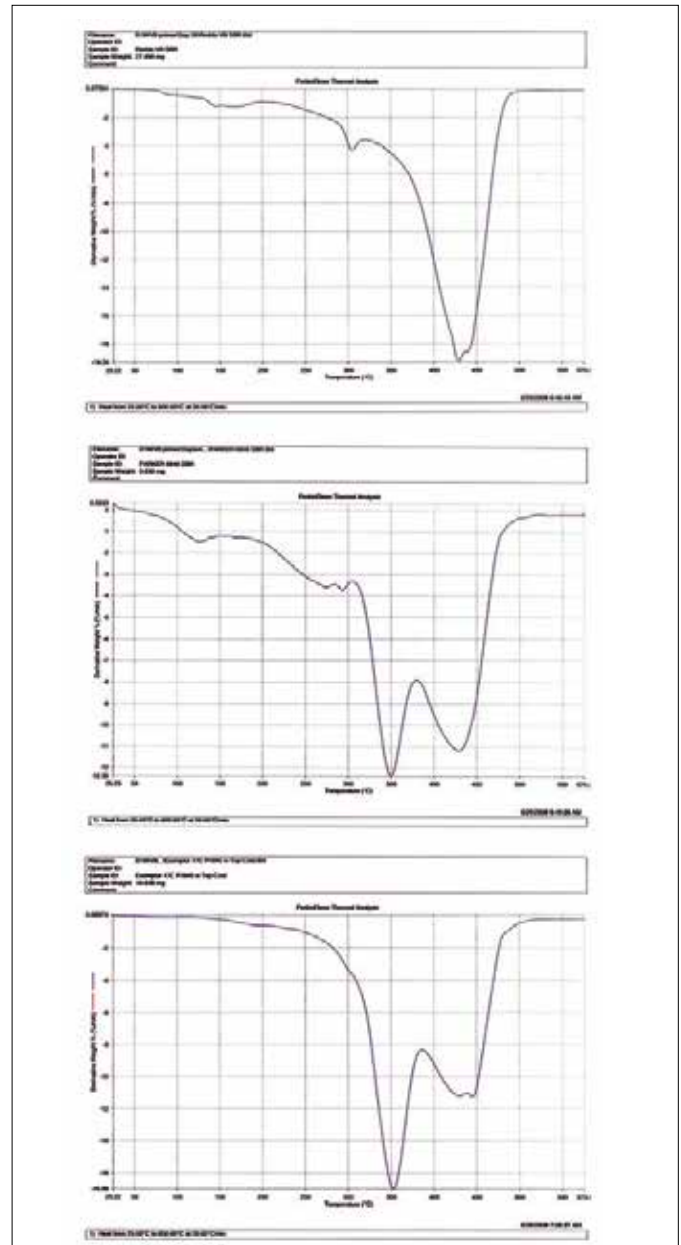


Figure 10. TGA 1st derivative curves of three different brands of vapor barrier primer. Each is a mixture of SBR and PVA resins.

Differential Scanning Calorimetry –
Raman Spectroscopy

Polymer Crystallinity Studies by DSC- Raman Spectroscopy

Differential scanning calorimetry (DSC) and Raman spectroscopy are both used to investigate crystallinity but in rather different ways. DSC can determine the degree of crystallinity very precisely and can also follow the kinetics of crystallization by measuring the associated enthalpy changes. Because of its ability to rapidly stabilize at temperature and its heating and cooling rates of up to 750 °C/min in control, the PerkinElmer® DSC 8000 or 8500 is often used for crystallization studies. Since the double-furnace design allows precise control at true isothermal temperatures, isothermal studies are best carried out in this model.

Raman spectra of crystalline and non-crystalline forms generally differ with the bands of the former being much narrower. Additional possibilities provided by Raman are to monitor very slow changes and also to identify situations where crystallization leads to a mixture of forms. As the PerkinElmer RamanStation™ 400 and RamanFlex™ lines allow the timing of its laser pulses to be adjusted, the collection of the Raman spectra can be tuned to match the scanning rate. Simultaneous measurements remove the uncertainties that arise when the behavior of the material may depend on the thermal history of the sample.

Semi-crystalline polyethylene oxide illustrates the complementary nature of the two techniques. This material has a variety of clinical applications and is widely used in consumer products such as toothpaste. A sample was heated from 10 °C to 75 °C through melting, then cooled back to 10 °C and the cycle was repeated. The maximum of the melting peak is at 70.0 °C in the first cycle and at 66.7 °C in the second. The heat of fusion is also lower in the second heating (Figure 1 – Page 2). This implies that the initial melting and solidification increases the proportion of amorphous material.

Raman spectra were obtained at 5-second intervals during the DSC runs. In the spectrum after the first heat/cool cycle, there are broad features associated with the amorphous component (Figure 2). The difference between the spectra before and after the first cycle is obtained by subtraction. Although noisy, it is very similar to the spectra obtained from the melt, which is amorphous. So the Raman spectra confirm directly the inference from the DSC data that the first heat/cool cycle increases the amorphous content. Spectra of crystalline and amorphous components can be obtained from these data (Figure 3 – Page 3).

Polyethylene terephthalate (PET) has been much studied by both techniques. The sample examined here has significant amorphous content after rapid cooling from the melt. The heat-flow curve shows a glass transition (T_g) at around 70 °C, crystallization, and then melting at 270 °C (Figure 4 – Page 3). Changes in the Raman spectra are small but can be followed by using principal components analysis (PCA). Analysis of the 1727 cm^{-1} C=O Raman band gives two principal components: PC 1 has the shape of a first derivative, corresponding to a band shift and PC 2 is second-derivative shape representing a change in peak width. The temperature profile for the peak-width change clearly matches that for crystallization and melting. However, the temperature profile for the peak shift does not correspond to the events seen in the DSC heat-flow curve but reflects a continuous shift to lower frequency with increasing temperature.

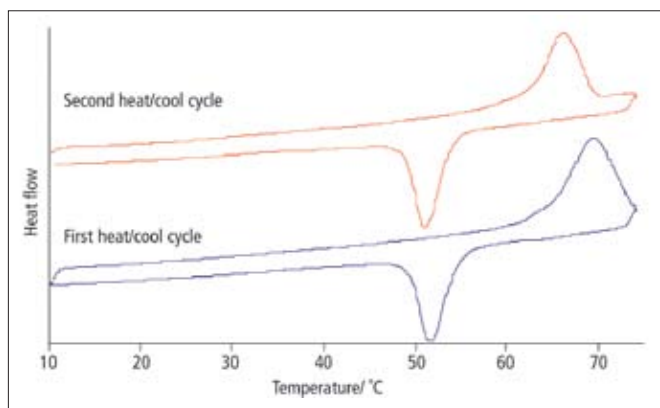


Figure 1. DSC run of polyethylene oxide (PEO). The first and second cycles have been offset for clarity.

Isothermal crystallization is readily monitored by DSC or Raman spectroscopy, with DSC being ideal for rapid processes while Raman is applicable even when crystallization is very slow. The comparability of the data from the two techniques is seen in a study of two blown polyethylene films, one of which was from a batch of bad material. Crystallization at 121 °C was measured after rapid cooling at 500 °C/min from the melt. This type of experiment requires a HyperDSC®-capable instrument like the DSC 8500 to cool rapidly and still precisely come to the isothermal holding temperature. After a stabilization transient, the DSC data (Figure 5a – Page 3) show that the bad material crystallizes more rapidly and with higher enthalpy than the good material. The Raman data (Figure 5b – Page 3) are shown for the initial heating and cooling of the samples as well as the isothermal period. In this case, a factor score from PCA is directly related to crystallinity. Here too the bad material is seen to crystallize more rapidly and also achieves a higher degree of crystallinity than the good material. From both sets of data, it appears that the final degree of crystallinity in the bad material is about 50% higher than the good. In both cases, the final degree of crystallinity is much lower than in the starting materials.

DSC-Raman spectroscopy allows us to precisely probe the crystallization behavior of polymers under various thermal conditions and correlate the energy changes from the DSC to changes in structure as seen in the Raman. This approach allows precise correlation of the two methods and promises a greater understanding of crystallization behavior.

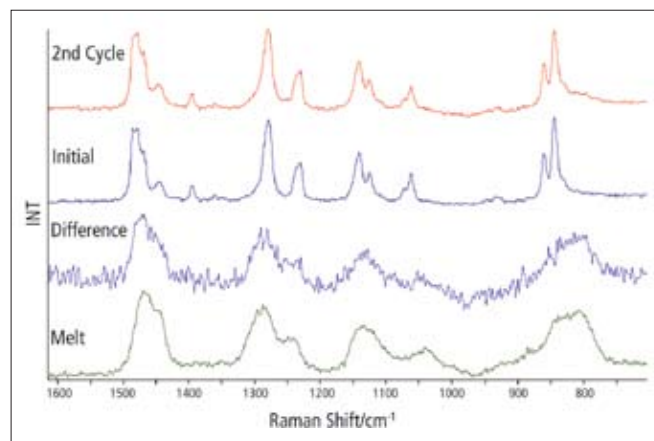


Figure 2. Spectra from DSC run of PEO.

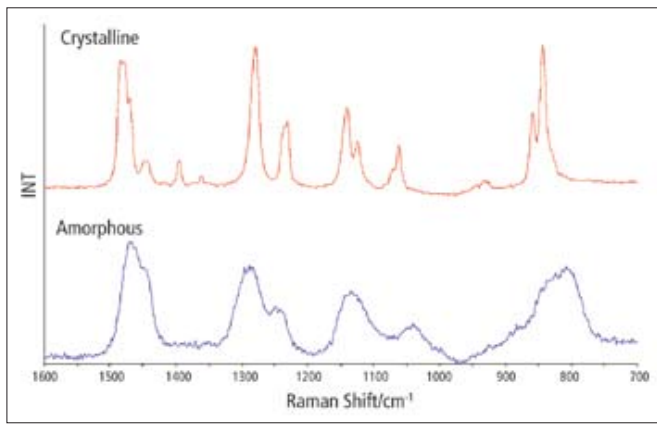


Figure 3. Raman spectra of crystalline and amorphous PEO.

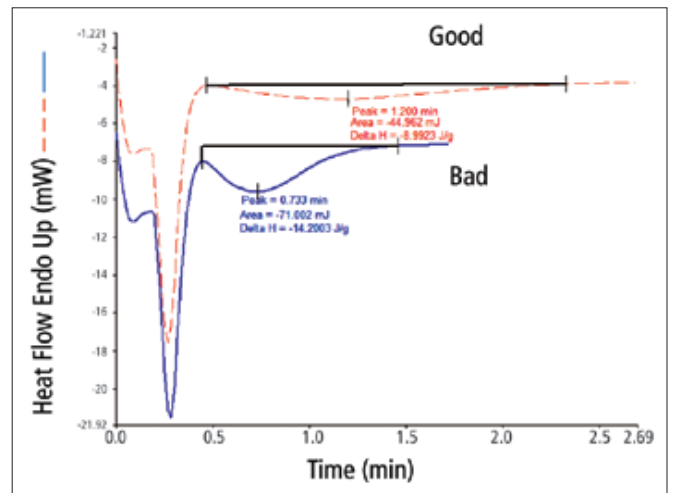


Figure 5a. DSC of HDPE isothermal crystallization.

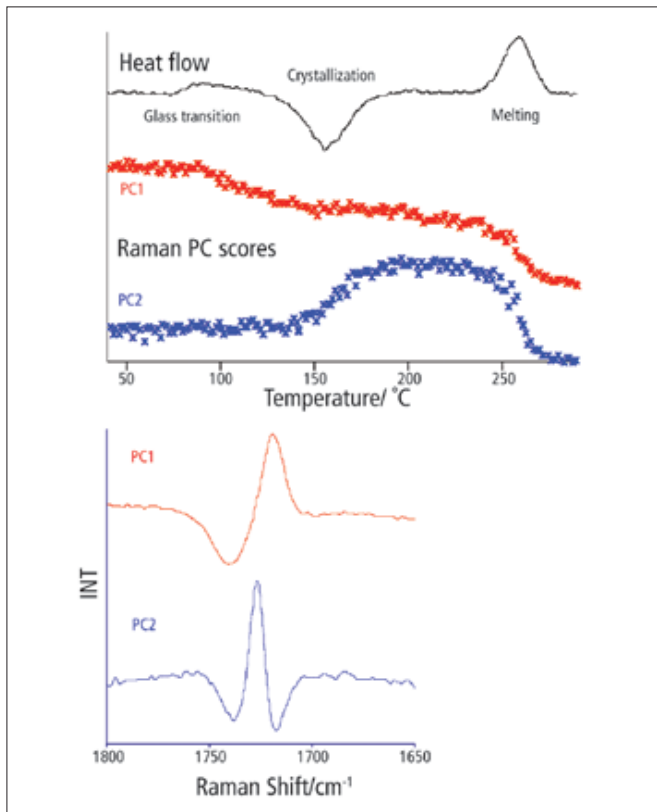


Figure 4. DSC and Raman data for PET.

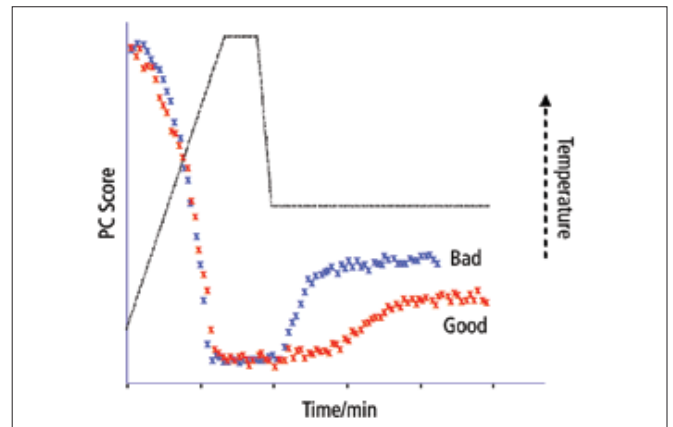


Figure 5b. Raman of HDPE melting and isothermal crystallization.

PerkinElmer, Inc.
 940 Winter Street
 Waltham, MA 02451 USA
 P: (800) 762-4000 or
 (+1) 203-925-4602
www.perkinelmer.com



For a complete listing of our global offices, visit www.perkinelmer.com/ContactUs

Copyright ©2009, PerkinElmer, Inc. All rights reserved. PerkinElmer® is a registered trademark of PerkinElmer, Inc. All other trademarks are the property of their respective owners.

008966_01

Thermogravimetric Analysis –
GC Mass Spectrometry**Author****Greg Johnson****PerkinElmer, Inc.**
Shelton, CT 06484 USA

Qualitative Analysis of Evolved Gases in Thermogravimetry by Gas Chromatography/ Mass Spectrometry

Introduction

Thermogravimetric analysis (TGA) measures the change in the weight of a sample as a function of temperature. A limitation of TGA is that it cannot identify what material is lost at a specific temperature. The analysis of gases evolved during a TGA experiment by gas chromatography mass spectrometry (GC/MS) provides laboratories with a way to identify the compound or groups of compounds evolved during a specific weight-loss event in a TGA analysis.

This application note discusses the utility of TG-GC/MS with an example application – the identification of specific organic acids evolved during TGA analysis of switchgrass.



Figure 1. Clarus 600 GC/MS interfaced to the Pyris 1 TGA.

Switchgrass (*Panicum Irgatum*) is a perennial warm-season grass native to the northern states of the USA; it is easily grown in difficult soils. Switchgrass is potentially useful in the production of biofuels, specifically cellulosic ethanol and bio-oil.

The instrumentation used in this study was a PerkinElmer® Pyris™ 1 TGA interfaced to the PerkinElmer Clarus® 600 GC/MS with the S-Swafer™ micro-channel flow splitting device (S4 configuration). The preferred mode of operation of the TGA maintains the atmosphere around the sample at ambient atmospheric pressure. The sample is collected from the TGA by allowing the high vacuum of the MS to create a pressure drop across the GC column, causing a flow of gas from the TGA through the transfer line and the analytical column to the MS. During the analysis, there are times when the TGA inlet will be surrounded by air, rather than an inert atmosphere. This would cause air to flow into the GC/MS; this is undesirable as it will cause oxidation to a number of different areas of the system. The S-Swafer device (shown in Figure 2) is used to switch between backflushing of the TGA transfer line during non-sampling time and sampling of the TGA environment during analysis.

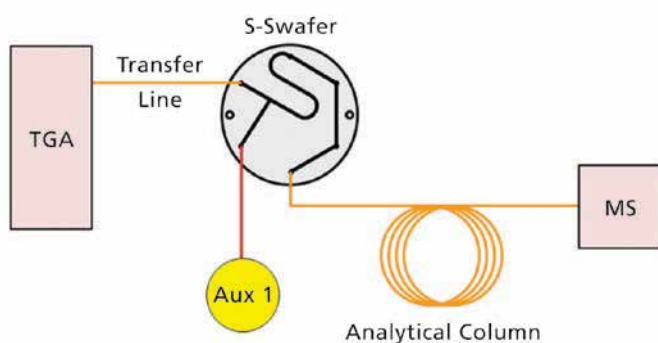


Figure 2. Schematic showing the pneumatic interfacing of the TG-GC/MS using the S-Swafer.

Figure 3 describes in greater detail the pneumatic supply to the S-Swafer device and assists in explaining why this approach is so well suited to interfacing the Pyris 1 TGA to the Clarus 600 GC/MS.

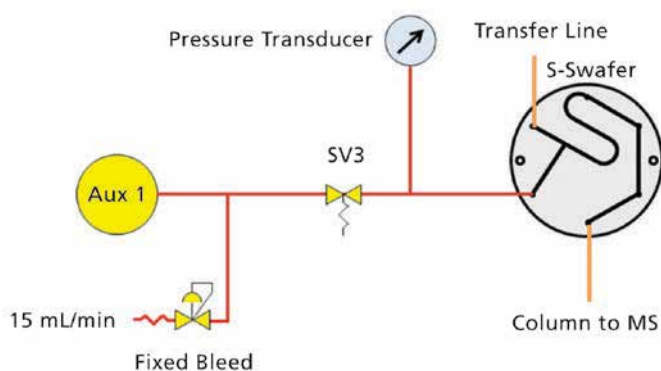


Figure 3. Schematic showing carrier-gas supply to the S-Swafer device.

The S-Swafer configuration is optimal because it will ensure a very rapid adjustment of carrier gas to the Swafer device, allowing for a rapid switch between backflush of the transfer line and sampling from the TGA. The samples of evolved gas are collected by setting a simple parameter in the GC method; multiple samples can be collected during a TGA analysis. Additionally, backflush of the transfer line will isolate the GC/MS and enable purge gas at the TGA to be switched from an inert gas (during analysis) to an air supply for cleaning of the TGA pan prior to the next sample.

Oven subambient cooling will be extremely useful in this application, allowing protracted sampling periods to be refocused into a narrow band of analytes on the column.

Experimental

The deactivated fused-silica transfer line used here was 1.6 m x 0.32 mm i.d. A few centimeters of the deactivated fused silica protrudes into the sample weighing area of the TGA. Approximately 30 cm of fused silica passes through the injector into the oven environment and is connected to the S-Swafer using specialized SilTite™ nuts and ferrules to ensure a leak-free connection that will not shrink and leak during normal or even extended thermal cycling of the main oven.

In all cases, a 30 m x 0.32 mm analytical column was employed as this allows a carrier flow of approximately 1 mL/min with the fixed 1.00 atmosphere pressure drop from ambient at the TGA to vacuum at the MS. Data was acquired using an Elite™ WAX stationary phase.

A small quantity of dried and ground switchgrass was placed on the TGA pan and weighed using Pyris software. A rapid TGA analysis based on heating the sample from 30 °C to 1000 °C at 100 °C/min in a nitrogen atmosphere was performed to determine which regions of the weight-loss curve were to be further studied using the TG-GC/MS technique.

The primary reason for using such rapid heating, which reduces the resolution of the weight-loss curve produced by the TGA, is to transfer the evolved gas quickly into the GC column. A quick transfer will improve GC peak shape, sensitivity and resolution.

After the sample was loaded onto the TGA and the furnace raised, the analysis was started immediately. The first step in the TGA heating program maintained the low initial furnace temperature for 5 to 10 min. During this time, the furnace environment is being purged with helium (or nitrogen/argon), and the carrier-gas pressure of 7.0 psig maintained at Aux 1 (Figures 2 and 3) ensures that no sample can enter the analytical column. After this initial hold period, the TGA furnace begins to heat the sample, and simultaneously, the GC/MS run is started using an external start command.

Based on previous TGA runs on the same sample, timed events within the GC method switch off the carrier gas supplied by the Aux 1 PPC module and then close the solenoid valve (SV3) shown in Figure 2 (Page 2). This begins the sampling and this procedure is reversed to bring the sampling period to an end. After the sampling is complete, both the GC oven-temperature program and MS data acquisition begins. The TGA can now be programmed to switch purge gases to clean the system using oxidation at elevated temperature, prior to the next analysis.

A typical TGA weight-loss curve for the switchgrass is shown in Figure 4 and reveals a typical weight % loss curve for the sample of switchgrass that was tested. In addition, superimposed on the weight-loss curve is the derivative of this curve which greatly assists the analyst in setting up the GC

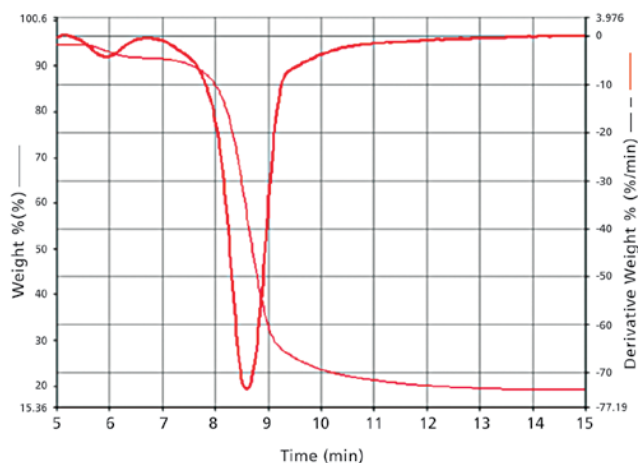


Figure 4. Typical result for the TGA analysis of switchgrass.

timed events that will be used to sample the evolved gases onto the GC/MS column. Note that the TGA is held isothermal for the first 5.0 min at which point heating begins. Simultaneously, the GC/MS analysis is started.

Figure 5 illustrates the TG-GC/MS analysis of the switchgrass based on timed events that collect the evolved gases from the main transition shown in Figure 4. The smaller earlier transition, also seen in the same figure, was also sampled onto the GC/MS but preliminary findings indicate that this is simply evolved water. The major transition produced large numbers of oxygenated volatile organic compounds (VOCs), including some very polar species. Earlier work using a non-polar capillary column had generated extremely smeared-out early-eluting peaks. The chromatogram below was generated using a thick-film polar Elite WAX column.

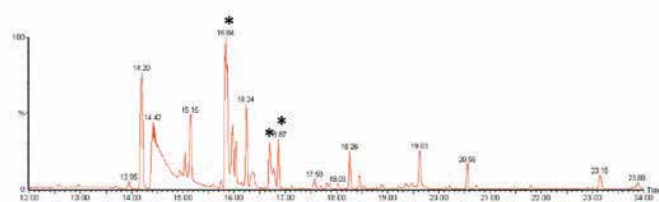


Figure 5. TG-GC/MS analysis of the switchgrass sample on a 30 m x 0.32 mm x 1 μ m Elite WAX column.

The three peaks labeled with asterisks in Figure 5 are identified as a homologous series of free fatty acids (Figure 6 – Page 4), based on a library search of their MS spectra (NIST® 2008). Usually in GC, a homologous series tends to elute in carbon-number order but here, the elution order appears to be acetic, followed by formic, followed by propanoic acid. As this retention behavior is not typical and in the absence of a literature reference or a similar chromatogram in the public domain, it seemed prudent to analyze a simple retention-time standard to confirm this tentative result. Figure 7 (Page 4) shows the same analysis again but with the retention-time standard shown in parallel. This standard was a simple mixture diluted in water with a small (5 μ L) aliquot of this aqueous solution deposited by syringe onto the TGA pan for analysis.

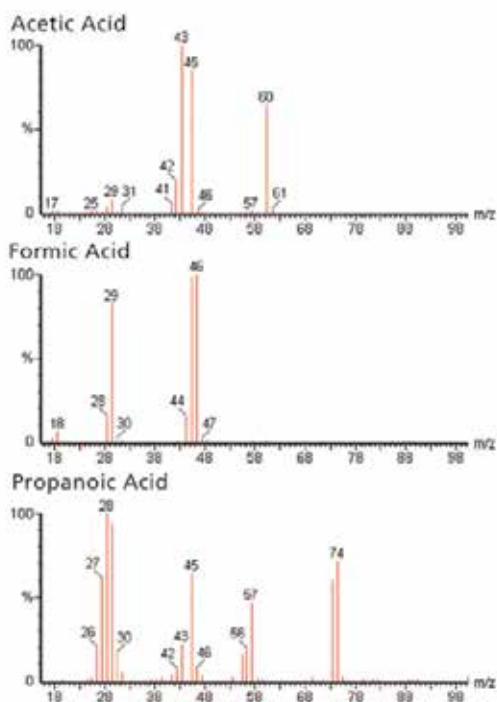


Figure 6. Mass spectra extracted from the total ion chromatogram of the switchgrass sample. The spectral data matches that of acetic, formic and propionic acid respectively available in the 2008 NIST® mass spectral library.

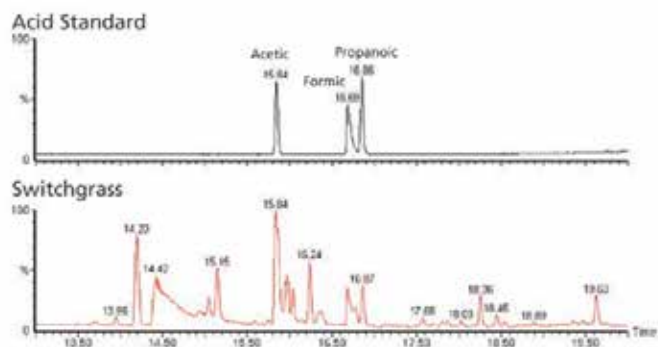


Figure 7. TG-GC/MS analysis of the switchgrass sample (bottom) on a 30 m x 0.32 mm x 1 µm Elite WAX column and the analysis of a simple retention time mix (top) under the same TGA and GC conditions.

Conclusions

In this application note, we describe the technique of TG-GC/MS through the analysis of switchgrass. TG-GC/MS is demonstrated to be a valuable technique in the separation and identification of complex mixtures of gas evolved during a TGA analysis. The S-Swafer device is demonstrated as a means to interface a TGA to GC/MS. The main benefits are its simplicity and the inertness of the entire sample path.

Thermographic Analysis –
Mass Spectrometry

The Analysis of Ethylene Vinyl Acetate by TG-MS

Introduction

The combination of thermogravimetric analyzers (TGA) with mass spectrometers (MS) to analyze the gases evolved during a TGA analysis is a fairly well-known technique. In this application, TG-MS technology is used to determine the components of an evolved gas from the TGA of ethylene vinyl acetate (EVA). EVA is a polymer used in many industries – two common applications are in solar panels and foam for footwear.

Experimental

This analysis was performed on a PerkinElmer® Pyris 1 TGA* using alumina pans and the standard furnace. The instrument was calibrated with nickel and iron and all samples were run under helium purge. Heating rates varied from 5 to 40 °C/min, depending on the sample under test. The furnace was burned off between runs in air. Samples were approximately 10-15 mg. Data analysis was performed using Pyris 9.0 Software.

During the TG-MS analysis, the PerkinElmer Clarus 600 GCMS* was used. In the TG-MS work, a 0.1 mm i.d. deactivated fused-silica transfer line was connected directly to the MS. The transfer line was heated to 210 °C. The data analysis was performed using TurboMass™ GC/MS Software.

Results

In this example, ethylene vinyl acetate (EVA) and the components of the evolved gas are analyzed to confirm their identity. Figure 1 (Page 2) shows the thermogram from the TGA of EVA.

*Pyris 1 TGA instrument is superseded. It has been replaced by TGA 8000.

*Clarus 600 GCMS instrument is superseded. It has been replaced by SQ8.

The thermogram demonstrates two weight losses, the first corresponding to acetic acid and the second corresponding to fragments from the polymer backbone. The MS analysis (Figure 2) of the evolved gas confirms the identity of acetic acid with spectral data included in Figure 3.

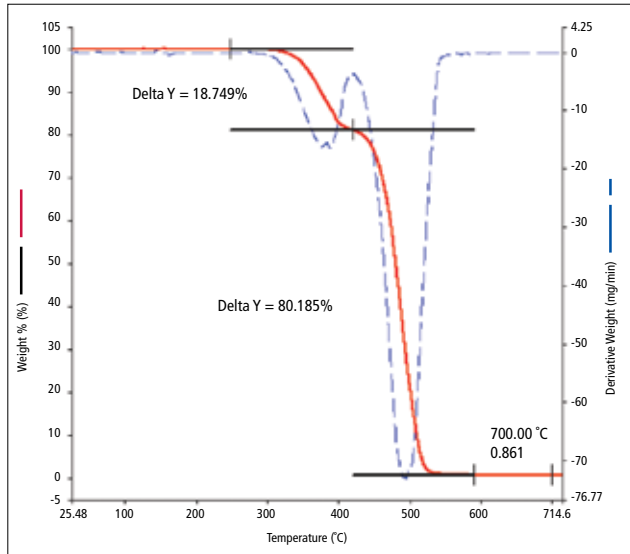


Figure 1. TGA curve generated from the analysis of EVA samples.

Conclusions

TGA analysis allows quantification of the weight loss of a material at specific temperatures. The coupling of the TGA with the MS increases the power of the technique by providing the ability to identify the species evolved during thermal analysis.

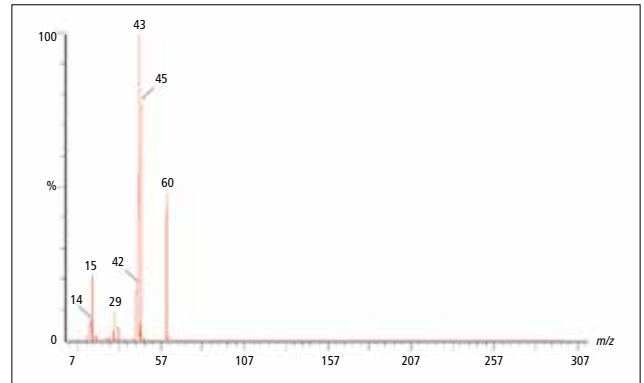


Figure 3. Spectral data verifying the identity of the evolved gas from the first transition of the TGA as acetic acid.

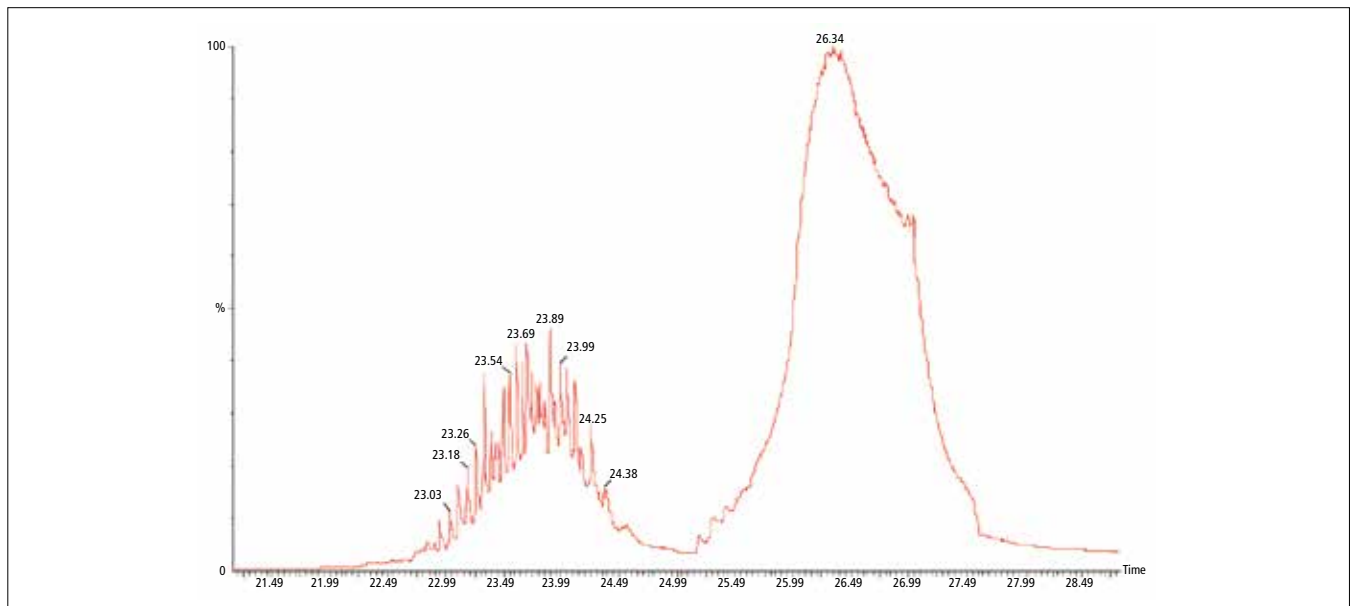


Figure 2. The MS analysis of the evolved gas generated during the TGA of EVA.

PerkinElmer, Inc.
940 Winter Street
Waltham, MA 02451 USA
P: (800) 762-4000 or
(+1) 203-925-4602
www.perkinelmer.com



For a complete listing of our global offices, visit www.perkinelmer.com/ContactUs

Copyright ©2010-2016, PerkinElmer, Inc. All rights reserved. PerkinElmer® is a registered trademark of PerkinElmer, Inc. All other trademarks are the property of their respective owners.



Thermogravimetric Analysis – GC Mass Spectrometry



The Analysis of PVC with Different Phthalate Content by TG-MS and TG-GC/MS

Introduction

The combination of thermogravimetric analyzers (TGA) with mass spectrometers (MS) to analyze the gases evolved during a TGA analysis is a fairly well-known technique. In cases of complex samples, TG-MS often results in data in which it is nearly impossible to differentiate gases that evolve simultaneously.

Combining TGA with gas chromatography mass spectrometry (GC/MS) allows for a more-complete characterization of the material under analysis and precisely determines the products from the TGA. This application will demonstrate the relative advantages of TG-MS and TG-GC/MS – a summary of the strengths of each technique is presented in Table 1 (Page 2).

Table 1. Relative Advantages of TG-MS and TG-GC/MS.

TG-MS	TG-GC/MS
Real-time analysis	Sequential analysis
No resolution capabilities	Resolves overlapping events
Limits to library effectiveness	Resolution improves GC libraries effectiveness
Oxygen sensitive	Oxygen sensitive
	Can use alternate/multiple detectors
Simple	More complicated

Experimental

This analysis was performed on a PerkinElmer® Pyris 1 TGA* 8000 using alumina pans and the standard furnace. The instrument was calibrated with nickel and iron and all samples were run under helium purge. Heating rates varied from 5 to 40 °C/min, depending on the sample under test. The furnace was burned off between runs in air. Samples were approximately 10-15 mg. Data analysis was performed using Pyris Software.

During the TG-GC/MS analysis, the PerkinElmer Clarus® 680 C GC/MS was used. In the TG-MS work, a 0.1 mm I.D. deactivated fused-silica transfer line was connected directly to the MS. The transfer line was heated to 210 °C. In the TG-GC/MS work, a 0.32 mm I.D. deactivated fused-silica transfer line was plumbed into the GC injector port where it was connected to the Elite™-1ms capillary GC column. In both cases, data analysis was performed using TurboMass™ GC/MS Software.

Results

In this example, polyvinylchloride (PVC) formulated with two different types of phthalates – disononyl phthalate (DINP) which is regulated and another formulation of non-regulated phthalates are analyzed to determine if a difference can be seen and correlated to the phthalate type.

Figure 1 is the thermogram from the analysis of the two different PVC samples. The purple line in the thermogram with a weight loss of 50.99% in the first event corresponds to the PVC sample with DINP. The green line with the weight loss of 64.82% corresponds to the PVC with the non-regulated mixture of phthalates.

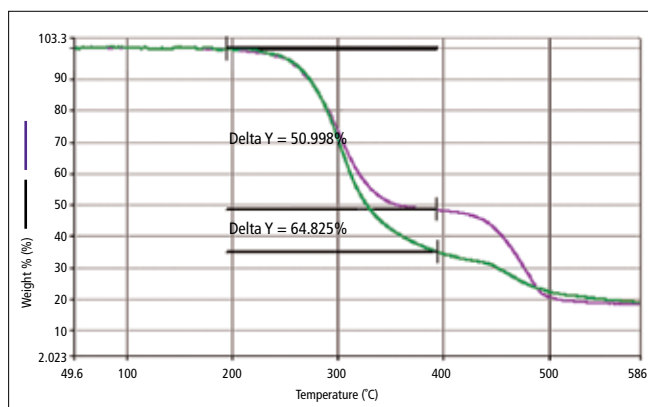


Figure 1. TGA percent-weight-loss curve generated from the analysis of two PVC samples: one with DINP (purple), a regulated phthalate, and a weight loss (delta y) of 50.998%; and a second with a mixture of non-regulated phthalates (green) and a weight loss (delta y) of 64.825%.

The weight-loss curve from TGA shows a clear difference between the two materials. This may be a result of either different additives or the amount of additive needed to achieve specific physical properties in the PVC sheeting.

The evolved gas from each sample was analyzed by both MS and GC/MS to determine if either technique would confirm the presence or absence of regulated vs. non-regulated phthalates. Figure 2 demonstrates the MS data obtained from the analysis of each sample.

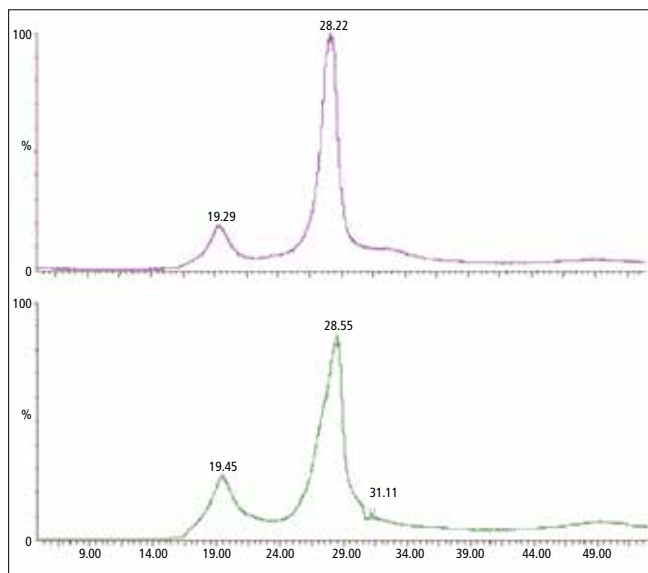


Figure 2. The MS analysis of the evolved gas generated during the TGA analysis of PVC materials with DINP (purple - top) and a mixture of non-regulated phthalates (green - bottom).

*Pyris 1 TGA instrument is superseded. It has been replaced by TGA 8000

In Figure 2, it is difficult to find a difference between each material. The gas evolved in the TGA showed little difference in the MS. Each of the two major weight-loss events generated a mixture of gases generating many ion fragments simultaneously. TG-MS is very useful when the evolved gases are relatively simple; here resolution of the evolved gas is needed to identify each component.

The TGA analysis was performed again; however, a sample of the first weight loss was collected and introduced into a GC column. This will allow some resolution of evolved gases and better identification of specific components. Figure 3 demonstrates the chromatogram of the analysis of the gas evolved during the first weight loss of the TGA. It can be seen that the gas evolved is indeed very complex with a chromatogram full of different components – many unresolved.

In this case, differences can be noted in the evolved gas of each TGA. Most significant were in the peaks around

30 minutes. These peaks contained a strong response at m/z 149 – an ion associated with many phthalates. Further work would need to be done to determine if qualitative and/or quantitative data is provided by the analytical approach used here, but differences are much more significant when TG-GC/MS is employed over TG-MS.

Conclusions

TGA analysis allows quantification of the weight loss of a material at specific temperatures. MS increases the power of the technique by providing the ability to identify the species evolved during thermal analysis; however, if a complex gas is evolved during a single event, the MS data is difficult to interpret. The use of TG-GC/MS adds chromatographic separation of co-evolved gases, enabling identification of individual components, making data interpretation easier than TG-MS.

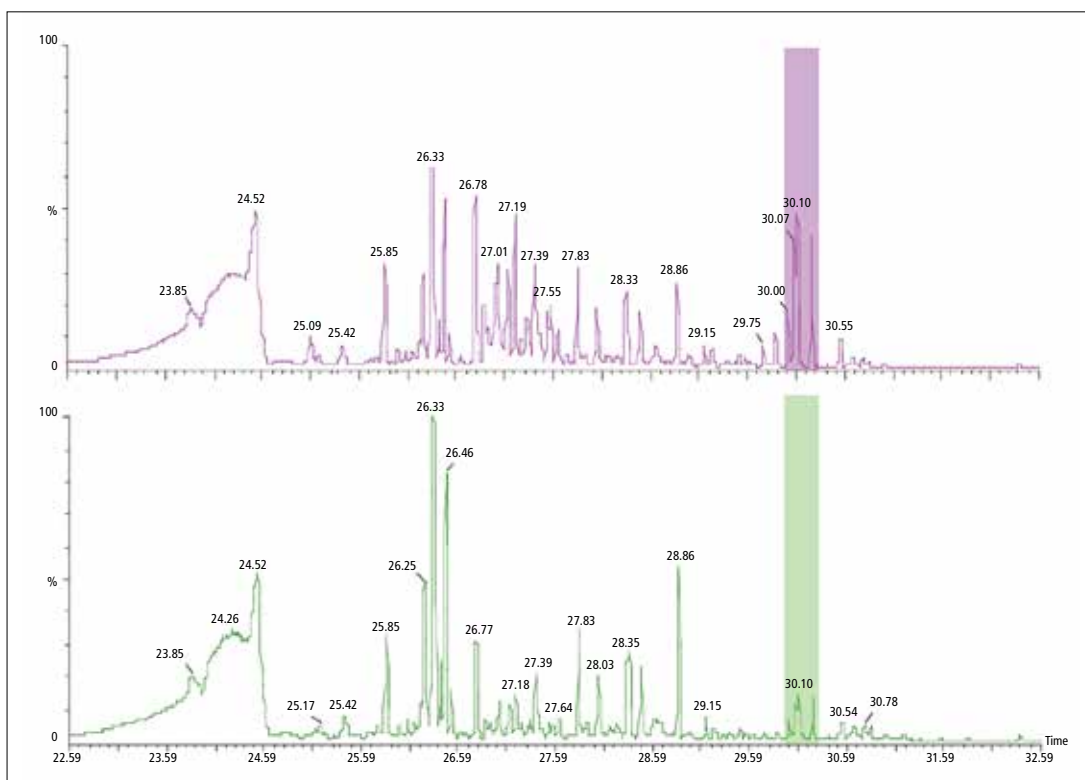


Figure 3. The GC/MS data collected during the TGA analysis of PVC with DINP (purple - top) and with a mixture of non-regulated phthalates (green - bottom). Differences are noted in peaks with tentative identification as phthalates around 30 minutes.

UV-DSC

Author

Peng Ye

PerkinElmer, Inc.
Shelton, CT 06484 USA

UV-DSC Study on New Double Furnace DSC

Abstract

The UV curing of resins is important in materials science. Direct energy measurement and true isothermal operation are essential to a successful UV curing experiment. Since the UV curing reaction is fast, a fast response DSC is needed to capture the process.

The double-furnace power-controlled DSC 8000/8500 with UV accessory is the ideal tool to study the UV curing process and to characterize the material properties before and after the UV curing.

Introduction

The major benefit of ultraviolet (UV) curing is that it is a cure-on-demand process. The photo-sensitive material will not cure until the UV light hits it, and when that occurs, it takes only a short time to cure. The process is fast, solvent-free, and economical. UV curing brings many benefits to product manufacturers. Among these are ease of use, process consistency and flexibility, reduced environmental considerations and the availability of high performance materials. The application of UV curing material is very broad. It includes adhesive, clear protective coatings, inks, dental material and pharmaceutical material. Cure conditions can favorably impact the performance properties of many UV-curing materials. However, both undercuring and overcuring should be avoided. DSC (Differential Scanning Calorimetry), together with a UV accessory can be used effectively to study UV curing reactions. In particular, it can be used to study

curing time, curing enthalpy, the effect of light source (wavelength, intensity), photo initiator concentration, curing temperature and purge gas (nitrogen or oxygen) etc. The new PerkinElmer® double-furnace power-controlled DSC is the ideal tool for the UV curing study because of its unique features compared with conventional heat flux DSC. It can perform true isothermal operation so that it can keep the sample temperature constant during the UV curing reaction. It has a fast response time so that it can capture the fast reaction of UV curing. It also measures the energy directly for accurate enthalpy results. This note will use a UV curing resin used in removable dental appliances as an example to demonstrate this application on the new power-controlled DSC 8000/8500. Experimental details such as sample preparation, method setup, data process and system optimization will be discussed. The effect of light intensity and isothermal temperature on curing will be studied.

Experimental

The instrument used is the new PerkinElmer power controlled DSC 8000/8500. The cooling accessory is the Intracooler III which is a new mechanical refrigerator for the DSC 8000/8500. It offers -100 °C as the lowest program temperature and can remove heat efficiently from a UV experiment. As a general rule, the cooling block temperature should be at least 30 °C lower than the isothermal temperature at which the curing is to be carried out. The UV light source is the OmniCure® 2000 (Figure 1). It comes with a 200 W mercury lamp and a bandwidth filter of 250 nm to 450 nm. For the DSC 8500/8000, the intensity range can be varied from approximately 2 mW/cm² (~1% iris opening) to about 180 mW/cm² (~70%). The light source is connected to the computer through a relay box which can be triggered by the Pyris™ software.

The sample is a fiber filled dental resin. It is a translucent, pink paste (Figure 2). Another optical adhesive sample with faster curing and higher curing energy is used for comparison purpose.

The curing experiment is conducted under isothermal conditions. Different experiment parameters including isothermal temperature and iris opening were used to investigate their effects on curing profile. The glass transition temperature (T_g) before and after the curing was also checked.



Figure 1. Picture of DSC 8000/8500 with the OmniCure® 2000 UV accessory showing sample and reference light guides.



Figure 2. Picture of the fiber filled dental resin used for the UV curing experiment.

Results

The sample weight must be optimized for each individual sample type depending on the kinetics of the curing reaction and the energy released during the curing. Basically, the greater the energy conversion and the faster the reaction, the smaller the sample should be. So 1 mg or less is recommended for samples like lacquers, printing inks and other fast-reacting systems with a high energy conversion. Several mg is appropriate for dental fillings or similar materials. In this experiment, about 3 mg sample was used. Since the sample is a paste, it needs to be spread as evenly as possible over the bottom of the sample pan. The thickness of the layer has a significant influence on the analysis results and reproducibility.

Table 1. Typical UV curing samples and sizes.

Sample size (mg)	Sample types
1 mg or less	lacquers, printing inks
Several mg	dental fillings

The heat flow signal will be changed when the shutter is open due to UV energy flowing to the pan. In order to minimize this effect, the heights of the sample and reference light guides need to be adjusted to give a near zero heat flow change on irradiation. As can be seen in Figure 3, there was a big baseline shift when the shutter opened. By using the thumbscrews to raise or lower the light guides, the heat flow can be brought back to the original level.

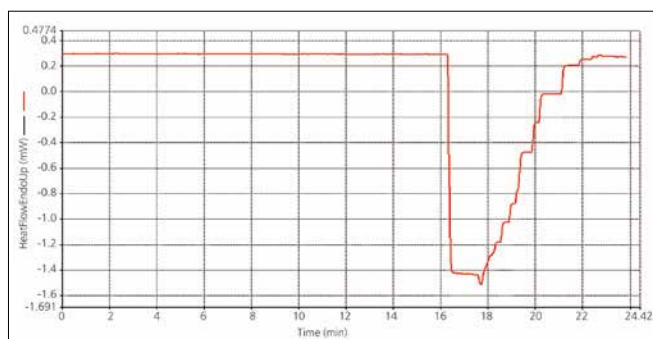


Figure 3. Adjust the heat flow baseline using the thumbscrews.

As a general rule, the light intensity should increase with the opacity of the sample and the thickness of the layer. The light intensity can be adjusted by opening the iris on the OmniCure® 2000 system. Since the DSC 8000/8500 measures energy directly, it is possible to estimate the light intensity by using graphite disk to adsorb the light energy. For such measurement, the graphite disks are inserted into the sample side and reference side. During irradiation, the reference side is covered with a piece of white paper. Figure 4 showed the results with the iris open 5%, 10% and 15%. With the iris 15% open, the heat flow change is about 6 mW. This value, divided by the surface area of the graphite disk (approximately 0.39 cm²), gives the value of the light intensity of 15.4 mW/cm². Because here the sample is translucent, a relatively big iris opening (15%) was used for the curing experiment.

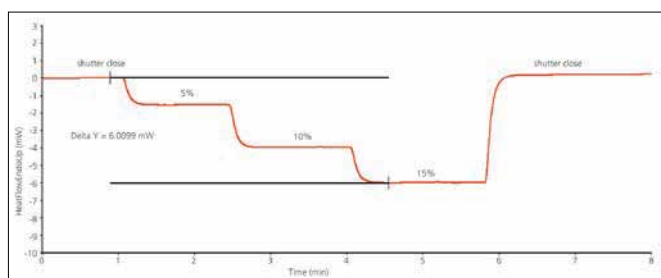


Figure 4. Light intensity determination by graphite disks.

For best results, two measurements under identical conditions are recommended in order to offset the baseline shift due to the light irradiation. The first run records the UV curing reaction. The second run helps to confirm if the curing reaction is complete (no exothermic peak observed) and establish the baseline shift due to light irradiation. Subtraction of the second run from the first run can eliminate any possible baseline shift and give an accurate calculation of curing energy (Figure 5). For all the following UV curing data, subtraction of a second run was performed.

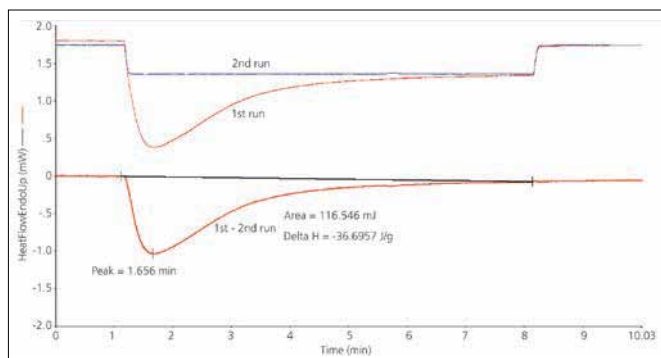


Figure 5. UV curing data process for the dental resin sample.

The uncured dental material has a subambient glass transition temperature. The Tg was determined by running a heating scan from -80 °C to 30 °C at 50 °C/min. The data (Figure 6)

shows a Tg at -27 °C. Since the curing process will change the Tg behavior, by comparing the Tg before and after curing, the effect of curing on Tg can be studied.

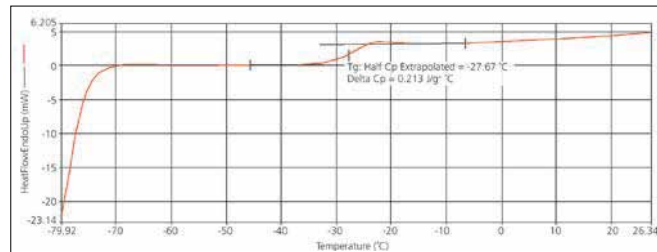


Figure 6. Uncured dental material showing a Tg at -27 °C.

Different UV curing materials may have quite different curing kinetics/energy based on their domain of application. The dental resin needs to be cured relatively fast and low curing energy is desirable. The UV curable optical adhesive is designed to cure very quickly and high energy is released to give a tough resilient bond. UV-DSC experiments can be used easily to show the different curing behaviors. Figure 7 demonstrates the different curing profile of dental resin and optical adhesive at 30 °C with 15% iris opening. The optical adhesive is cured faster than dental resin and has much more energy released (189 J/g vs. 44 J/g).

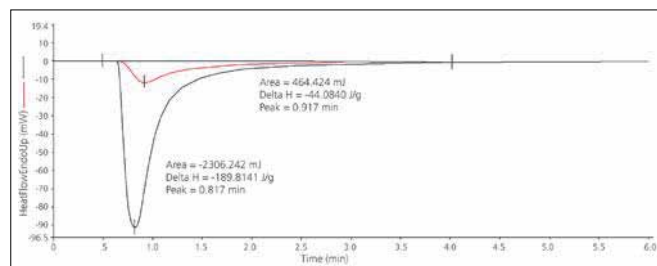


Figure 7. UV curing data at 30 °C with 15% iris, dental resin (red) vs. optical adhesive (black) showing different peak time and energy.

The curing reaction will change the Tg behavior. With the increasing curing time, the curing degree will increase and the original Tg of uncured material will diminish. A partial UV curing experiment was conducted on dental resin with the curing time of 0, 0.1, 0.2, 0.3, 0.5, 1, 2 and 4 min. The original Tg was checked after each UV curing period. As can be seen in Figure 8, the Tg strongly diminished with increasing UV exposure time. After 0.5 min curing, the Tg has become difficult to see.

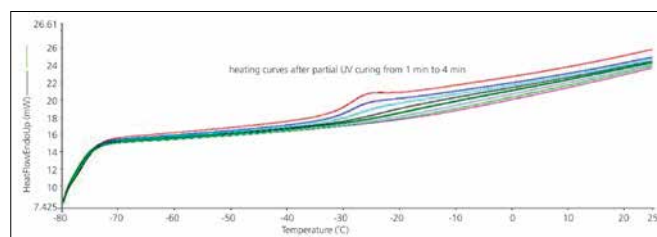


Figure 8. Heating curve after partial UV curing for 0, 0.1, 0.2, 0.3, 0.5, 1, 2 and 4 min, showing the diminishing Tg of uncured material after UV curing.

After the dental resin was UV cured fully at 30 °C, a heating scan from -80 °C to 145 °C was performed (Figure 9). The subambient T_g of uncured resin has disappeared. The 1st heating shows a residual curing above the UV curing temperature and finally a small T_g around 128 °C of the cured resin. The 2nd heating curve indicates no residual curing and the T_g of cured resin as expected.

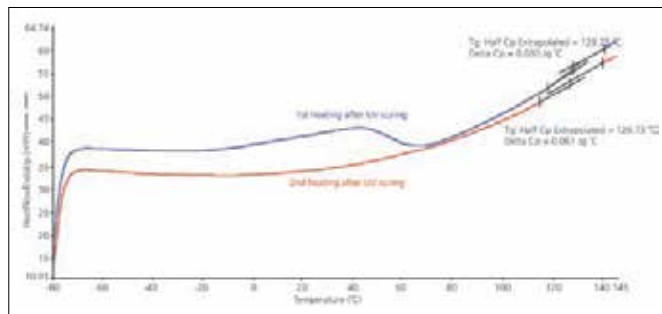


Figure 9. 1st and 2nd heating curves after UV curing, showing residue curing and T_g after that.

Two important parameters for UV curing experiments are light intensity and isothermal temperature under which the UV curing is conducted. Their effects on curing behavior of dental resin are studied. The effect of light intensity was studied by adjusting the iris opening from 5% to 25% (Figure 11) and three isothermal

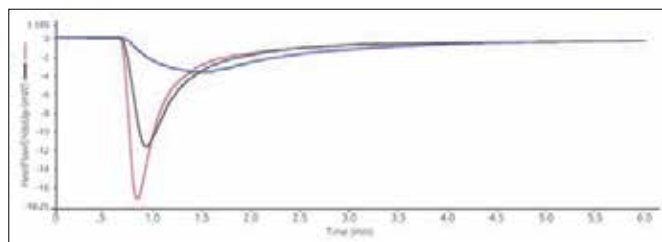


Figure 10. Effect of light intensity with iris opening at 5% (blue), 15% (black) and 25% (pink) at 30 °C on dental resin.

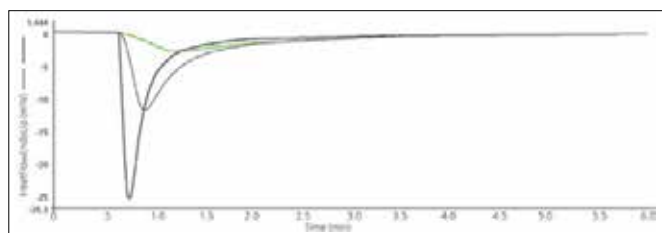


Figure 11. Effect of isothermal temperature at 10 °C (green), 30 °C (blue), 50 °C (black) on dental resin curing with 15% iris opening.

temperatures 10 °C, 30 °C and 50 °C were used to study its influence on curing profile (Figure 12). Clearly both factors have a big effect on the curing profile. Increasing light intensity or isothermal temperature will shorten the UV curing time and increase the degree of curing generally as shown by Figures 10 and 11.

Summary

The UV curing of the dental resin can be studied on the new DSC 8000/8500 with UV accessory. Since the UV curing reaction is usually fast, a fast response DSC is needed to capture the curing process. In addition, direct energy measurement and true isothermal operation are essential to a successful UV curing experiment. The light source can be easily controlled by the Pyris software. The double furnace power controlled DSC 8000/8500 with UV accessory is the ideal tool to study the UV curing process and to characterize the material properties before and after UV curing.

Appendix – control software interface

A typical method is shown below (Figure 12). A key part of the method is to use the “trigger an external event” actions to switch the external channel used by the OmniCure® 2000 curing system On and Off, to open and close the lamp shutter. Four switch external channel actions must be included in the method to trigger the lamp shutter open and close at the end of the irradiation time. In the method here, a 10 minute isothermal hold was used. During the isothermal period, the lamp shutter was opened and UV curing started at 1 minute. The shutter was closed at 8 minutes for a 7 minute UV curing experiment.

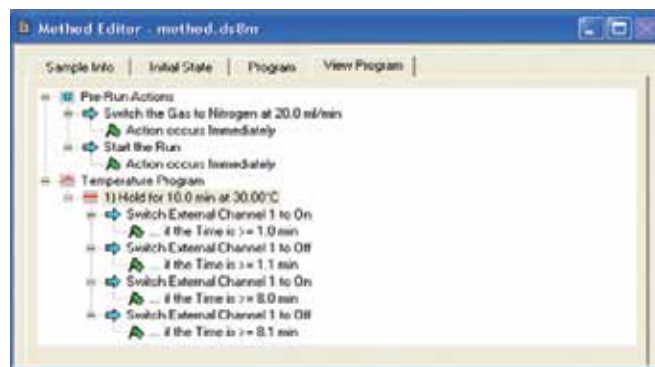


Figure 12. A typical UV curing method window. Note the parameters set by the user.

Thermogravimetric- Infrared Analysis

Authors

Maria Grazia Garavaglia

Peng Ye

PerkinElmer, Inc.
Shelton, CT 06484 USA

Plasticizer Characterization by TG-IR

Introduction

Plasticizers are additives that are added to polymeric material to increase flexibility. For example, phthalates are usually added to hard PVC plastics to make it soft. Many properties of the polymer will be changed by the addition of a plasticizer, such as the glass transition temperature (T_g) which will be reduced dramatically; the hardness which will be reduced; the strength which will decrease and the processability which will be improved. Since

plasticizer is often made up of small molecules, it will migrate to the surface and evaporate from the polymer matrix over time or upon heating. One common example is the smell of a new car which is caused by the plasticizer evaporating from the car's interior polymer parts. Because the plasticizer may be toxic and be harmful to human health, restrictions often apply to some types of phthalates such as in children's toys in the United States and European Union. It may be important to know the plasticizer added to the polymer product and its content.

Thermogravimetric analysis (TGA) is a common technique that is used to study the weight loss during heating. It can tell you the percentage of weight loss quantitatively and accurately. But TGA alone will not tell you anything about the chemical components of the evolved off gas. The hyphenation between TGA and FT-IR is able to identify the off gas from TGA and give a more complete picture of material characterization.

In this note, the sample is a complex mixture of solvent, plasticizer and polymers from a paint and varnish producer who require data concerning the plasticizer and its percentage.

Instrument

A PerkinElmer TGA 8000 and Frontier FT-IR system connected by the state-of-the-art TL 8000 transfer line was used for this analysis (Figure 1)



Figure 1. The TL 8000 transfer line couples a Frontier FT-IR to a TGA 8000.

The advantages of this system include:

- Insulated heated transfer line with replaceable SilcoSteel® liner.
- Heated zero-gravity-effect 'ZGCell' gas cell for the Spectrum instrument incorporating automatic accessory identification, low volume, and efficient sample area purging.
- Control unit incorporating a mass flow controller, particle filters, flow smoothing system, independent transfer line and gas cell temperature controllers, and vacuum pump with exhaust line.
- Automatic triggering of IR data collection from the Pyris software.
- Spectrum Timebase software for time resolved experiments.

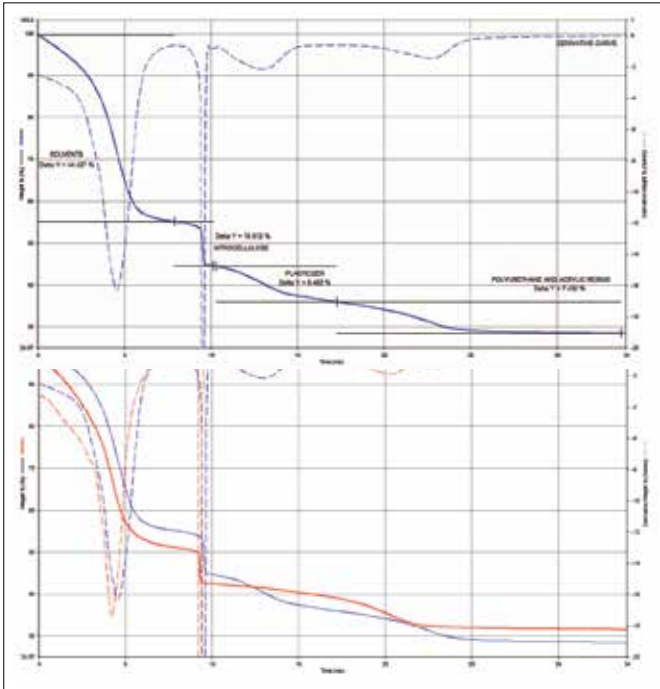


Figure 2. TGA and its derivative curve. Red curve: sample without plasticizer; Blue curve: sample with about 8% plasticizer.

Analysis of an Unknown Aqueous Sample by TG-IR-GC/MS

Thermal Analysis

Author

Maria Garavaglia

PerkinElmer

Monza, Italy

Introduction

A laboratory often must analyze an unknown mixture to determine the primary components and identify additives or contaminants. This information may be needed, for example, to evaluate a competitor's product or to determine compliance with regulations. The use of spectroscopic techniques to identify isolated molecular components is well established, and the separation and isolation can be accomplished by thermogravimetric analysis (TGA), FT-IR, and gas chromatography (GC). However, often combining these techniques is more powerful approach for complex mixture. PerkinElmer makes a range of hyphenated solutions and in this case, the TL-9000 transfer line is used to allow TG-IR-GCMS analysis on one sample. The laboratory apparatus combining these techniques can be seen in Figure 1.



Figure 1. From left to right: PerkinElmer® Clarus® 6000 GC/MS, PerkinElmer® Frontier® FT-IR, The Pyris® 1 TGA and the TL9000 temperature control module. The black transfer lines are part of the TL9000 interface system.

Consider the recent example: An analytical lab has received a pigmented aqueous sample for analysis.

Since water interferes strongly with the analysis, the sample was first dried at ambient temperatures. When the drying process was complete the film thus obtained was detached from the drying tray and warmed briefly in a dry air flow. A sample was then taken from the resultant film and placed in a TGA coupled to an infrared spectrophotometer (TG-IR). The twenty milligram sample was heated from 20 to 850 °C at a rate of 20 °C/min in a nitrogen atmosphere. During the heating of the sample, the gas released by the sample was directed to the gas cell of an infrared spectrophotometer via the TL8000 heated transfer line and interface. So during the TGA analysis, spectra of the gas released by the sample during heating were analyzed iteratively. See Figure 2 for the thermal weight loss versus temperature curve.

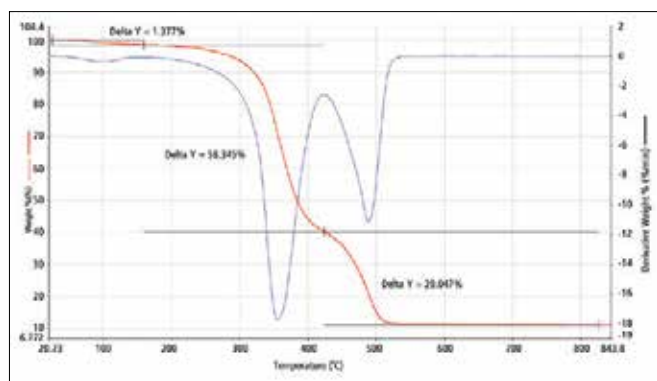


Figure 2. Weight loss (red curve) and rate of weight loss (blue curve) versus temperature from ambient to 850 °C.

Between 20 and 150 °C there was a weight loss of 1.38% from residual moisture in the sample. Between 200 and 410 °C there was a significant weight loss from evaporation of volatile fractions, accompanied by an initial decomposition of the polymer. The final decomposition of the polymer occurred between 410 and 510 °C.

During the TGA thermal separation, the gases released by the sample were sent to the FT-IR for spectral analysis. The TG-IR data consists of a sequence of spectra, acquired at intervals of around 8 seconds. The standard presentation of the data is the adsorption versus wave number, and this spectral profile of the gases released by the sample is generated for each roughly two degree interval. The TG-IR Spectrum Time Base software provides a 3D graphical representation, consisting of stacked IR spectra, a feature that provides a snapshot of the entire TG-IR separation (see Figure 3). This aids in interpreting the kinetics of the decomposition process and deciding which temperature cuts to analyze. Furthermore, the analyst can view the absorption versus time at any chosen wavelength to track the relative concentration of a particular decomposition product versus time, hence, temperature.

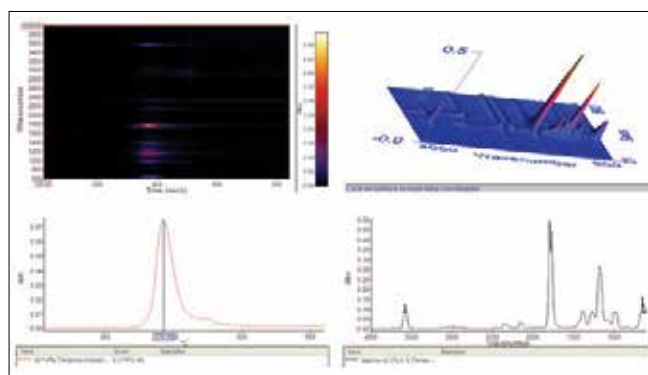


Figure 3. Spectrum Time-Based software outputs, which aid in interpreting the decomposition process. With experience, an operator will look at the stacked spectra (upper right plot) and see an “unexpected mountain range” that represents the transient presence of a particular species of off-gassing product of potential interest.

With reference to the data in Figure 3 the author observed the evaporation of an unknown substance which reached a concentration maximum at about 280 °C. The spectrum at this temperature was selected for a database search. From this library search the unknown substance was found to be triethylene glycol dibenzoate – or a very similar substance. Figure 4 shows that spectra of the unknown and that of the best search match. Figure 5 lists other match candidates together with the relative statistical likelihood of each match.

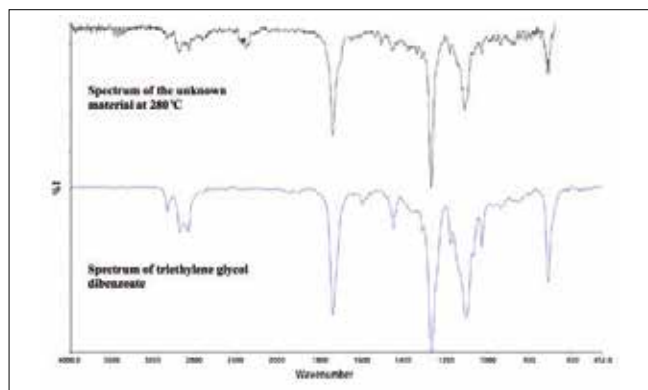


Figure 4. Best match spectra using PerkinElmer Spectrum Search software.



Figure 5. Output of Search software, showing match candidates.

Next, the TL9000 interface was enlisted to perform a subsequent analysis to confirm the identity of the unknown substance in the sample. At the time of maximum concentration absorbance of the substance being analyzed, the gas in the IR gas cell was sent to a GC/MS. The gas chromatogram can be seen in Figure 6.

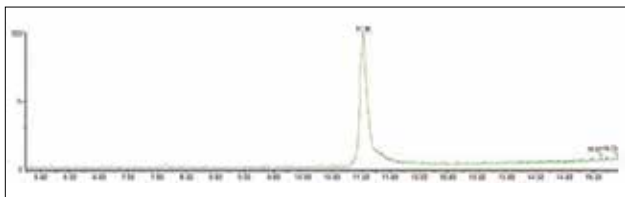


Figure 6. GC Chromatogram, detection amplitude versus time in minutes.

The material which came off the TGA at 280 °C, and which was further resolved by GC, was then evaluated by mass spectrometry (MS), whereby the unknown molecular structure is broken up into constituent ions that are then identified by their flight response in a magnetic field. The results are compared to a library of established MS data.

The National Institute of Science and Technology (NIST®) MS database search for the unknown substance yielded the output in Figure 7.

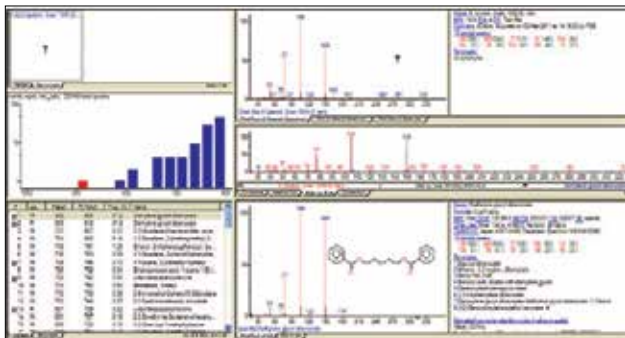


Figure 7. Output of TurboMass™ software showing the MS spectral results and the results of the search of the NIST® MS database.

The unknown substance was found to be diethylene glycol dibenzoate, chemically very similar to the substance identified by infrared analysis, and one with a substantially indistinguishable IR spectrum.

A literature search on diethylene glycol dibenzoate reveals it to be a clear liquid with chemically stable properties and a very high boiling point. It is slightly soluble in water and very soluble in polymers. It is used as a plasticizer for PVA homopolymer and copolymer emulsions, due to its excellent compatibility with polyvinylacetates and polyvinyl chloride. It is also used for PVC coatings, food packaging adhesives and paints. It can be used as a plasticizer in the cosmetics industry. There may be regulatory issues regarding these uses and the disposal of materials containing this material because of its apparent toxicity as indicated by testing on rodents.

In further analysis the TG-IR showed that between 300 and 450 °C the polymer in the sample decomposes releasing acetic acid, as shown in the graph below; the polymer in the sample is therefore very likely polyvinyl acetate:

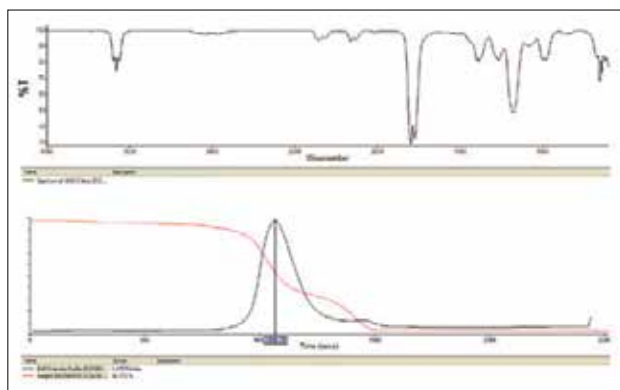


Figure 8. The IR spectrum (upper plot) taken at the peak rate of weight loss (lower plot) of the first stage of the decomposition of the polymer substrate of the analyzed film.

Summary

The use of "hyphenated techniques", TG-IR and TG-GC-MS, which link separation and identification instrumentation, together with search software and established research data bases has enabled an unknown aqueous mixture to be effectively analyzed and its components identified.

Differential Scanning Calorimetry

Authors

Wunpen Chonkaew^{a,b}, Peyman Dehkordi^c
 Kevin P. Menard^d, Witold Brostow^b, Noah Menard^b
 Osman Gencel^{b,e}

^a Department of Chemistry, Faculty of Science,
 King Mongkut's University of Technology Thonburi,
 Bangkok, Thailand

^b Laboratory of Advanced Polymers & Optimized
 Materials (LAPOM), Department of Materials Science
 and Engineering and Center for Advanced Research
 and Technology (CART), University of North Texas,
 Denton TX, USA

^c Digital Light Labs, Knoxville, TN, USA

^d PerkinElmer, Inc., Shelton, CT USA

^e Department of Civil Engineering, Faculty of
 Engineering, Bartın University, Turkey



Photo Differential Scanning Calorimetry, UV-Thermal Mechanical Analysis and UV-Dynamic Mechanical Analysis of Light Cured Acrylics

Abstract

Polymers and composites cured by ultraviolet (UV) light exhibit similar shrinkage on curing as those cured by heat, with the associated distortion in the product shape. We report results pertaining to effects of light intensity and temperature on properties of the cured materials. UV differential scanning calorimetry (UV-DSC) and UV dynamic mechanical analysis (UV-DMA) were performed. The degree of distortion was measured by the displacement of the static probe position in the DMA.

The results are represented as Time-Intensity-

Transition (TIT) diagrams and as 3D plots of intensity, temperature and time. The largest distortion is seen when high intensity light is used to cure the sample through the gelation point. Curing the sample using low intensity light until gelation, then completing the cure at higher intensities results in minimal distortions.

Introduction

Network polymers have a very wide range of applications.¹ Network formation is variously called crosslinking, curing, or vulcanization in the case of natural rubber. The term curing will be used in this article. The curing of epoxies,^{2,3,4,5,6,7} other thermosets as well as thermoset-based composites^{8,9,10,11} is most often performed by providing heat – a procedure called thermal curing. Another option is photocuring. It is also called light curing or optical curing and consists in application of irradiation; ultra violet (UV) light is used often but sometimes an electron beam or gamma radiation¹² is used instead. In both types of curing processes, either bulk materials or else films and coatings can be cured. Photo-initiated systems have several advantages: short curing times, low amounts of volatile organic compounds (VOCs) and relative ease of application.¹³

One problem with both photo-cured and thermally cured materials is that curing cause shrinkage in samples.¹⁴ The shrinkage can be as much as 6% by volume in aerospace composites. In photo-cured materials shrinkage leads to a significantly higher amount of residual stresses, misshapen parts, and increased failures in use. Finding a remedy is complicated by several factors. Curing is function of temperature and time; there is an equation representing effects of both.¹⁵ At the fundamental level, the progress of curing depends on the functional groups present.¹⁶ During curing two distinct phenomena occur, gelation and vitrification.^{17,18,19} These two phenomena can be separated but such separation requires application of two different techniques¹⁹ namely temperature modulated differential scanning calorimetry (TMDSC) and dynamic mechanical analysis (DMA).

In this situation we have decided to investigate whether the shrinkage during photo curing can be mitigated. A commercial obturation resin used in dentistry was the material studied. As already noted, DSC and DMA are the techniques used often to characterize progress of curing^{14,19,20,21,22} and we have used them. These techniques have been described in some detail by Lucas and her colleagues²³, by Gedde²⁴, by one of us^{25,26} and DSC also by Saiter and coworkers.²⁷

Experimental

The material used was a commercial dental resin used for filling cavities. Donated to us by the University of Colorado Dental School, the material consists of a N,N-dimethylaminoethyl methacrylate and bis-glycidyl methacrylate in a mixture of 60% and 40% by weight. No silicate fillers were present. This represents a fairly standard composition for dental obturation materials.

The PerkinElmer Diamond DSC was used with N₂ purge and recirculation cooling (-20 °C). One of the advantages of power compensation DSC is that it controls temperature

and measures energy. This means temperature spikes seen in sometimes in heat flux DSC do not happen when using this particular apparatus with adequate cooling as the instrument controls sample temperature. The modified DSC was fitted with a specialized lid to allow the light source to reach the material tested. The UV energy used in the DSC was measured and calibrated using graphite targets.²⁰ Samples for DSC experiments were weighted before and after runs, showing little to no weight loss across the run. For the optically curing system used here, weight loss was about 0.05% in the worst case. Results from DSC runs were used to measure the energy of cure, the activation energy of the curing reaction and the glass transition temperature T_g of cured samples. Details of this approach may be found in Gabbott.²⁸

The PerkinElmer DMA 8000 with the LN2 cooling attachment was used to test mechanical properties and to track deformation. Distortion of the samples was measured in the DMA by tracking the static position of the probe; see Figure 1. The T_g as well as progress of curing of samples were evaluated by DMA. Since UV light generates heat, cooling during DMA testing is especially necessary so that temperature remains fairly constant during the run. Without effective cooling, temperature spikes can give the impression in the DMA results that a modulus change has occurred. Cooling with liquid nitrogen has been found by us to provide sufficient control to prevent said abnormalities within the data and no temperature drift was seen in DMA samples. The LN2 cooling attachment is controlled by the DMA firmware and maintains sample temperature by adjusting the flow rate of LN2. We recall that in DMA a sinusoidal stress σ is applied as a function of time t :

$$\sigma(t) = \sigma_0 \sin(2\pi\nu t) \quad (1)$$

Here ν is the frequency in Hertz = cycles/s. The result of imposition of the sinusoidal load results in the following behavior of the strain ϵ :

$$\epsilon(t) = \epsilon_0 \sin(2\pi\nu t - \delta) \quad (2)$$

The results provide us the storage modulus E' representing the elastic (solid-like) behavior and the loss modulus E'' representing the viscous flow (liquid-like) behavior.^{23,24,25,26} Sometimes one works also with $\tan \delta = E''/E'$.

Samples were prepared by coating the material on paper backing and then run in single cantilever geometry. A LED curing unit from Digital Light Labs, Knoxville, TN was used with 365 nm LED source. Light was applied to the samples under temperatures of 25, 37.5, and 50 °C, for times ranging from 10 to 30 minutes, and at intensities of 40 to 110 W/cm². Light intensity was measured in the DMA using a radiometer to calibrate for intensity. More information on the curing of photo-initiated materials in DMA can be found in the references.²⁶

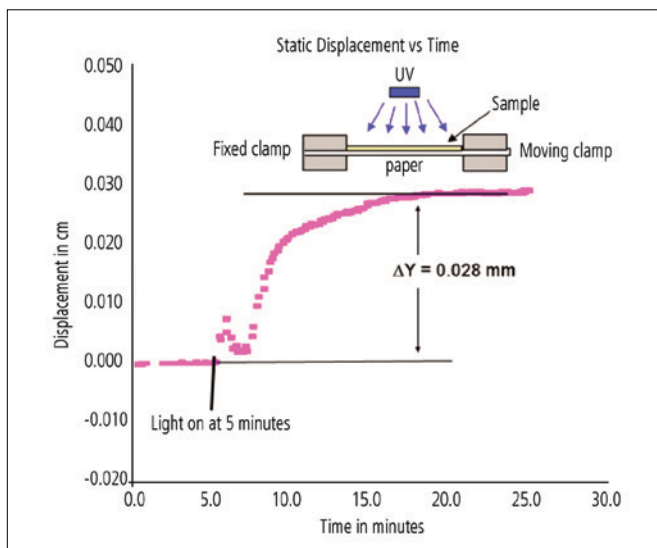


Figure 1. Determination of sample distortion by DMA under UV irradiation, showing the change in sample size as measured by the static position of the DMA probe. Work was performed at 25 °C and 365 nm.

Following standard experimental design protocols,²⁹ we used a factorial design to define the conditions run in the experiment to characterize both the amount of cure and the degree of distortion as functions of the light intensity, exposure time, and temperature used. This approach allowed us to minimize the number of experiments used to characterize the material. Experiment conditions are reported in Table 1, in the first three columns. These values can be graphic envisioned as the points shown in Figure 2. A commercial software package, Design-Ease, was used to analyze the results (Stat-ease Software, Minneapolis, MN).

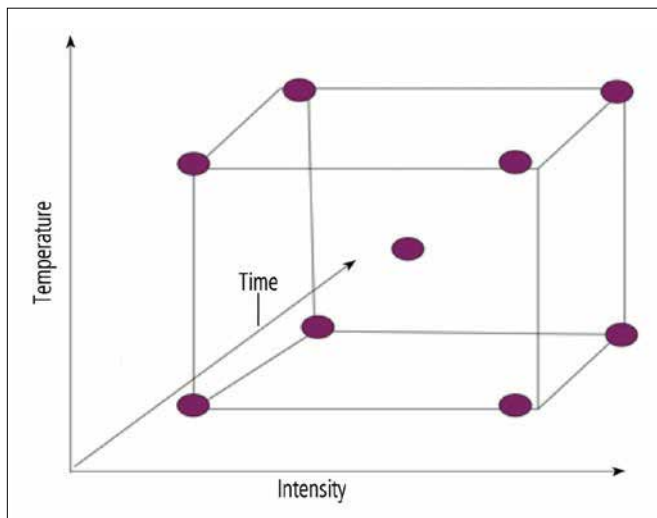


Figure 2. Graphical representation of the factorial design used. This design is referred to as a 2³ centered factorial design, the boundary points of the region of interest are measured as is the center point of the experimental conditions.²⁹

Results and discussion

Analyzing the results, we need to remember that most materials reach functional mechanical strength at less than 100% cure.³⁰ In most cases, reaching a value above the T_g^c (Critical Glass transition value where the material begins to act as a high polymer) gains sufficient strength for most uses. However, it is important to remember other physical properties do not always track strength.³¹ Hence the relationship of degree of cure to a particular property will need to be determined for the system of interest.

Examples of the data obtained from DSC and DMA are shown in Figures 3 and 4, respectively. The enthalpy change is used to calculate the degree of cure by dividing a given value during the process by the value for complete cure.²⁸ This gives the amount of uncured material.

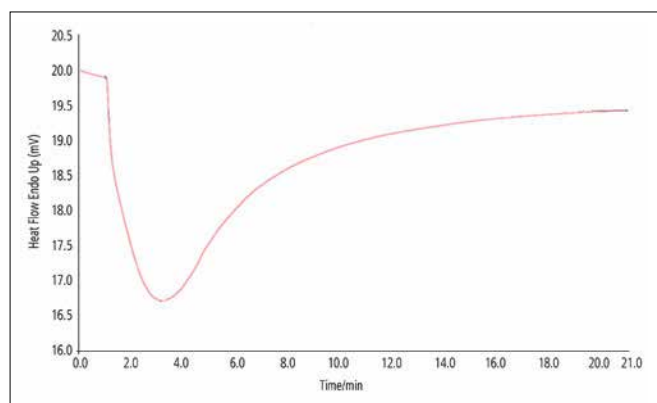


Figure 3. DSC results from a typical photocure experiment. The DSC data was used to calculate the residual cure by measuring the enthalpy of the exothermic reaction and comparing to the known value for 100% curing. In this instance, it was cured at 365 nm and at 25 °C.

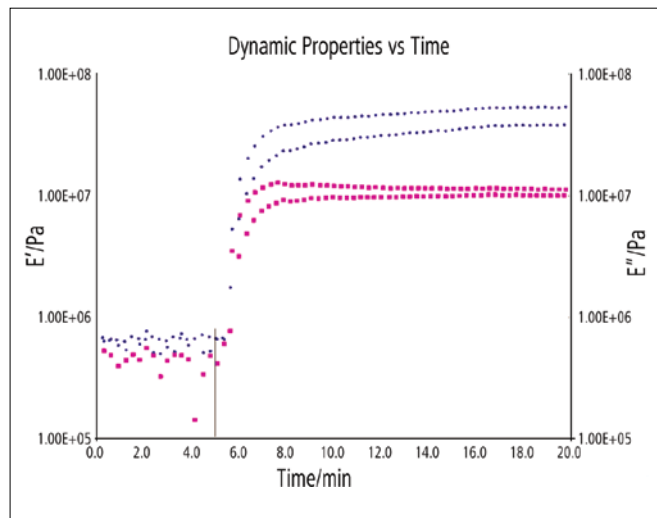


Figure 4. DMA results from a typical photocure experiment at 25 °C and 365 nm. The mark at 5.0 minutes indicates the initialization of the light. The results were used to calculate the temperature of gelification t_{gel} , the temperature of vitrification t_{vit} and the distortion of the sample. Small dots represent the storage modulus E' , filled squares represent the loss modulus E'' .

The method we use is easier than the volumetric method used in thermomechanical analysis (TMA) and can be applied in the same run as measuring gelation and vitrification temperatures. A variety of trials were undertaken, and we found that the gelation of the sample varied widely depending on the intensity of the light. With a high intensity of light there was significant distortion of the sample; as opposed to a low intensity of UV, where very little shrinkage of the sample occurred. The same occurred on the vitrification of the sample, but on a much higher order of magnitude. Since an initial high intensity of UV light causes a rapid deformation of the sample, we are able to conclude that both gelation and vitrification occur almost simultaneously at a high intensity. Gilham has developed time-temperature-transformation (TTT) diagrams³² for the process of curing.³³ Following his example, we have developed from our results time-intensity-transformation (TIT) relationships. Needless to say, intensity pertains here to UV light intensity in curing.

Since ultimately the goal is to minimize of distortion of the material as much as possible, we determined that the best method to use was low intensity UV light to photocure the sample at the beginning of the experiment, and then after to increase the UV light significantly in order to finish the vitrification of the sample. The results are also reported numerically in Table 1. Factorial design shown schematically in Figure 2 was used.

Table 1. Experimental conditions and results from factorial design experiments. Digital Light Labs, Knoxville, TN.

Temp. (°C)	Intensity (W/cm ²)	Time (min)	t _{gel} (min)	t _{vit} (min)	Delta Y (mm)	% Cure
25	110	30	0.1	11	0.019	95.4
50	110	30	0.1	10	0.016	96.3
25	40	30	0.4	14	0.003	89.1
50	40	30	0.4	13	0.004	90.3
50	40	10	0.4	13	0.004	90.8
25	40	10	0.5	15	0.003	90.1
25	110	10	0.1	15	0.013	96.7
50	110	10	0.1	10	0.015	97
37.5	75	20	0.3	12	0.006	94.6

First, from the results in Table 1 an intensity equivalent of the Gilhams-Enns or TTT diagram was generated as shown in Figure 5. This displays how the transitions in the material are affected by constant intensity at 25 °C. Note that at high intensities the gelation occurs almost instantly.

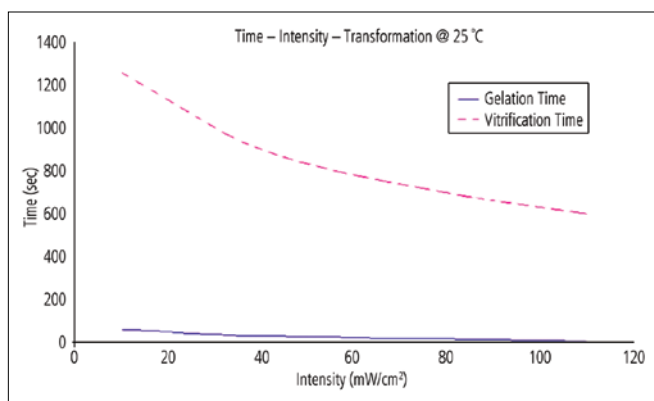


Figure 5. The Time-Intensity-Transformation Diagram showing how intensity and time interact to cause vitrification and gelation. This example is at 25 °C and 365 nm.

Then we have developed a cure profile to minimize distortion for reasonable curing times. Finally, the distortion was plotted as a function of temperature and light intensity (Figure 6). We find that temperature has little effect; the higher the intensity of the light, the greater distortion is seen in the material. Based on this, we tried low intensity light until gelation and then finishing the cure with higher intensity and found that such procedure minimized the changes in the sample shape. Finally, the distortion was plotted as a function of temperature and light intensity (Figure 6). In the case of these materials, the response surface is smooth and well behaved.

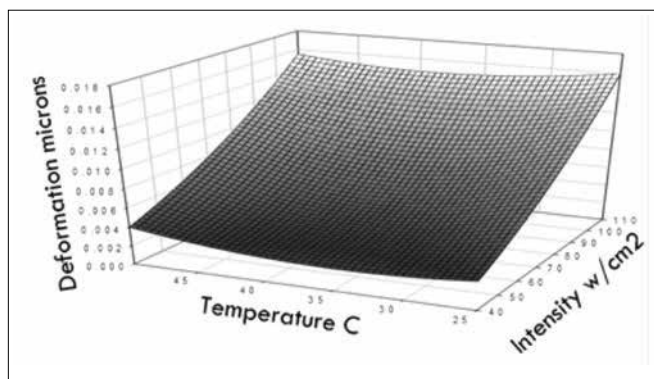


Figure 6. A response surface mapping showing the distortion of the sample (Z) as function of intensity (X) and temperature (Y). Shading represents similar distortion values with the darkest shades indicating the least distortion.

The results displayed in Figure 6 show that temperature has only little effect on sample distortion. This can be summarized as the higher the intensity of the light, the greater distortion is seen in the material. Based on this, we have tried low intensity light until gelation and then finishing the cure with higher intensity; this procedure minimized the changes in the sample shape.

Conclusions

The use of an experimental design approach to the characterization of a light cured acrylic resin has promise for allowing characterization of the shrinkage, curing time, time to gelation, and time to vitrification to be obtained from one sequence of experiments. Interestingly, the greatest driver for distortion was the intensity of the light, indicating the initial network formation is vital to controlling this. By utilizing a variation of the Gillham diagram and response surfaces, it is possible to determine the best conditions for a minimally distorted product from a UV driven cure.

With this new approach of analysis including photo-differential scanning calorimeter, UV-thermomechanical analysis, and UV-dynamic mechanical analysis, it was possible to find which parameter had the greatest effect on the curing of acrylic resins. We believe that our findings will be generally applicable for other light curing materials.

Acknowledgements

We would like to thank Digital Light Labs of Knoxville, TN for the loan of the UV LED light source, PerkinElmer, Inc. of Shelton, CT for the use of the DSC and DMA, and Dr. Jeffery Stansbury of U. Colorado Denver's Dental School for the resin studied.

References

1. J.E. Mark and B. Erman, in 'Performance of Plastics', (ed. W. Brostow), Chap. 17; Munich/Cincinnati, OH, Hanser (2000).
2. B. Bilyeu, W. Brostow and K.P. Menard, *J. Mater. Ed.* **21**, 281 (1999).
3. L. Bazyliak, M. Bratychak and W. Brostow, *Mater. Res. Innovat.* **3**, 132 (1999).
4. B. Bilyeu, W. Brostow and K.P. Menard, *J. Mater. Ed.* **22**, 107 (2001).
5. B. Bilyeu, W. Brostow and K.P. Menard, *J. Mater. Ed.* **23**, 189 (2002).
6. I.M. Kalogeras, M. Roussos, I. Christiakis, A. Spanoudaki, D. Pietkiewicz, W. Brostow and A. Vassilikou-Dova, *J. Non-Cryst. Solids* **351**, 2728 (2005).
7. I.M. Kalogeras, A. Vassilikou-Dova, I. Christakis, D. Pietkiewicz and W. Brostow, *Macromol. Chem. & Phys.* **207**, 879 (2006).
8. E. Pisanova and S. Zhandarov, in 'Performance of plastics', (ed. W. Brostow), Chap. 19; Munich/Cincinnati, OH, Hanser (2000).
9. P. Panchaipetch, V. Ambrogi, M. Giamberini, C. Carfagna, W. Brostow and N.A. D'Souza, *Polymer* **42**, 2067 (2001).
10. P. Panchaipetch, A.E. Akinay, W. Brostow, N.A. D'Souza and J. Reed, *Polymer Composites*, **22**, 32 (2001).
11. K. Pingkarawat, C.H. Whang, R.J. Varley and A.P. Mouritz, *J. Mater. Sci.* **47**, 4449 (2012).
12. S. Alessi, A. Parlato, C. Dispenza, M. De Maria and G. Spadaro, *Radn. Phys. & Chem.* **76**, 1347 (2007).
13. J. Koleske, *Radiation Curing of Coatings*, Chap 1, West Conshohocken, PA, ASTM®, (2002).
14. B. Bilyeu, W. Brostow and K.P. Menard, *Polimery* **46**, 799 (2001).
15. W. Brostow and N.M. Glass, *Mater. Res. Innovat.* **7**, 125 (2003).
16. M. Bratychak, W. Brostow, V.M. Castaño, V. Donchak and H. Gargai, *Mater. Res. Innovat.* **6**, 153 (2002).
17. C. Schick, J. Dobberth, M. Potter, H. Dehne, A. Hensel, A. Wurm, A. M. Ghoneim and S. Weyer, *J. Thermal Analysis*, **49**, 499 (1997).
18. G. VanAssche, A. Van Hemelrijck, H. Rahler and B. Van Mele, *Thermochim. Acta* **317**, 041505 (1997).
19. B. Bilyeu, W. Brostow and K.P. Menard, *Polymer Composites* **23**, 1111 (2002).
20. PerkinElmer Service Bulletin ACCY-01-022A, PerkinElmer, Inc., Shelton, CT (2005).
21. B. Bilyeu, W. Brostow and K.P. Menard, *J. ASTM® Internat.* **2** (10), 1 (2005).
22. B. Bilyeu, W. Brostow and K.P. Menard, *Mater. Res. Innovat.* **10**, 110 (2006).
23. E.F. Lucas, B.G. Soares and E. Monteiro, *Caracterização de polimeros*, Rio de Janeiro, e-Papers (2001).
24. U.W. Gedde, *Polymer Physics*, Dordrecht-Boston, Springer – Kluwer (2001).
25. K.P. Menard, in 'Performance of plastics', (ed. W. Brostow), Chap. 8; Munich – Cincinnati, Hanser (2000).
26. K.P. Menard, *Dynamic Mechanical Analysis*, 2nd ed. Boca Raton, FL, CRC Press (2008).
27. J.-M. Saiter, M. Negahban, P. dos Santos Claro, P. Delabare and M.-R. Garda, *J. Mater. Ed.* **30**, 51 (2008).

28. P. Gabbott, in Principles and Applications of Thermal Analysis, (ed. P. Gabbott), Chap 1, Oxford, UK, Blackwell Publishing, (2008).
29. G. Box, W. Hunter, and J. Hunter, Statistics for Experimenters, New York, NY, John Wiley and Sons, (1974)
30. L. Sperling, Introduction to Physical Polymer Science, New York, NY, Wiley, (1994)
31. R. Seymour and C. Carrahers, Structure Property Relationships in Polymers, New York, Plenum Press, (1984)
32. J. K. Gillham, AIChE Journal, **20**, 1066 (1974).
33. J. Gillham, Polymer Engineering And Science, **26**(20), 1429, (1986).

PerkinElmer, Inc.
940 Winter Street
Waltham, MA 02451 USA
P: (800) 762-4000 or
(+1) 203-925-4602
www.perkinelmer.com



For a complete listing of our global offices, visit www.perkinelmer.com/ContactUs

Copyright ©2012, PerkinElmer, Inc. All rights reserved. PerkinElmer® is a registered trademark of PerkinElmer, Inc. All other trademarks are the property of their respective owners.

Differential Scanning Calorimetry

Author

Tiffany Kang

PerkinElmer, Inc.
Shelton, CT USA

Curing of an Optical Adhesive by UV Irradiation in the DSC 8000

Introduction

Optical adhesives are used in many industries where solvents are undesirable. Semiconductors and chip manufacturers for example can not afford solvents depositing on components. Photo-DSC allows fast analysis of the curing profile and measurement of the energy of the curing reactions. Because photo-initiated reactions are fast and energetic, good temperature control and responsiveness are needed to get good data. Power compensated instruments are the best choice for these applications

Experimental

A specialized DSC pan with a quartz cover can be used although an open pan often is acceptable. The sample is heated or cooled to the isothermal temperature and allowed to equilibrate. Pyris™ software allows triggering the shutter of the light source to open and close for irradiation of the sample. Data can be collected at various intensities and times to develop the best cure cycle for the material.



Figure 1. **DSC 8000.** The DSC's high sensitivity and excellent temperature control makes it ideally for demanding applications like photo curing studies.

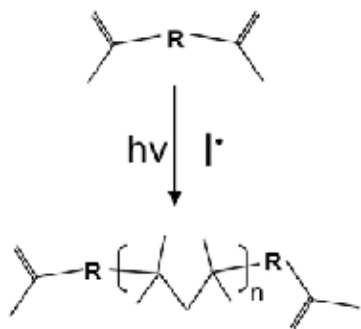


Figure 2. UV curing materials are commonly used as adhesives. UV light generates a free radical which causes the cure.

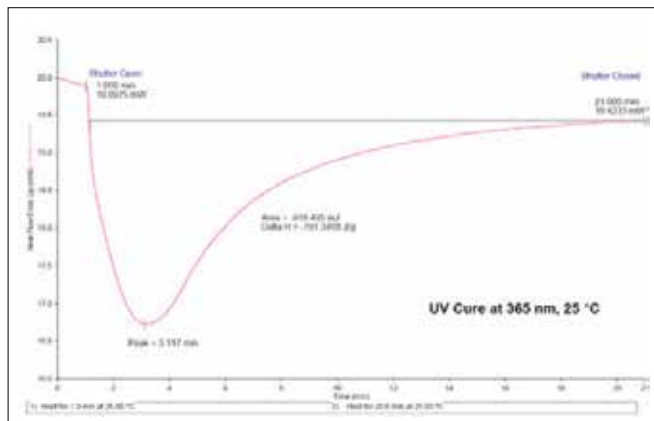


Figure 3. DSC results from the UV driven cure of an adhesive. Light turned on at 3 minutes (red line marked shutter open) for 30 seconds.

The DSC 8000 (Figure 1) is the ideal choice for these studies because the power compensated design allows the instrument to quickly detect and respond to the optical material. The design allows us to maintain a true isothermal through the cure so the sample temperature does not increase. All of the recorded energy therefore comes from the reaction shown in Figure 2.

Results

When the UV source is triggered, the sample is exposed to the UV light. A curing exotherm develops as the material undergoes polymerization. The energy in this peak can be used to calculate the kinetics of the curing process. Figure 3 shows an example of this. When the light is applied at 3 minutes for 30 seconds, an exothermic reaction occurs as the material crosslinks and forms a solid. Since the material is its own solvent, no volatiles are lost and contamination of the circuit board is minimized. Looking at the thermogram, one sees the maximum of the exotherm occurs very quickly after applying the light, emphasizing the need for fast response. The energy of the reaction is calculated from the area under the peak, which is why the ability to compensate for the heat coming from the UV lamp is important.

Depending on the material, the exposure can be varied in terms of time as well as the number of exposures. Light frequency and intensity can be varied using filters on the UV source. As UV sources generate heat, the DSC's temperature control must be able to compensate for the energy from the lamp.

Conclusion

Photo-DSC is a powerful tool for studying and characterizing optically curing materials. For more information go to <http://www.perkinelmer.com>.

Hyphenated Technology

Author:

Hua Cheng

PerkinElmer, Inc.
Shanghai, China

In-situ Evolved Gas Analysis During the 3D Printing Procedure

zero residual feedstock^{1,2,3}. The invention and development of low-cost desktop printers has made this technology widely acceptable for applications both in industry and home⁴. Normally, thermoplastic materials are utilized as the raw material of 3D printers, while more advanced and sophisticated prototype uses the precursor of thermoset materials (or a prepreg) as the feedstock sources. Due to the reaction nature of the precursor, various unpleasant gases would emit during the printing procedure which may include regulation prohibited chemicals from time to time.

PerkinElmer can provide effective hyphenated solutions to in-situ study the chemical nature of evolved gases during the 3D printing. At the same time, since the TGA 8000™ can cover the temperature range up to 1200 °C, we may also count on the TG-GC/MS platform to reverse-engineer target products regardless of a fully cured product or an additive included prepreg.

Introduction

Three-dimensional (3D) printing technology has received tremendous interests due to its capability of generating complex-shaped structures, unparalleled high efficiency and

Experimental

The study utilized the TG-GC/MS hyphenated module to obtain accurate thermal decomposition data with subsequent identification of the evolved breakdown products.

The TGA 8000 was programmed for a linear temperature range from room temperature to 800 °C with a sweep rate of 20 °C/min. High purity helium (45 mL/min) was used to purge the whole system and to transfer the breakdown products to the GC/MS.

The online mode and the separation mode are both applied to monitor the molecule debris, Total Ion Chromatogram (TIC) 15~500 amu with SIR at 44 amu and 94 amu.

Maintain the temperature of lines and adaptors at 280 °C, with a pumping rate of 30 mL/min the TL9000 sampling split ratio is 1.:1.5.

Table 1. Gas Chromatograph method parameters.

Gas Chromatograph		Clarus 680 GC	
GC Column	Elite-5 MS 30 m × 0.25 mm × 0.25 μm		
Injector Type	TL-9000		
Injector Temperature	280 °C		
Injector Liner	TL-9000		
Carrier Gas	Helium		
Split Flow	None		
Transfer Line Program			
	Online Mode GC Oven Program		
GC Oven Program	Set Point	Hold Time	
Isothermal	280 °C	40 min	
	Separation Mode GC Oven Program		
GC Oven Program	Set Point	Hold Time	
Initial	35 °C	3 min	
10 °C/min	290 °C	3 min	

Table 2. Mass Spectrometer method parameters.

Mass Spectrometer:		Clarus 680 GC	
Inlet Line Temperature	280 °C		
Source Temperature	280 °C		
Scan Conditions			
Mass Range	15 – 500 m/z		
Scan Duration	0.10 sec		
Run Time	30 min		

Results

A sample of (26.264 mg) printing stock was heated as shown in Figure 1.

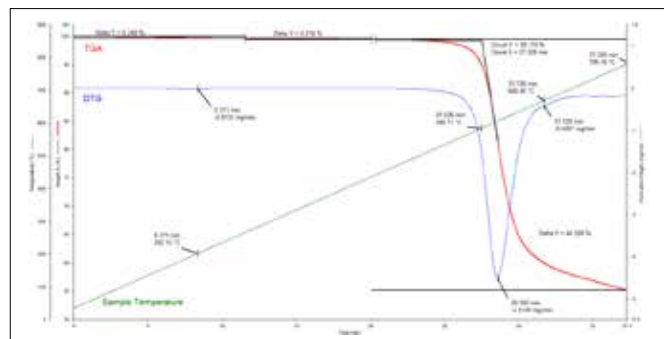


Figure 1. Initial polymer pyrolysis.

Three weight loss steps can be observed from the obtained curve. The polymer system starts to pyrolysis at 585.17 °C with a total weight loss of around 44.268%. There are two small steps existing within the low temperature range which might be the origin of the unpleasant gas during the 3D printing procedure.

The initial mass spectrometry (Figure 2) of the evolved gas at 29.856 min (approximately 630 °C) shows the presence of aromatic compounds with further separation by chromatography required to correctly identify which aromatic compounds and to separate the aromatics from other thermal breakdown compounds that are evolved at the same temperature.

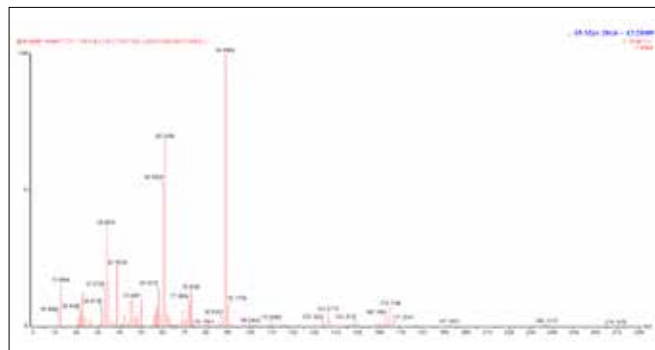


Figure 2. Total spectra at 29.856 minutes.

In order to understand the rough distribution of the evolved mixing gas debris, the online TGA-MS mode is applied firstly. As shown in Figure 3, the primary MS signals reach peaks at 315 °C and 605 °C respectively. Based on this fact, we will focus our attention on these two points using the separation mode.

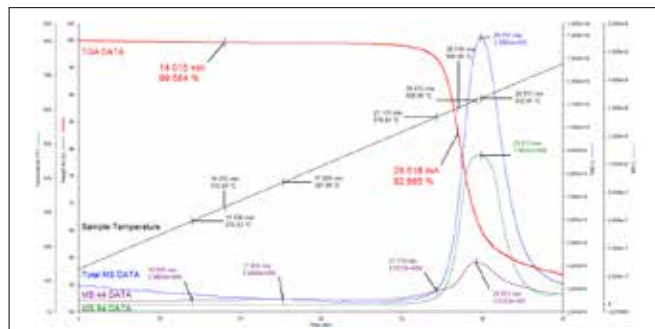


Figure 3. MS data in relation to the thermal program demonstrating the evolved components.

In order to qualitatively study the unpleasant gas evolved during the 3D printing procedure, we've collected 80~100 μL of evolved gas at 315 °C and injected it into the GC column to fully study its components using the method described in Table 1. As can be seen in the obtained chromatogram (Figure 4), there are many degradation components that can be identified to discern the polymer engineering.

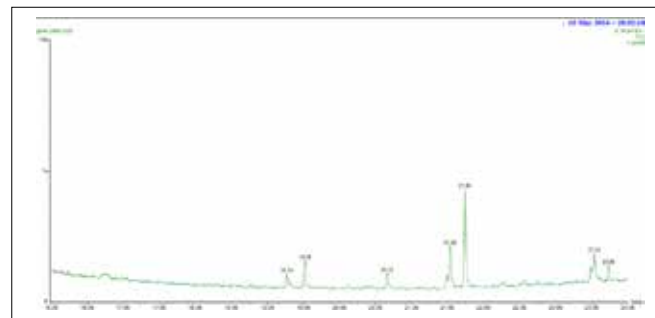


Figure 4. Separated breakdown products at 315 °C for analysis.

Analysis of the peaks evolved at 315 °C tentatively identified the peaks to consist of linear hydrocarbons terminated with a triple bonded nitrogen atom such as Figure 5.

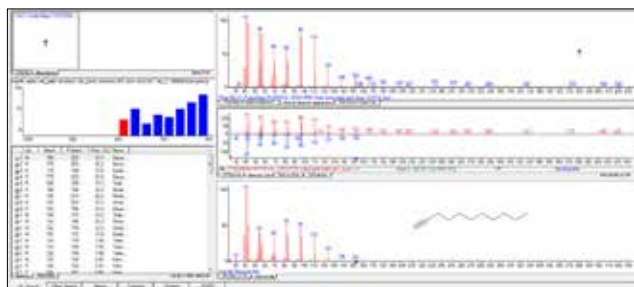


Figure 5. Linear hydrocarbon breakdown product generated at 315 °C.

A similar 80~100 µL evolved gas at 605 °C was injected and analysed in the same manner with the chromatogram shown in Figure 6.

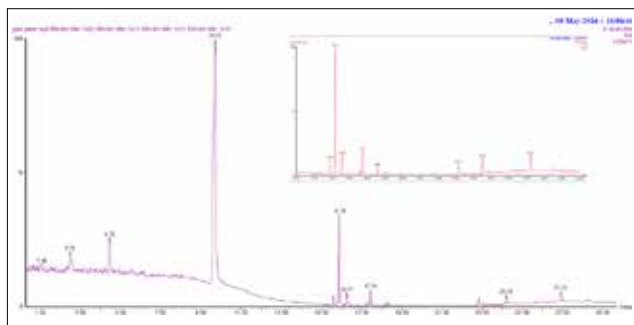


Figure 6. Separation of evolved components at 605 °C.

Analysis of the evolved gases at 605 °C identified many aromatic structures such as shown in Figures 7 and 8.

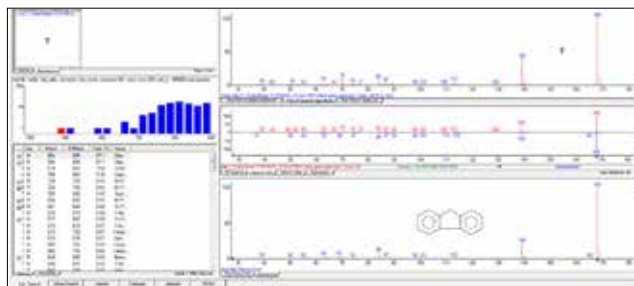


Figure 7. Evolved product of thermal degradation at a retention time of 17.74 minutes.

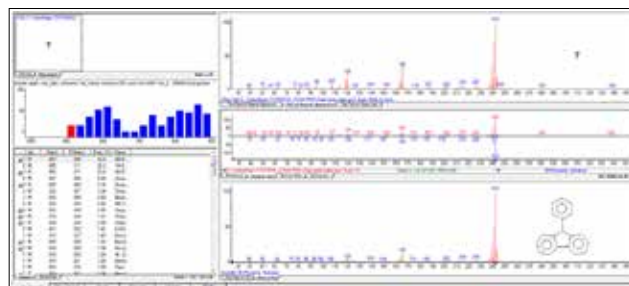


Figure 8. Evolved product of thermal degradation at a retention time of 24.50 minutes.

Conclusion

The 3D-printed polymer starts to degrade at 585.17 °C under helium atmosphere. It gives us a hint that this polymer should belong to the high performance engineering polymer category;

The primary pyrolytic products are phenol, biphenyl derivative and other aromatic derivatives, this is the characteristic fingerprints of aramid group polymers (such as Kevlar or Nomex);

The evolved "unpleasant gas" during the 3D printing procedure are mostly azoic compounds as revealed by the TG-GC/MS data, and they are most likely used as the initiator of the chain extension reaction.

References

1. Mohammad Vaezi, Hermann Seitz, Shoufeng Yang, A review on 3D micro-additive manufacturing technologies, *Int. J. Adv. Manuf. Technol.*, 2013, 67: 1721.
2. Brent Stephens, Parham Azimi, Zeineb El Orch, Tiffanie Ramos, Ultrafine particle emissions from desktop 3D printers, *Atmos. Environ.*, 2013, 79: 334.
3. J.M. Taboas, R.D. Maddox, P.H. Krebsbach, S.J. Hollister, Indirect solid free form fabrication of local and global porous, biomimetic and composite 3D polymer-ceramic scaffolds, *Biomater.*, 2003, 24: 181.
4. Matt Zarek, Michael Layani, Ido Cooperstein, Ela Sachyani, Daniel Cohn, Shlomo Magdassi, 3D printing of shape memory polymers for flexible electronic devices, *Adv. Mater.*, 2015, 28: 4449.



Hyphenated Technology

Authors:

Jia Yi Ling

PerkinElmer, Inc.
Selangor, Malaysia

Tiffany Kang

Joe Lee

PerkinElmer, Inc.
Taiwan

Detection of Additive Used in Gloves by TG-GC/MS Hyphenation System

The quality of gloves is associated with the raw materials used and its manufacturing processes. For this reason, understanding the various rubber additives and raw materials used and its application advantages has becoming very important.

Glove manufacturing processes begin by mixing latex with latex compounding ingredients which include sulfur, zinc oxide, accelerators, pigments, stabilizers, dewebbing agent and antioxidant. The mixture is then leave to cure, before it undergoes glove dipping, vulcanization, and leaching process that produce stretchable gloves.

Introduction

Producing consistently high quality gloves with minimum cost has always been the top mission for glove manufacturers.

One of the additives commonly used in glove manufacturing is dispersing agent, which keep solid particles in latex dispersion from agglomerating or joining with other particles to form a cluster¹. In this study, two glove samples formulated with and without dispersing agent are analyzed to see if a difference can be seen.



Figure 1. TG-GC/MS (Clarus SQ 8 GC/MS, TL8500, TGA 8000).

Experimental

The experiment was conducted using PerkinElmer TGA 8000™ hyphenated with Clarus® SQ 8 GC/MS. The hyphenation transfer line system used is TL-8500. A survey run was performed using TGA system to characterize the thermal degradation of dispersing agent.

The percent weight loss (TG) and derivative percent weight loss (DTG) curves of dispersing agent were plotted against temperature in Figure 2. As sample is in liquid form, the weight loss plot has shown immediate weight loss due to the drying or vaporization of volatile content of about 30% between room temperature to 200 °C. From the TG-DTG curves, it was determined that dispersing agent has shown greatest decomposition rate at approximately 455 °C, 28%/min.

Therefore, in subsequent runs, the evolved gas from each glove samples were analyzed at the same temperature region using TG-GC/MS hyphenation system. The setting of the experiment is shown in Table 1.

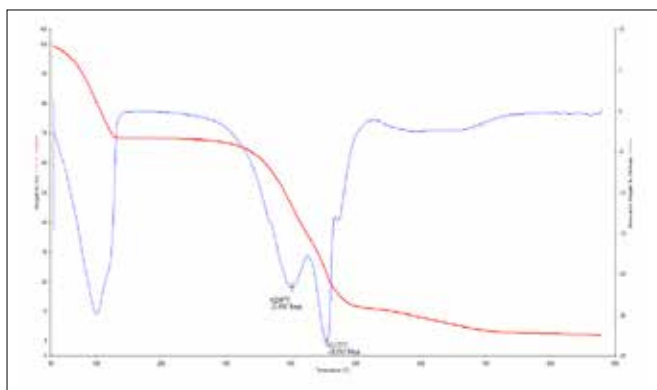


Figure 2. Dispersing agent survey run – Percent weight loss (in red) and derivative weight loss (in blue) curves versus temperature.

Table 1. Hyphenation system experimental setup.

TGA Program		
TGA 8000	Purge gas	Helium at 40 ml/min
	Temperature profile	Heat from 30 to 650 °C at 50 °C/min
	Sample size	10 ~ 15 mg
Transfer Line Program		
TL 8500	TL Temperature	280 °C
	Pump rate	70 mL/min
GC/MS Program		
Clarus 680 GC	GC column	Elite-5 MS, 30 m * 0.25 mm * 0.25 µm
SQ8 MS	Temperature profile	50 °C for 1 min, 10 °C/min to 300 °C, hold for 10 min
	Scan range	40-300 amu, SIR 44, SIR 54
	Ionization mode	EI, 70eV
	Ion source Temp	230 °C

Results

Glove samples A and B, one formulated with dispersing agent, another one without are analyzed. Figure 3 (a) and (b) showed the weight loss profile of both samples, with very similar trend at the temperature region of interest. A more sensitive instrument is in need to differentiate the two.

The evolved gas from each sample was analyzed by GC/MS to determine if hyphenation technique would confirm the presence or absence of trace amount of dispersing agent in glove samples. Figure 4 demonstrates the MS data obtained from the analysis of each sample.

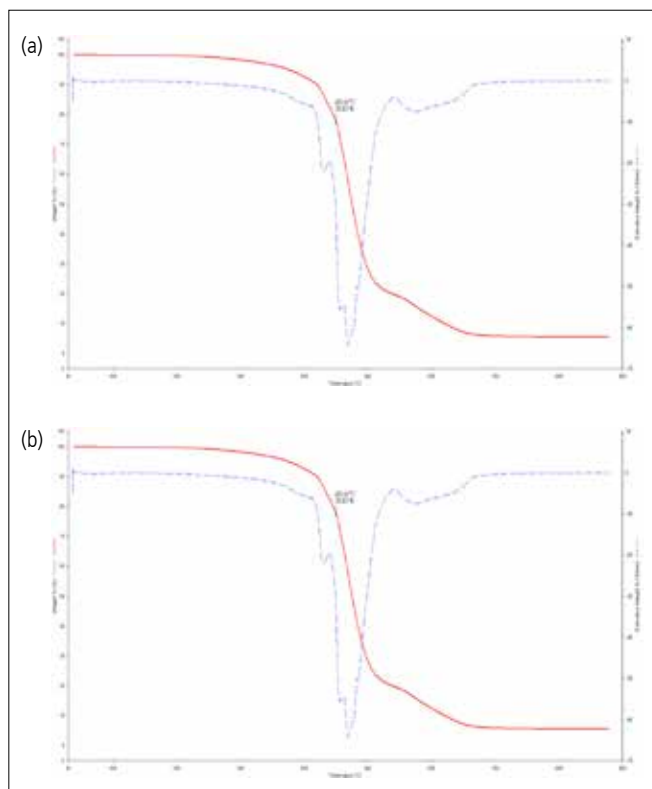


Figure 3. Weight loss profile of (a) Glove A and (b) Glove B.

It can be seen that the gas evolved are very complex, with major compounds detected at Retention Time (RT) between two to four minutes for both glove samples. However, it is not comparable to those eluted out from dispersive agent. This is because the major compounds detected in glove samples are mainly contributed by the decomposition of latex. As the content of dispersing agent used is very low, it becomes challenging to resolve the peaks coming from dispersing agent from those of latex gloves.

Hence, two other peaks detected between RT between 11 to 12 minutes in the TIC diagram of dispersing agent (Figure 5) were identified and used for further interpretation.

Figure 6 demonstrated three major mass to ion charge ratio (m/z) detected at RT 11.205 minute and 11.563 minute which are being monitored. Profile searching via MS software, has shown evidence of low levels of dispersing agent detected in Glove B, that is not seen in Glove A, refer to Figure 7.

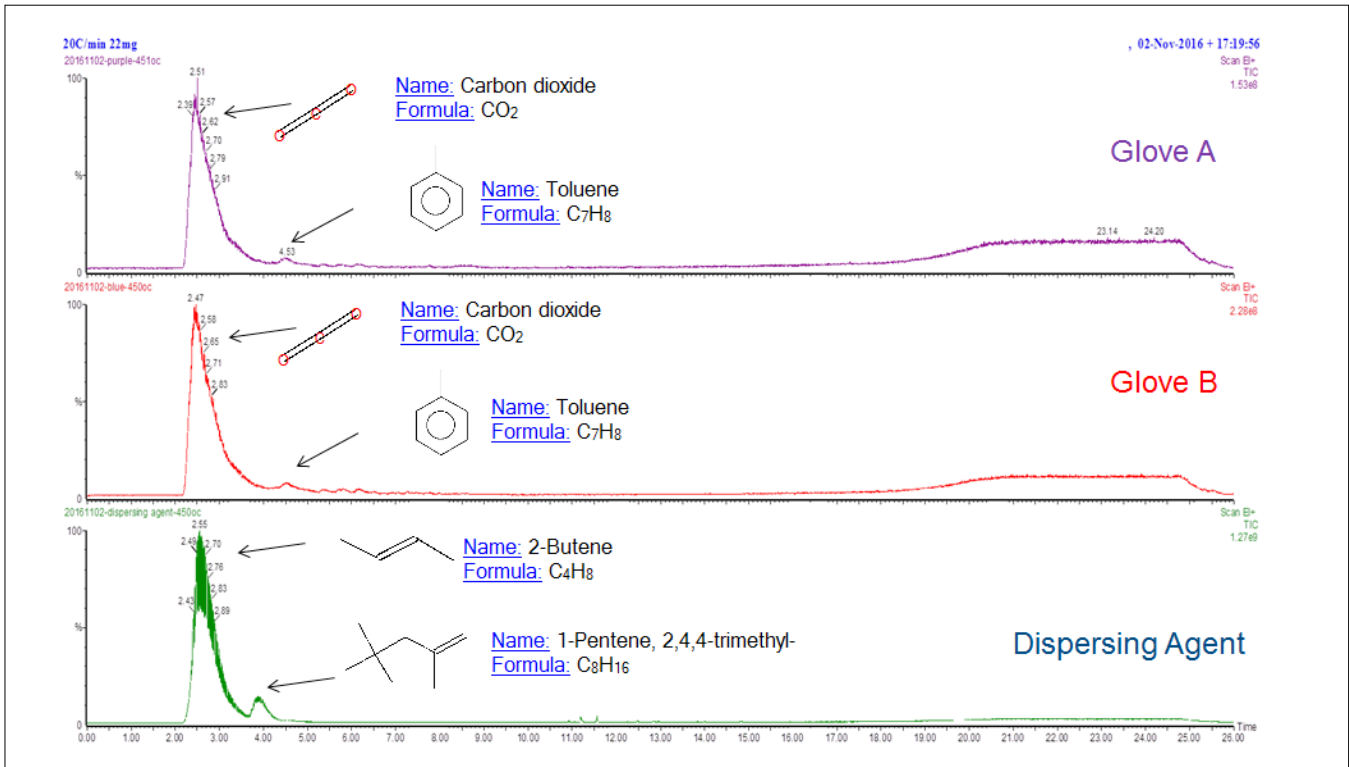


Figure 4. Comparison of GC/MS TIC Diagram of the evolved gas of Glove A, Glove B and dispersing agent injected at 450°C.

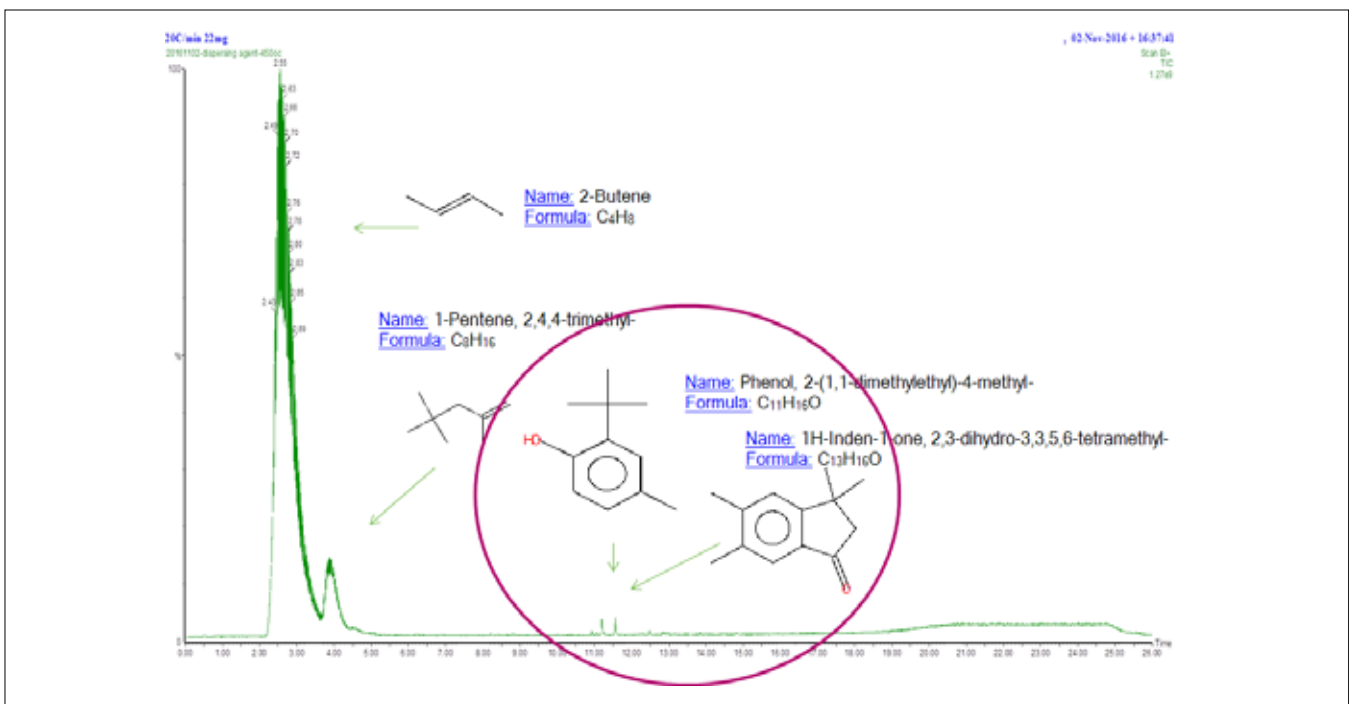


Figure 5. Dispersive Agent – GC/MS TIC Diagram after injection of evolved gas at 450°C.

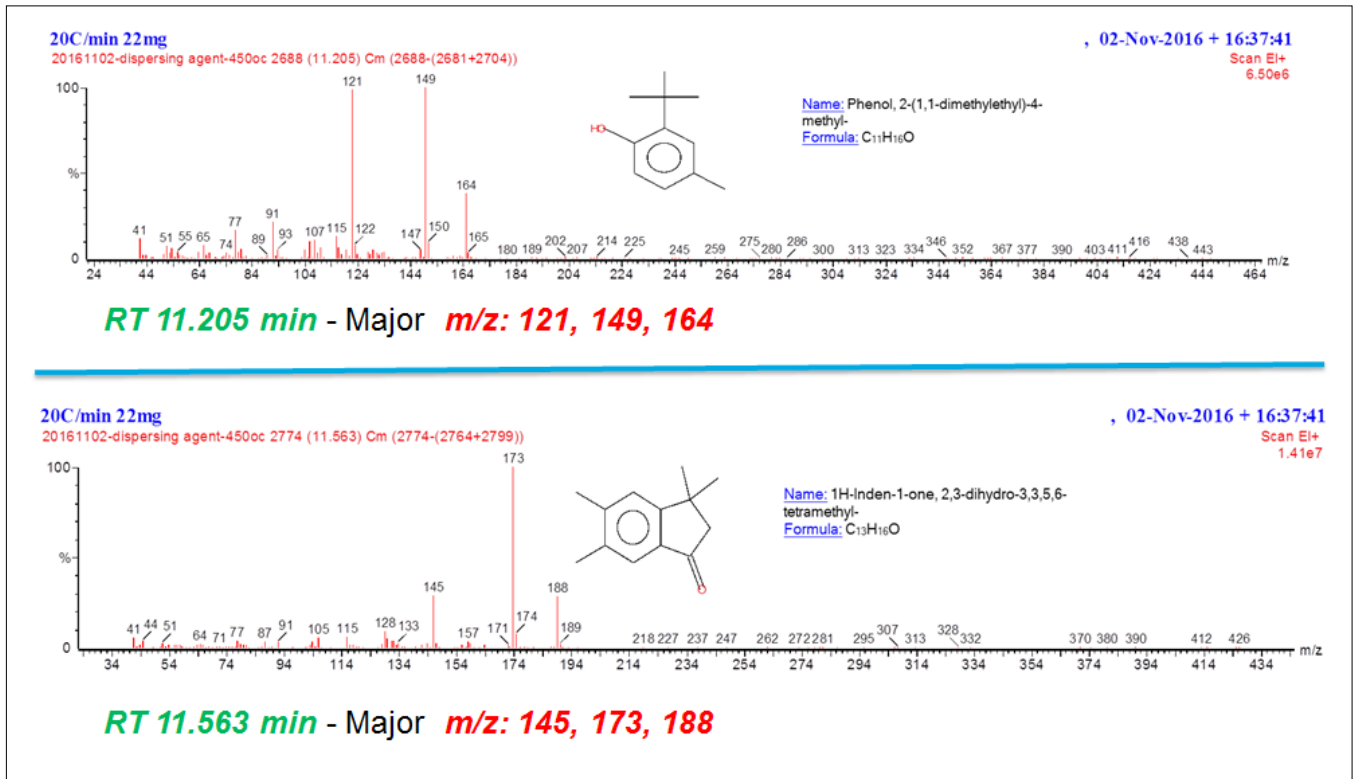


Figure 6. Dispersive Agent – Mass spectrum of selected peaks at RT 11.205 min and 11.563 min.

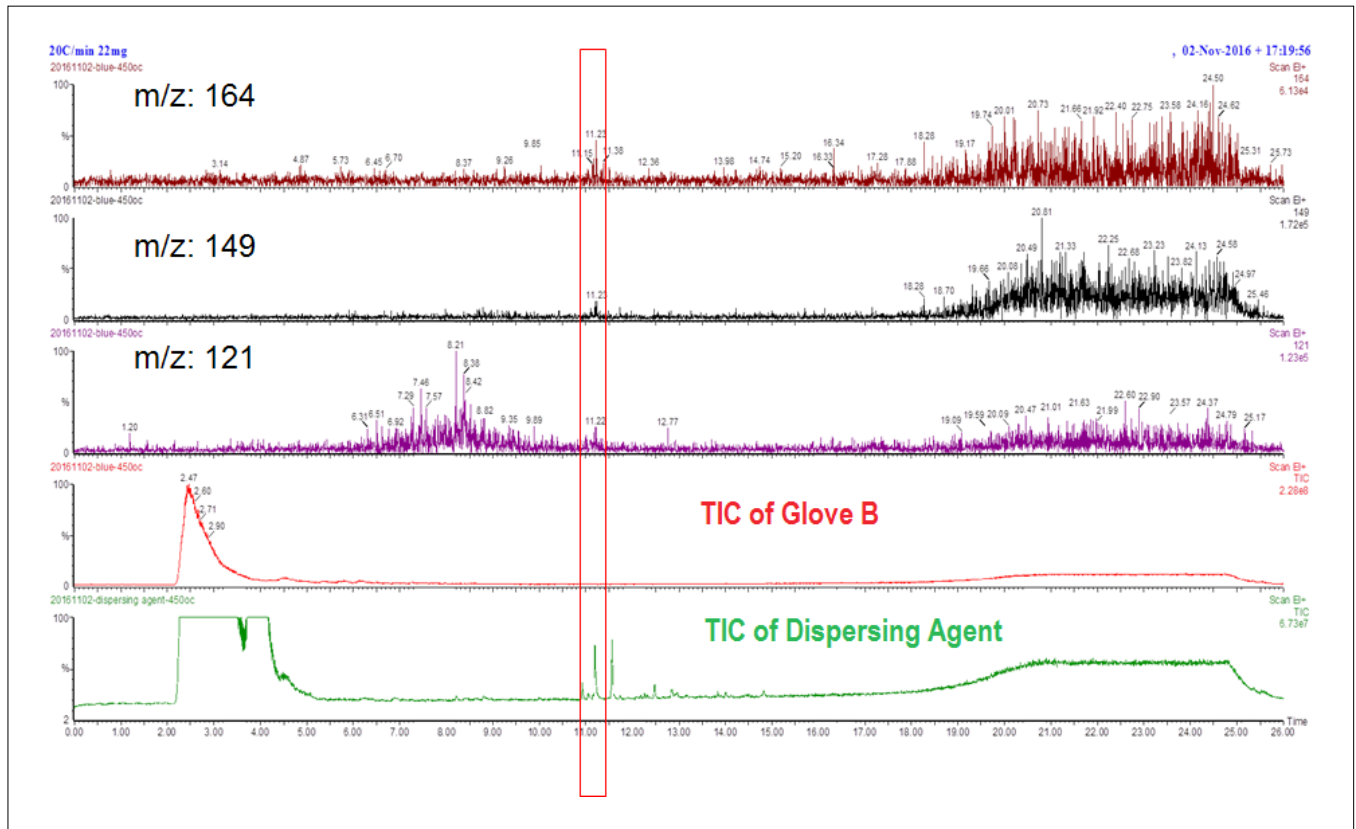


Figure 7. Blue glove – Peak monitoring at RT 11.205 min, m/z 121, 149 & 164, showing trace amount of dispersing agent detected.

Conclusions

TGA is a useful tool when it comes to compositional analysis as it allows quantification of weight loss of a material at targeted temperature region. By hyphenating TGA to a GC/MS system, further identification of evolved gases can be carried out.

In this case, TG-GC/MS hyphenation system successfully detect trace amount of additive used in glove manufacturing process. With minimum sample preparation, the TG-GC/MS serves as a

much faster approach when it comes to sample differentiation, at the same time allowing a more complete thermal characterization of material.

References

1. Vanderbilt Chemicals Product Information, Latex Glossary.

Thermogravimetric Analysis –
Mass Spectrometry

Evolved Gas Analysis: a High Sensitivity Study of a Solvent of Recrystallization in a Pharmaceutical

Typical applications of TG-MS include:

- Detection of moisture/solvent loss from a sample (e.g. loss on drying or dehydration of a pharmaceutical)
- Thermal stability (degradation) processes
- Study reactions (e.g. polymerizations)
- Analysis of trace volatiles in a sample (e.g. volatile organic compound (VOC) testing)

Introduction

Thermogravimetric analysis (TGA) of materials is commonly used to measure weight loss as a sample is heated or held isothermally. In the pharmaceutical industry, materials often show weight losses associated with the loss of solvent/water, desolvation or decomposition of the sample. This information is then used to assess the purity and stability of the material and its suitability for use. The TGA gives a quantitative measure of mass lost from the sample, but it does not provide information on the nature of the products that are lost from the sample, and this information is often required for complete characterization.

Coupling a mass spectrometer (MS) to a TGA allows evolved gases to be analyzed and identified giving this additional valuable information.

Instrumental Setup

All of the TGA systems supplied by PerkinElmer (Pyris™ 1 TGA, STA 6000 and TGA 4000) can be easily interfaced to MS systems. PerkinElmer can supply systems with either the PerkinElmer Clarus® MS or with a Hiden Analytical MS. In this study, a Pyris 1 TGA interfaced to a Hiden Analytical HPR-20 MS was used.



Figure 1. Pyris 1 TGA is shown interfaced to a HPR-20 MS (left) and a Clarus 600 MS (right).

The HPR-20 MS is optimized for the analysis of the evolved gases from the TGA and offers the following benefits:

- The ability to use either Faraday cup or secondary electron multiplier (SEM) detectors, depending on the sensitivity levels required. The SEM offers the ability to detect very low partial pressures of evolved gases below 10^{-8} bar, allowing identification of very low levels of contaminants. The system is able to operate in air, posing no issues for sample changing.
- Optional foreline and bypass vacuum pumping permits the most efficient pumping of helium which is normally used as a purge gas since it produces no interfering mass ions.
- A very flexible heated transfer line allows simple interfacing to the TGA systems. The lightweight heated line can be moved around in use without damage, making the system very robust. Gas transfer uses a wide-bore fused-silica capillary which gives 16 mL/min flow to the mass spectrometer for highest sensitivity.
- An anti-blockage filter has been added to catch high-molecular-weight material that might block the capillary. This single feature prevents hours of down time and cleaning with no loss of vacuum in the mass spectrometer.
- Soft ionization so the system can be optimized to reduce the splitting of ions leading to a simpler spectrum for analysis.

Experiment

In the following study, a Pyris 1 TGA was interfaced to a HPR-20 MS. The sample was heated to 200 °C at 10 °C/min with helium purge gas at 30 mL/min. A sample weight of 6.1374 mg was used.

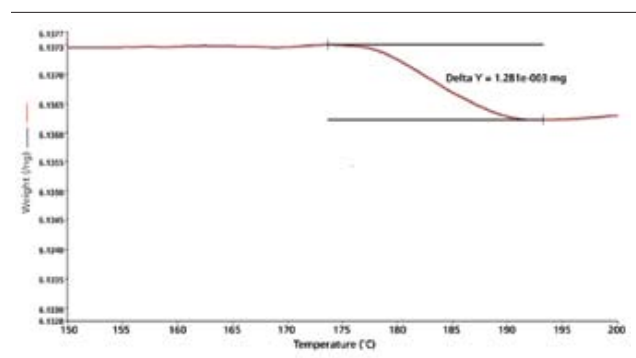


Figure 2. Weight loss due to the loss of solvent from the sample. Data has been expanded to show the weight loss clearly.

A sample of a pharmaceutical was found to exhibit an unusual recrystallization behavior over a period of time. This behavior is often associated with the loss of a solvent from the sample. A method was required to confirm the suspected identity of the solvent which had been used in the production of the sample.

6.1374 mg of the sample was run in the TGA; the HPR-20 MS was used in multiple ion detection (MID) mode using the high-sensitivity SEM detector. The mass ion chosen to identify the presence of the solvent was 49 amu (atomic mass units) for dichloromethane.

The thermogram in Figure 2 shows the TGA trace collected for the sample. An extremely small weight loss of just 1.2 µg (0.026%) was found, indicating the outstanding performance of the Pyris 1 TGA.

The gases evolved during this very small amount of weight loss were analyzed. The background partial pressure of mass 49 was observed at a 2×10^{-11} bar and a slight peak to 5×10^{-11} bar observed in the weight loss region as shown below (Figure 3). Despite the very small amount of volatile loss and the correspondingly small increase in partial pressure, the MS was clearly able to detect this small change. This trace clearly indicates the loss of dichloromethane from the sample, as suspected, and shows the power of this technique to identify very small amounts of residual contaminants in a sample.

The application of TG-MS to low-level contaminants that would be undetectable by TG-IR is an example of the power of this technique. For more information, please contact your sales representative.

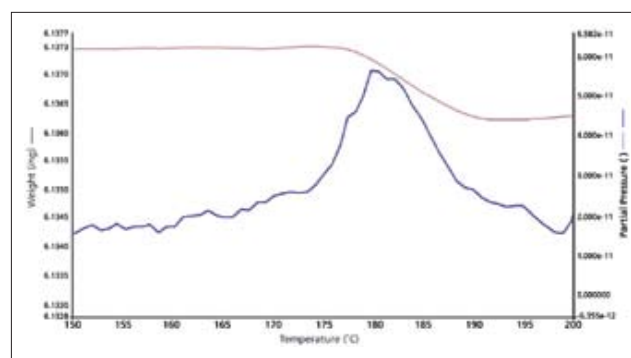


Figure 3. Weight loss curve and mass 49 (dichloromethane) in the 10^{-11} bar region.

Differential Scanning Calorimetry –
Raman Spectroscopy

Polymorphism in Acetaminophen Studied by Simultaneous DSC and Raman Spectroscopy

Introduction

Differential scanning calorimetry (DSC) and Raman spectroscopy are complementary techniques that are often applied to the same problems, principally to study phase transitions in solids. Simultaneous Raman and DSC measurements add a qualitative dimension to DSC data which simply measure heat flow. A typical example is the identification of polymorphs. Acetaminophen has several polymorphic forms which can interconvert with thermal treatment. A single Raman spectrum can identify a polymorph, while DSC uses a temperature scan to observe the relationship between forms that are not all stable at ambient temperatures. Simultaneous measurements are necessary to ensure that the Raman data correspond to the different stages identified by DSC.

Coupling thermal and spectroscopic techniques raises the question of how the methods affect each other. In this case, the main issue is the potential of the laser energy to perturb the temperature of the sample. By exploiting the double-furnace design of PerkinElmer®'s DSC to assure accurate temperature control on the bulk of the sample and the fast response of this design to compensate for the heat induced by the Raman laser, the effects of the Raman on the sample can be minimized. Similarly, the ability of the PerkinElmer RamanStation™ to apply laser only while spectra are being collected also helps maintain sample temperature. This allows accurate measurements with minimal induced artifacts.

Experimental

The system used here combines a PerkinElmer DSC 8500 with a PerkinElmer RamanStation connected by a fiber optic probe. The probe fits into the lid of the DSC with an additional lens to focus the laser onto the sample pan and collect the Raman scatter. Spectra are measured with an open sample pan or through a quartz lid. For the data shown here, the heating rates were 10 or 20 K/min with spectra typically obtained at 1 or 2 degree intervals. The power of the laser used to generate the Raman spectra affects the DSC, but the rapid response of the dual-furnace design of the DSC 8500 minimizes any perturbation of the sample temperature. Changes in the Raman spectra recorded during the temperature cycle can generate a curve for direct comparison with the DSC heat-flow curve, confirming that the two techniques are responding to the same changes. Thermal transitions appear as peaks in the DSC heat-flow curve but they appear as steps when generated from band intensities in the Raman spectra (Figure 1).

Results

Raman spectra of the various forms are seen in Figure 2. Although the spectra of Forms I and III appear very similar, there are significant band shifts, while the spectrum of Form II is clearly different. The spectra of the melt and the amorphous solid are extremely similar to each other with much broader bands than the crystalline forms.

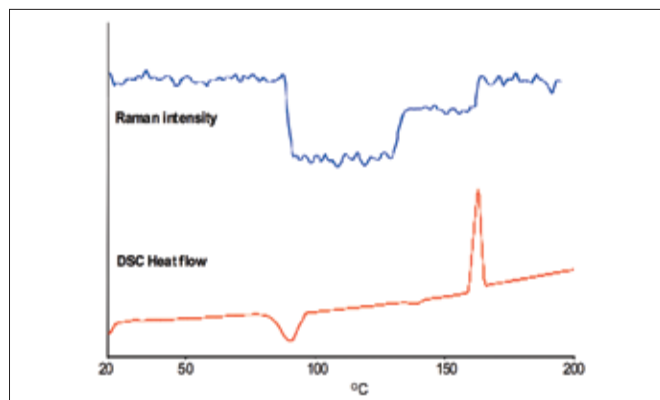


Figure 1. Thermograms from DSC and Raman spectra.

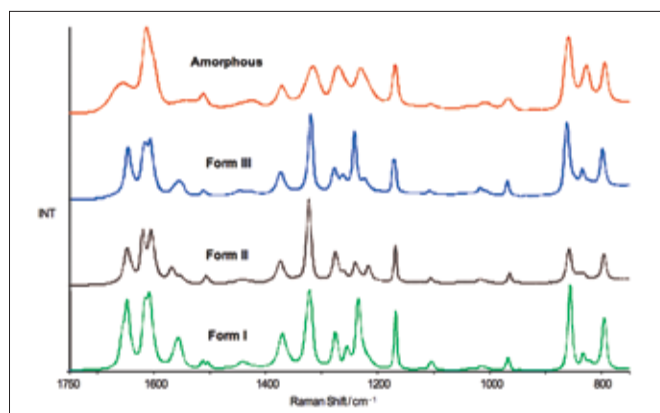


Figure 2. Raman spectra of samples of acetaminophen with different thermal histories.

DSC is needed to understand the relationship between the different forms. Commercial products contain Form I which is the thermodynamically most-stable polymorph. However, cooling from the melt normally produces an amorphous glass. Figure 3 shows a thermogram and spectra obtained by heating the amorphous material from 30 to 200 °C. The glass crystallizes at about 80 °C to Form III. At about 130 °C, this is transformed into Form II which melts at about 160 °C.

When the amorphous glass is allowed to crystallize at room temperature, it can convert to Form II. Although Form II melts at 160 °C as in Figure 3, it may convert to Form I when heated from ambient temperature. Figure 4 shows a Raman thermogram and spectra obtained by heating a sample of Form II from 20 to 200 °C, cooling to 20 °C and heating to 200 °C again. Conversion to Form I occurs at about 120 °C with subsequent melting at 170 °C. After cooling, the amorphous glass undergoes the expected transitions to Form III and then to Form II. The conversion from Form II to Form I is not always seen.

The amorphous glass crystallizes very slowly unless heated. However, the presence of small particles to act as nuclei can promote crystallization. A sample of acetaminophen containing a small concentration of zinc oxide crystallizes at around 100 °C on cooling from the melt at 10 K/min. Spectra from before and after the transition in Figure 5 (Page 3) show that, in this case, crystallization results in Form III.

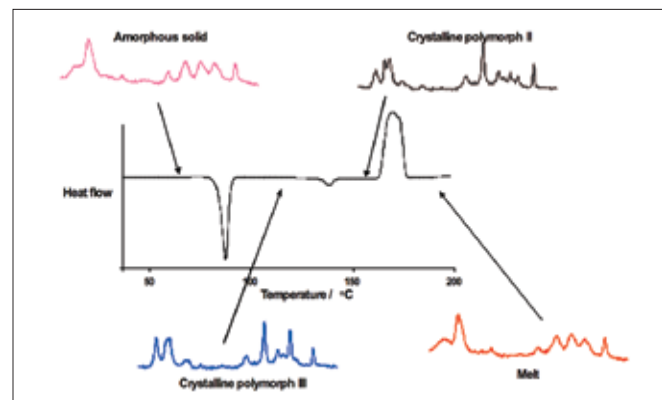


Figure 3. Raman spectra (1700-1100 cm^{-1}) from a DSC run.

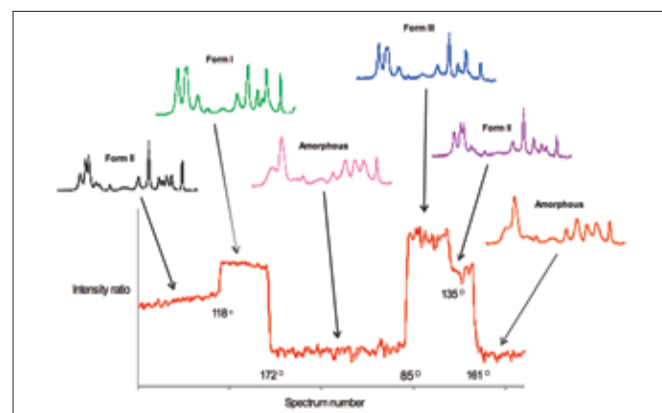


Figure 4. Thermogram and spectra from heating acetaminophen Form II.

Summary

Acetaminophen exhibits a number of transitions between different forms and the behavior is not always reproducible. Simultaneous DSC and Raman measurements can identify unambiguously which forms are involved in any transition.

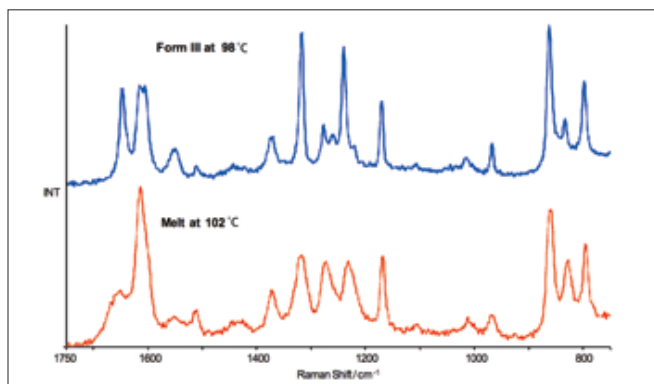


Figure 5. Spectra before and after crystallization on cooling.

Thermogravimetric Analysis

Evolved Gas Analysis: a High Sensitivity Study of a Solvent of Recrystallization in a Pharmaceutical

Introduction

Thermogravimetric analysis (TGA) of materials is commonly used to measure weight loss as a sample is heated or held isothermally. In the pharmaceutical industry, materials often show weight losses associated with the loss of solvent/water, desolvation or decomposition of the sample. This information is then used to assess the purity and stability of the material and its suitability for use. The TGA gives a quantitative measure of mass

lost from the sample, but it does not provide information on the nature of the products that are lost from the sample, and this information is often required for complete characterization.

Coupling a mass spectrometer (MS) to a TGA allows evolved gases to be analyzed and identified giving this additional valuable information.

Typical applications of TGA-MS include:

- Detection of moisture/solvent loss from a sample (e.g. loss on drying or dehydration of a pharmaceutical)
- Thermal stability (degradation) processes
- Study reactions (e.g. polymerizations)
- Analysis of trace volatiles in a sample (e.g. volatile organic compound (VOC) testing)

Instrumental Setup

All of the TGA systems supplied by PerkinElmer (Pyris™ 1 TGA, STA 6000 and TGA 4000) can be easily interfaced to MS systems. PerkinElmer can supply systems with either the PerkinElmer Clarus® MS or with a Hiden Analytical MS. In this study, a Pyris 1 TGA interfaced to a Hiden Analytical HPR-20 MS was used.



Figure 1. Pyris 1 TGA is shown interfaced to a HPR-20M (left) and a TurboMass 600 MS (right).

The HPR-20 MS is optimized for the analysis of the evolved gases from the TGA and offers the following benefits:

- The ability to use either Faraday cup or secondary electron multiplier (SEM) detectors, depending on the sensitivity levels required. The SEM offers the ability to detect very low partial pressures of evolved gases below 10^{-8} bar, allowing identification of very low levels of contaminants. The system is able to operate in air, posing no issues for sample changing.
- Optional foreline and bypass vacuum pumping permits the most efficient pumping of helium which is normally used as a purge gas since it produces no interfering mass ions.
- A very flexible heated transfer line allows simple interfacing to the TGA systems. The lightweight heated line can be moved around in use without damage, making the system very robust. Gas transfer uses a wide-bore fused-silica capillary which gives 16 mL/min flow to the mass spectrometer for highest sensitivity.

- An anti-blockage filter has been added to catch high-molecular-weight material that might block the capillary. This single feature prevents hours of down time and cleaning with no loss of vacuum in the mass spectrometer.
- Soft ionization so the system can be optimized to reduce the splitting of ions leading to a simpler spectrum for analysis.

Experiment

In the following study, a Pyris 1 TGA was interfaced to a HPR-20 MS. The sample was heated to 200 °C at 10 °C/min with helium purge gas at 30 mL/min. A sample weight of 6.1374 mg was used.

Results and Conclusions

A sample of a pharmaceutical was found to exhibit an unusual recrystallization behavior over a period of time. This behavior is often associated with the loss of a solvent from the sample. A method was required to confirm the suspected identity of the solvent which had been used in the production of the sample.

6.1374 mg of the sample was run in the TGA, the HPR-20 MS was used in multiple ion detection (MID) mode using the high-sensitivity SEM detector. The mass ion chosen to identify the presence of the solvent was 49 amu (atomic mass units) for dichloromethane.

The thermogram in Figure 2 shows the TGA trace collected for the sample. An extremely small weight loss of just 1.2 µg (0.026%) was found, indicating the outstanding performance of the Pyris 1 TGA.

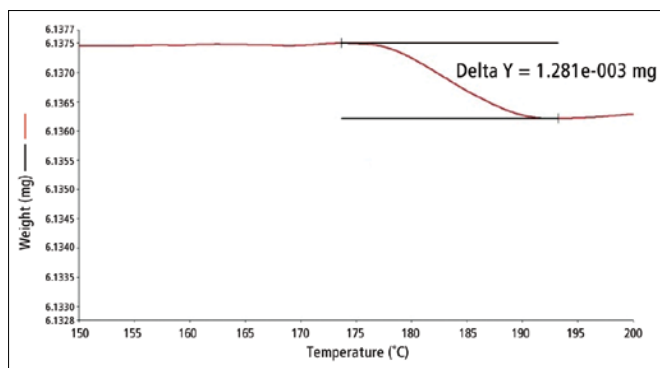


Figure 2. Weight loss due to the loss of solvent from the sample. Data has been expanded to show the weight loss clearly.

The gases evolved during this very small amount of weight loss were analyzed. The background partial pressure of mass 49 was observed at a 2×10^{-11} bar and a slight peak to 5×10^{-11} bar observed in the weight loss region as shown below. Despite the very small amount of volatile loss and the correspondingly small increase in partial pressure, the MS was clearly able to detect this small change. This trace clearly indicates the loss of dichloromethane from the sample, as suspected, and shows the power of this technique to identify very small amounts of residual contaminants in a sample.

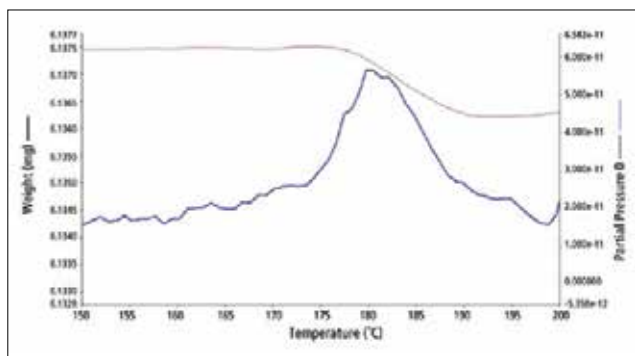


Figure 3. Weight loss curve and mass 49 (dichloromethane) in the 10^{-11} bar region.

The application of TG-MS to low level of contaminates that would be undetectable by TG-IR is an example of the power of this technique. For more information, please contact your sales representative.

Hyphenation

Authors:

Kathryn Lawson-Wood

Ian Robertson

PerkinElmer, Inc.
Seer Green, England

Study of the Decomposition of Calcium Oxalate Monohydrate using a Hyphenated Thermogravimetric Analyser - FT-IR System (TG-IR)

instrument on their own. The combination of a Thermogravimetric Analyser (TGA) with an Infrared Spectrometer (TG-IR) is the most common type of evolved gas analysis. TGA accurately measures the percentage weight loss of a sample as a function of temperature, but will not provide any information regarding the chemical composition of the evolved gases. Interfacing a TGA with an FT-IR Spectrometer allows identification of the gases evolved, thus more comprehensive studies of the processes which occur in thermal analysis may be conducted.

TG-IR is suited to a variety of applications which require identification of evolved gases upon sample heating. Such applications include residual solvents in pharmaceuticals, and polymer and plastic decomposition¹. In this application, the thermal decomposition of calcium oxalate monohydrate ($\text{CaC}_2\text{O}_4 \cdot \text{H}_2\text{O}$) has been studied.

Introduction

Hyphenation is the combination of different instruments to gain analytical insights which would previously not be observed by either



Figure 1. PerkinElmer TGA 8000, Frontier FT-IR Spectrometer and TL8000 mass flow controller.

Decomposition of Calcium Oxalate Monohydrates

Calcium oxalate monohydrate ($\text{CaC}_2\text{O}_4 \cdot \text{H}_2\text{O}$), also known as whewellite, is a main component in kidney stones and is an industrially useful compound used to make oxalic acid and organic oxalates. $\text{CaC}_2\text{O}_4 \cdot \text{H}_2\text{O}$ is commonly used as a standard to test TGA performance due to its well-known decomposition steps and products².

When heated, $\text{CaC}_2\text{O}_4 \cdot \text{H}_2\text{O}$ decomposes in three well defined steps as shown below with the overall reaction equation. Step 1 involves loss of water of crystallisation to form anhydrous calcium oxalate. Calcium oxalate then thermally decomposes to calcium carbonate in step 2 with the loss of carbon monoxide. The final step involves thermal decomposition of calcium carbonate to calcium oxide with the loss of carbon dioxide². The theoretical stoichiometric percent weight loss of each step, calculated using the molar masses of each compound, is shown in Table 1.

Overall Reaction: $\text{CaC}_2\text{O}_4 \cdot \text{H}_2\text{O} \rightarrow \text{CaO} + \text{H}_2\text{O} + \text{CO} + \text{CO}_2$

- 1) $\text{CaC}_2\text{O}_4 \cdot \text{H}_2\text{O} \rightarrow \text{CaC}_2\text{O}_4 + \text{H}_2\text{O}$
- 2) $\text{CaC}_2\text{O}_4 \rightarrow \text{CaCO}_3 + \text{CO}$
- 3) $\text{CaCO}_3 \rightarrow \text{CaO} + \text{CO}_2$

Table 1. Theoretical stoichiometric weight loss for each TGA step.

Step	Theoretical stoichiometric weight loss (%)
1	12.3
2	19.2
3	30.1

Experimental

$\text{CaC}_2\text{O}_4 \cdot \text{H}_2\text{O}$ (Puratronic®, 99.9985 % (metals basis)) was obtained from Alfa Aesar. Thermal decomposition and evolved gas analysis of $\text{CaC}_2\text{O}_4 \cdot \text{H}_2\text{O}$ was performed on the PerkinElmer TG-IR hyphenated system.

The IR background scan was taken after zeroing the ceramic pan in the nitrogen gas flow. $\text{CaC}_2\text{O}_4 \cdot \text{H}_2\text{O}$, 6.8170 mg (typically between 5-25 mg), was placed in the pan and analysis performed according to the conditions shown in Table 2. The final hold for five minutes in air at 950 °C was implemented to clean the crucible. The IR spectrometer parameters were set to collect a co-added scan every 20 seconds.

Table 2. Experimental parameters for the TG-IR experiment.

TGA Parameters	
Temperature Program	1. Hold for 1min at 30 °C 2. Heat from 30 °C to 950 °C at 20 °C/min 3. Hold for 5 min at 950 °C
Pan Used	Ceramic
Balance Purge	50 ml/min
Sample Purge	N ₂ , 30 ml/min for Step 1 to 2 Air, 30 ml/min for Step 3
Sample Quantity	6.8170 mg
Transfer Line	270 °C
FT-IR Parameters	
Scan Range	4000-450 cm ⁻¹
Resolution	4 cm ⁻¹
Co-added Scans	4

Results and Discussion

The TGA thermogram for the decomposition of $\text{CaC}_2\text{O}_4 \cdot \text{H}_2\text{O}$ is shown in Figure 2, which illustrates the occurrence of three weight loss steps. After the third step, the weight stabilized at 38%. Using Pyris software, the percent change in weight, onset temperature, and inflection point were calculated as shown in Figure 2. The measured percent weight losses of each step were close to the theoretical stoichiometric values (Table 3). The inflection point is the point at which the greatest rate of change on the weight loss curve occurs. The extrapolated onset temperature is a reproducible calculation for further characterisation of a sample and is the temperature at which the weight loss initiates.

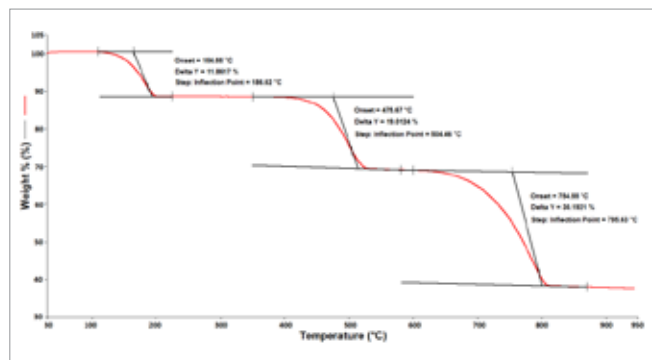


Figure 2. $\text{CaC}_2\text{O}_4 \cdot \text{H}_2\text{O}$ thermogram.

Table 3. Theoretical stoichiometric weight loss for each TGA step.

Step	Theoretical Stoichiometric Weight Loss (%)	Measured Weight Loss (%)
1	12.3	11.9
2	19.2	19.0
3	30.1	30.2

Evolved gas analysis by FT-IR was carried out to provide confirmation of the identity of gases evolved. The FT-IR generated a Gram-Schmidt profile of absorbance versus temperature, shown in Figure 3 overlaid with the TGA weightloss curve. The peaks in the Gram-Schmidt profile correlate directly with the steps in the TGA weightloss curve.

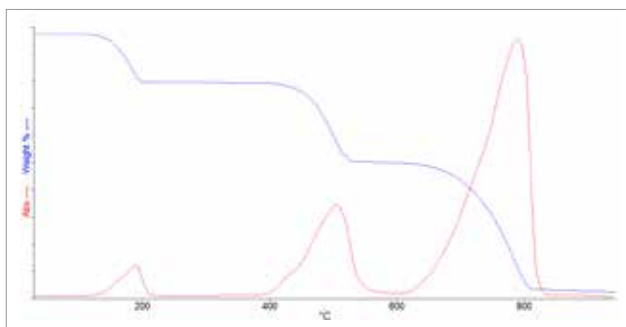


Figure 3. $\text{CaC}_2\text{O}_4 \cdot \text{H}_2\text{O}$ Weight loss curve (blue) and Gram-Schmidt profile (red).

Figure 4 shows the IR spectra at each of the three weight loss steps. At temperatures ranging 100 - 200 °C, a first weight loss of 11.9% was observed, corresponding to the loss of water of crystallization. The IR spectrum of the evolved gas at 186 °C confirmed the weight loss to be due to water vapour being evolved from the sample.

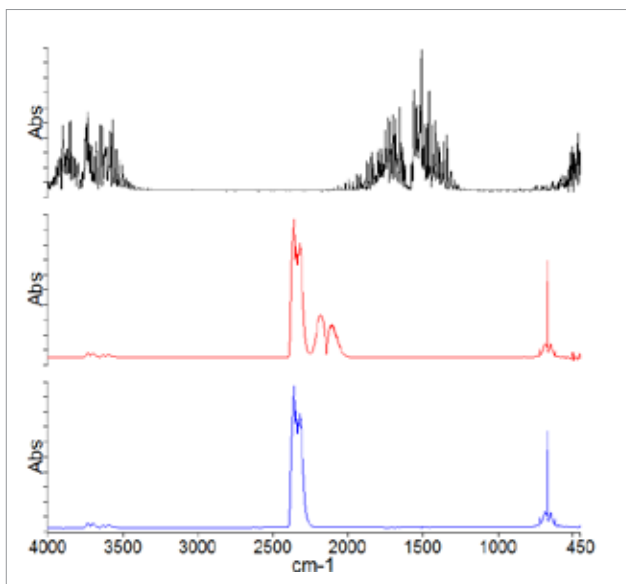
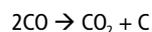


Figure 4. IR spectra from top to bottom; Spectrum at 186°C, 504°C and 789°C.

At temperatures ranging 400 – 530 °C, a second weight loss of 19.1% was observed, corresponding to the decomposition of anhydrous calcium oxalate, with the loss of carbon monoxide. The IR spectrum at 504 °C provided confirmation of evolved CO with the two peaks centered around 2100 cm^{-1} . However, peaks at 667 cm^{-1} and 2350 cm^{-1} indicated that CO_2 was also produced during the second step. Carbon dioxide forms as a result of the disproportionation reaction of CO to CO_2 and carbon (Equation 1).



Equation 1: Disproportionation reaction of CO

The third and final weight loss, at temperatures ranging 600 – 810 °C, was determined to be 30.2%, corresponding to the decomposition of calcium carbonate to calcium oxide with the loss of carbon dioxide. The peaks at 667 cm^{-1} and 2350 cm^{-1} in the IR spectrum at 789 °C provide confirmation of evolved CO_2 .

Conclusion

Calcium oxalate monohydrate showed three decomposition steps with obtained weight losses matching the theoretical values. Hyphenating IR analysis to the TGA provided confirmation of the identity of the evolved gases and insights into data which would otherwise not be observed in TGA alone. The PerkinElmer TG-IR system is fully optimised to obtain the highest quality data from the TGA, the FT-IR and the hyphenation of both techniques.

References

1. Nishikida, K., Nishio, E., and Hannah, R. (1995) "Selected Applications of Modern FT-IR Techniques", Kodansha.
2. Haines, P.J., (2002) "Principles of Thermal Analysis and Calorimetry", The Royal Society of Chemistry.
3. Nair, C. and Ninan, K. (1978) "Thermal decomposition studies: Part X. Thermal decomposition kinetics of calcium oxalate monohydrate — correlations with heating rate and samples mass", Elsevier, Volume 23, Issue 1.

Thermogravimetric Analysis – GC
Mass Spectrometry

TG-GC/MS Technology – Enabling the Analysis of Complex Matrices in Coffee Beans

Introduction

The combination of a thermogravimetric analyzer (TGA) with a mass spectrometer (MS) to analyze the gases evolved during a TGA analysis is a fairly well-known technique. In cases of complex samples, TG-MS often results in data in which it is nearly impossible to differentiate gases that evolve simultaneously.

Combining TGA with gas chromatography mass spectrometry (GC/MS) allows for a more complete characterization of the material under analysis and precisely determines the products from the TGA.

Experimental

This analysis was performed on a PerkinElmer® Pyris™ 1 TGA using alumina pans and the standard furnace. The instrument was calibrated with nickel and iron and all samples were run under helium purge. Heating rates varied from 5 to 40 °C/min, depending on the sample under test. The furnace was burned off between runs in air. Samples were approximately 10-15 mg. Data analysis was performed using Pyris 9.0 Software.

During the TG-GC/MS analysis, the PerkinElmer Clarus® 680 C GC/MS was used. A 0.32 mm I.D. deactivated fused-silica transfer line was connected to the GC injector port. The transfer line was heated to 210 °C and connected to the Elite™-1ms capillary GC column. In both cases, data analysis was performed using TurboMass™ GC/MS Software.

Results

In this TG-GC/MS application, coffee beans were analyzed. The TGA resulted in a complex thermogram with many different transitions (Figure 1).

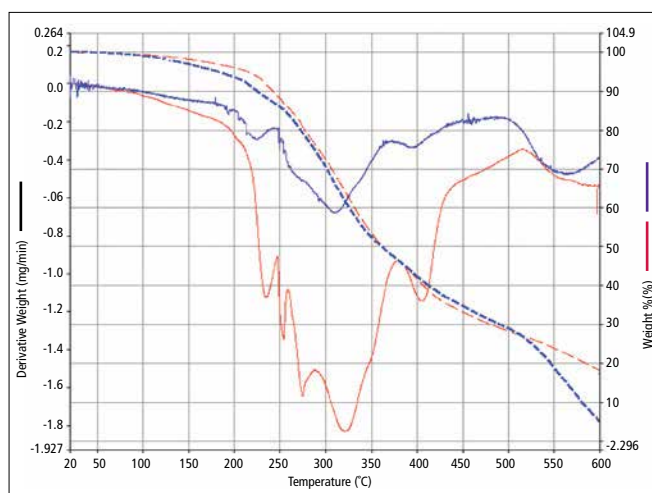


Figure 1. Resultant thermogram from the analysis of coffee beans. The blue curve is unroasted beans from Africa; the red curve is unroasted beans from Sumatra. The weight loss and the first derivative are shown.

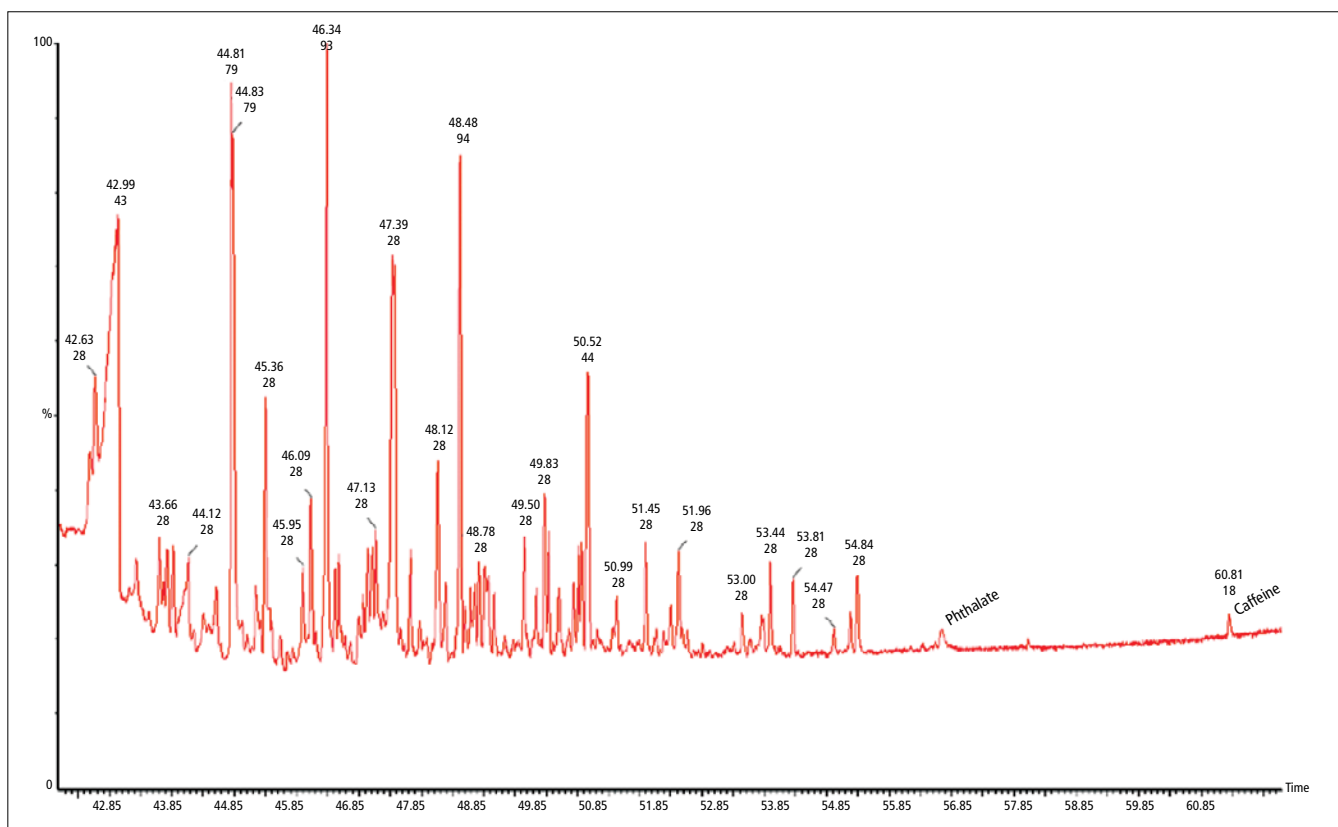


Figure 2. The GC/MS data resultant from the TGA of African coffee beans.

Complex data was expected as coffee beans are known to contain many different compounds. As a result, it was determined that the evolved gas would likely be too complex for TG-MS, thus TG-GC/MS was determined to be a better approach for this matrix.

The goal of the analysis was to search the complex data for two compounds that would be expected in a coffee sample, caffeine (m/z 194) and phthalates (m/z 149). The caffeine is obviously present in coffee, while the phthalates were a possibility as a result of storage in and contact with plastics. The resultant GC/MS data is shown in Figure 2 (Page 2), demonstrating a very complex chromatogram.

A search for significant peaks resulted in a spectral match for a phthalate (56 minutes), while a search for m/z 194 resulted in a spectral match for caffeine at 60 minutes. As expected, the TGA of coffee beans results in the simultaneous evolution of a large number of gases – TG-GC/MS is able to resolve many of these compounds enabling deeper investigation.

Conclusions

TGA analysis allows quantification of the weight loss of a material at specific temperatures. MS increases the power of the technique by providing the ability to identify the species evolved during thermal analysis. TG-GC/MS adds the additional capability of chromatographic separation of co-evolved gases. While not realtime, the improved separation by the GC/MS makes data interpretation easier than TG-MS. This allows the separation of fairly complex mixtures with minimal sample preparation by using the TGA to volatilize components.

Thermogravimetric Analysis

Authors

E. Sahle-Demessie

A. Zhao

U.S. EPA, Office of Research and Development
National Risk Management Research Laboratory
Cincinnati, OH 45268

A. W. Salamon

PerkinElmer, Inc.
Shelton, CT 06484 USA

A Study of Aged Carbon Nanotubes by Thermogravimetric Analysis

Introduction

Increased use of carbon nanotubes in consumer and industrial products have scientists asking about the implications of CNTs in our environment. Many end product applications include polymer composites, drug delivery systems, coatings and films, military applications, electronics, cosmetics, healthcare, among others.

CNTs are desirable for many applications because of their high surface area to weight ratio. They are lightweight and highly elastic compared to carbon fibers, and deliver higher surface area for increased chemical interaction in its specific application.

Thermogravimetry a simple analytical technique that is frequently used to characterize carbon nanotubes.¹ The Pyris™ 1 TGA delivers accurate results quickly because of its low mass furnace. The Pyris 1 TGA low mass furnace has accurate temperature control and fast cooling for higher sample throughput.

There are various carbon-nano-material classifications, such as single wall carbon nanotubes (SWCNT), or multi-wall carbon nanotubes (MWCNT). A SWCNT is a single tube of some length with its tubular wall having a hexagonal hollow geometry, similar in shape to a fullerene. A MWCNT is one or more tubes within a tube. Fullerenes, also known as Bucky Balls, are hollow spheres. Graphene is a flat sheet of carbon, one atom thick that has the same hexagonal structural geometry as CNTs. CNTs are made from graphene by wrapping the graphene into cylindrical shapes. Specifications of CNTs may describe their diameter and length, as well as the orientation of the lattice wall in regards to the CNT's centerline. There are three types of lattice orientations, armchair, zigzag, and chiral. The difference between these CNT types is the bias or angle that they are wrapped.^{2,4}

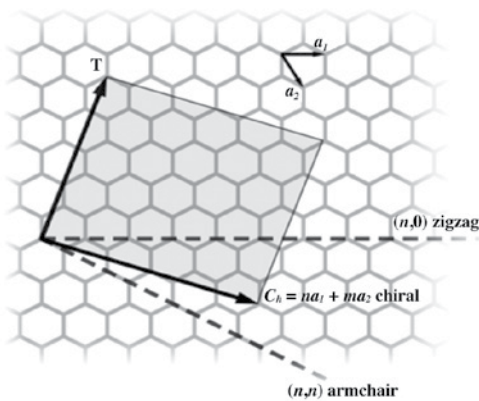


Figure 1. Types of carbon nanotubes, armchair (n,n), zigzag (n,0) and chiral (C_h). The (n,m) nanotube naming scheme can be thought of as a vector (C_h) in an infinite graphene sheet that describes how to “roll up” the graphene sheet to make the nanotube. **T** denotes the tube axis, and a_1 and a_2 are the unit vectors of graphene in real space. This image is the courtesy of Wikipedia.⁴

Materials Used

Commercially available high purity MWCNT samples were obtained. Analysis of acid washed samples using ICP showed less than 1% of trace elements.

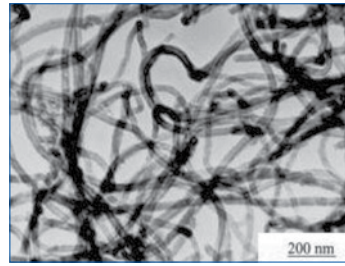


Figure 2. Above, the Transmission Electron Microscope (TEM) image of CNTs indicates that the CNTs have a ~ 20 nm outside diameter and their lengths are much larger than 200 nm.

Table 1 is the manufacturer’s product description before the samples were subjected to UV aging. The far right column explains one of the foremost features of NMs, that is their high surface area in relationship to weight. One gram of Type B CNTs have a surface area that is larger than 200 square meters (>200 m²/g). The manufacturer’s CNT outside diameters are verified by the TEM image in Figure 2.

Table 1. MWCNT Characterization.

Type	Purity	Outside Diameter	Length	Specific Surface Area
Type A	>95%	8-15 nm	~50µm	>233 m ² /g
Type B	>95%	10-20 nm	10-30 µm	>200 m ² /g
Type C	>95%	> 50 nm	10-20 µm	>40 m ² /g

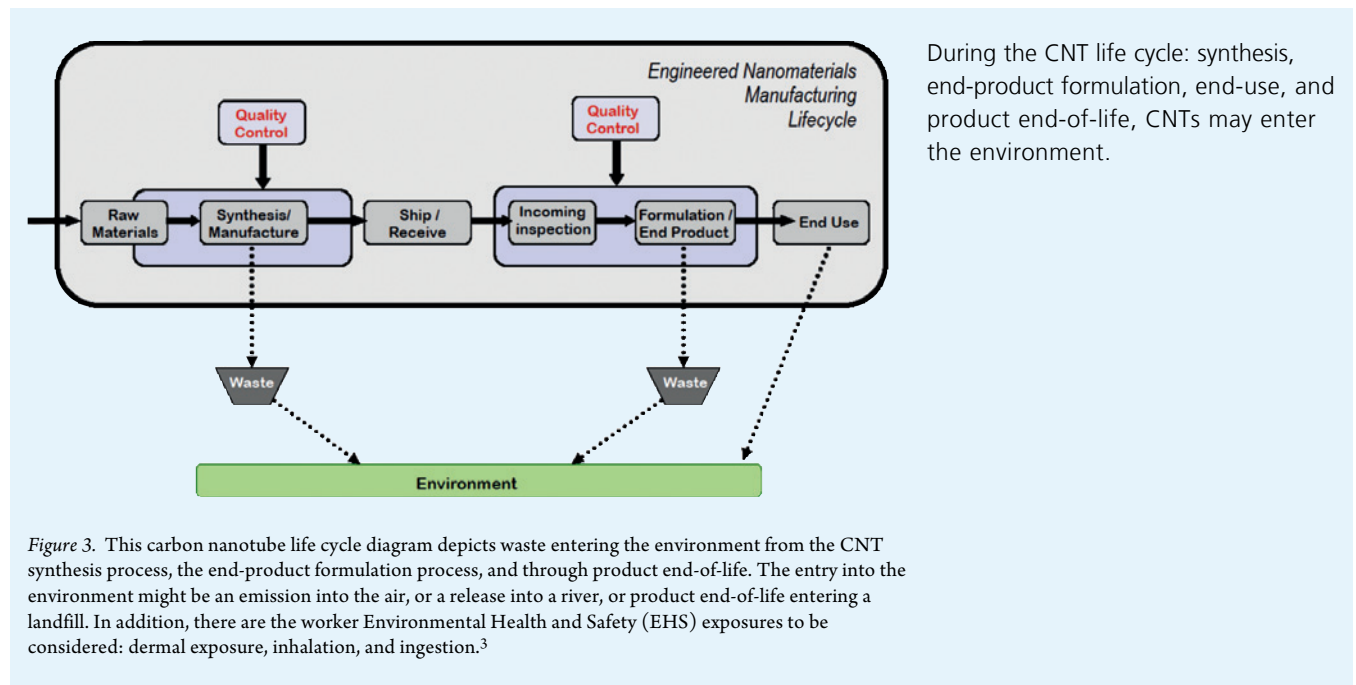




Figure 4. The Pyris 1 TGA.

Definition: Thermogravimetric Analysis (TGA) also called Thermogravimetry is a technique in which the mass of a material is monitored as that material is subjected to a controlled temperature program in a controlled atmosphere.

Method

A general method follows:

Instrument:	Pyris 1 TGA
Sample Size:	> 1 mg, usually 3 mg to 50 mg
Sample Pan:	Ceramic
Temperature Range:	30 °C to 800 °C
Scanning rate:	10 °C/minute or faster
Sample Purge Gas and Rate:	Air at 20 mL/min
Balance Gas and Rate:	Nitrogen at a rate at least 10 mL/min higher than the sample purge rate

Characterization of nanotubes with TGA

Thermogravimetric Analysis was the first analytical technique chosen to compare the effects of the UV exposure times on the CNTs. TGA is very simple, yet a very accurate analytical technique that delivers results quickly. Studying the oxidation of fullerene C₆₀ using TGA has been reported.^{5,7} The high sensitivity of the TGA, which is in the order of 0.1 micro-gram/min, permitted weight loss determinations at a given

heating rate, within a short time without consuming too much material. The oxidation rates of carbon nanotubes measured in air at atmospheric pressure within the TGA are unique for each CNT sample of different wall thicknesses. Figure 5 shows the decomposition temperatures (i.e. oxidation) for samples run at the same heating rate, varies up to ±40 °C depending on the characteristics of the carbon tubes.

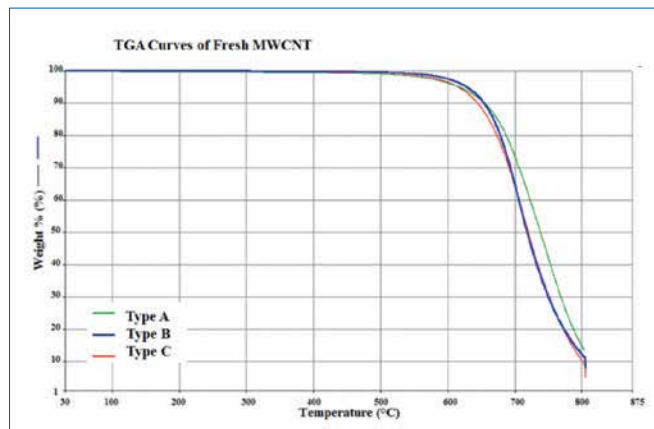


Figure 5. Thermogravimetric analysis of CNTs showing weight loss. Sample weight was about 10 mg, oxygen flow was 20 mL/min. Samples A, B, C, had varying wall thicknesses. See Table 1 for specifications.

Measuring Aging of Carbon nanotubes

In a laboratory environment, three high purity MWCNT samples that had no specific wrap were analyzed. They were all nearly the same weight and came from the same manufacturing lot. They were subjected to the same UV light source. The intent of the UV light is to simulate sunlight in a controlled manner. Three “A” samples in Figure 5 were exposed to UV for:

- An exposure of 9.0 hours
- An exposure of 5.5 hours
- An exposure of 4.0 hours

Results

This experiment results in the CNT amorphous carbon decomposing before the structural carbon. All carbon should decompose in the oxidative environment before reaching 900 °C.

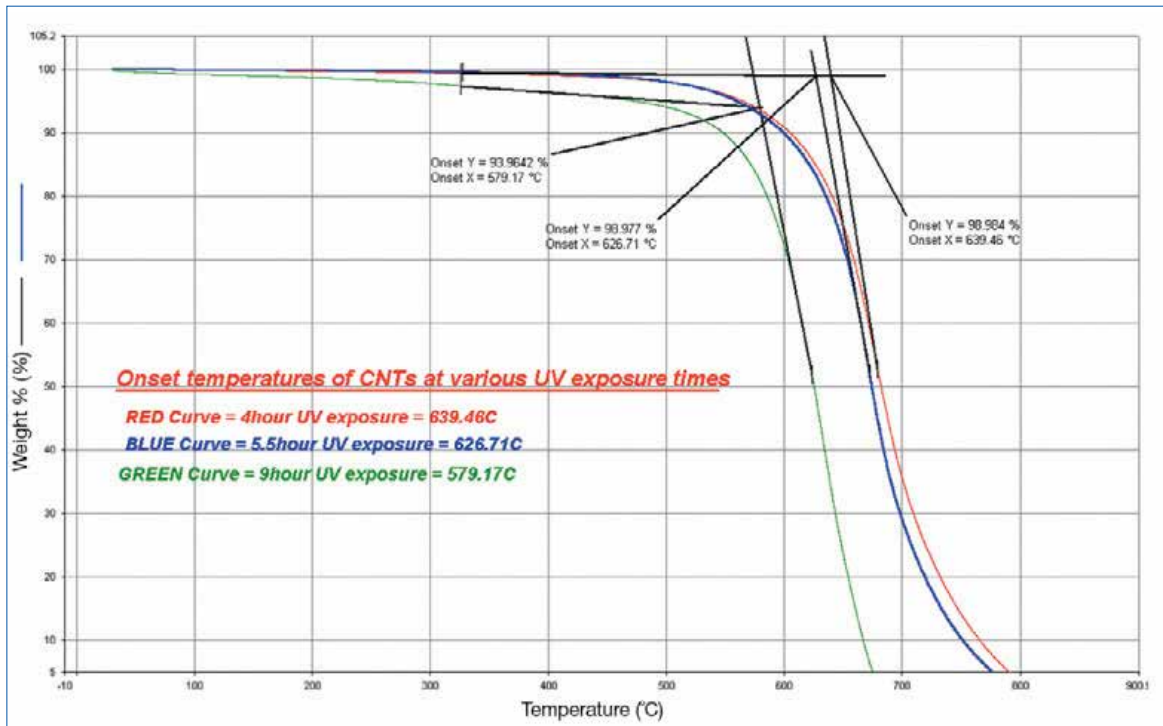


Figure 6. X Axis = Temperature: When observing Thermogravimetric weight loss curves in regards to temperature, the weight loss curves above indicate that CNTs exposed to UV light for 9 hours began decomposition at a lower temperature than the other two samples of shorter exposures.

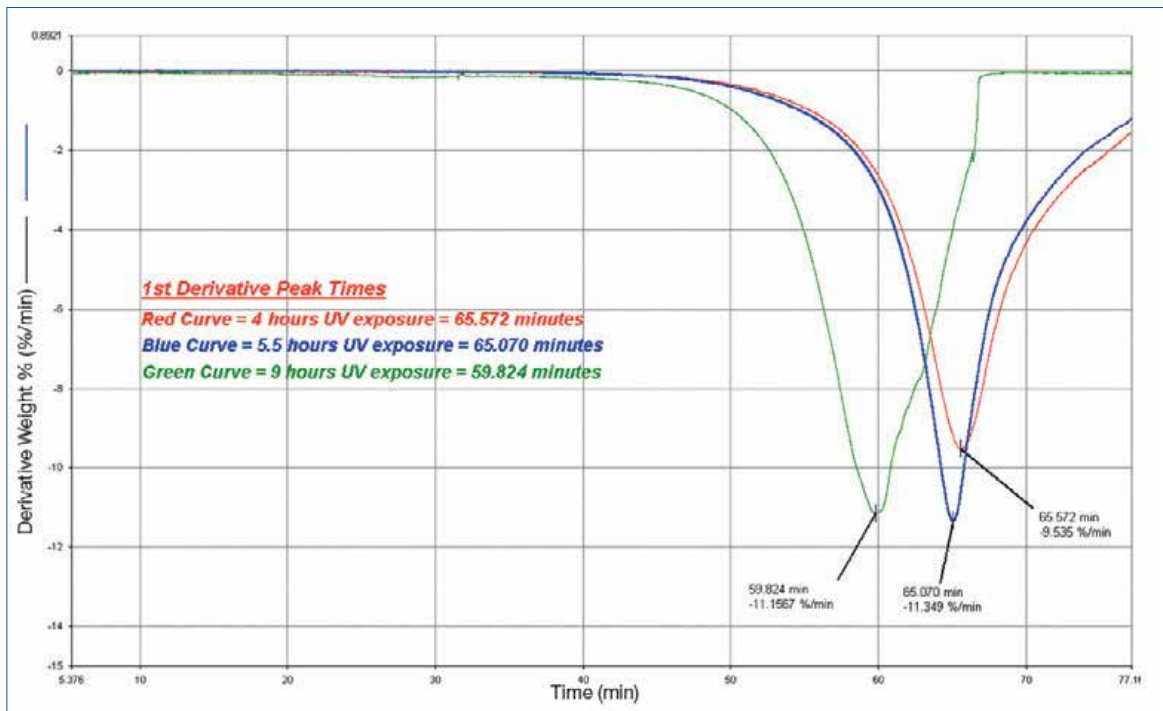


Figure 7. X Axis = Time: To gain a better understanding of the results, the same data file is displayed on a Time X-axis. The 1st derivative curve of each weight loss curve is displayed. The 1st derivative is a widely used tool to compliment the TGA weight loss curve, and like the weight loss curve, the 1st derivative curve is very reproducible. Upon examination of the 1st derivative curves above, the CNT sample with the longest UV exposure decomposes more than 5 minutes before the other two samples of shorter exposure times.

Summary

Based on the Pyris 1 TGA data collected, UV light has an effect on CNTs. As this study suggests, the longer the CNTs are subjected to UV light, the sooner CNTs decompose when heated to elevated temperatures.

Further investigation

Because this is early in an entire series of CNT analytical experiments, there are more TGA tests to conduct. It is suggested that a series of isothermal tests be conducted next. They should involve longer UV exposures and similar exposures to this experiment. Based on the scanning data provided, it is suggested that isothermal tests be conducted at 500 °C, 550 °C, 600 °C, and 650 °C. These future isothermal tests would help define the test protocol needed to examine CNTs found in water, soils, or air.

Conclusion

Thermogravimetry by the Pyris 1 TGA is a simple analytical technique that is frequently used to characterize carbon nanotubes. The Pyris 1 TGA delivers accurate results quickly because of its low mass furnace. The Pyris 1 TGA low mass furnace has accurate temperature control and fast cooling for higher sample throughput.

References

1. Mansfield, E., Kar, A., Hooker, S.A., Applications of TGA in Quality control of SWCNTs, Analytical and Bioanalytical Chemistry, Vol. 369, Number 3, 1071-1077. 2009.
2. Ozin, G.A., Arsenault, A.C., and Cademartiri, L., *Nanotechnology – A Chemical Approach to Nanomaterials*, Royal Society of Chemistry, Cambridge, U.K., 2009. Page 209.
3. National Nanotechnology Initiative – Human Health Workshop, November 2009, Washington D.C., US.
4. Wikipedia, Carbon Nanotubes, Nov. 2010, http://en.wikipedia.org/wiki/Carbon_nanotube#Structural
5. Pang L.S.K., Saxby, J.D., and Chatfield, S.P., *Thermogravimetric Analysis of Carbon Nanotubes and Nanoparticles*, J. Physical Chemistry, 97, 27, 1993.
6. Saxby, J.D., Chatfield, S.P., et al, *Thermogravimetric analysis of Buckminsterfullerene and Related Materials in Air*, J. Phys. Chem. 1992, 96,17-18.
7. Joshi, A., Nimmagadda, R., and Herrington, J., *Oxidation Kinetics of Diamond, Graphite and Chemical Vapor Deposited Diamond Films by Thermal Gravimetry*, J. Vac. Sci. Technol. A 8(3), May/June, 1990.

Additional Reading

PerkinElmer, *Nanotechnology and Engineered Nanomaterials – A Primer*, www.perkinelmer.com/nano

PerkinElmer, Nanomaterials Reference Library
www.perkinelmer.com/nano

Acknowledgement

Special thanks to E. Sahle-Demessie and A. Zhao of the U.S. EPA, January 2011, for providing the TGA data. This thermogravimetric data is from an on-going study of environmental effects on carbon nanotubes.

TGA-GC-MS

Authors

E. Sahle-Demessie
Amy Zhao

U.S. Environmental Protection Agency
Cincinnati, OH USA

Andrew W. Salamon

PerkinElmer, Inc.
Shelton, CT USA

Characterizing Interaction of Nanoparticles with Organic Pollutants Using Coupling Thermal Analysis with Spectroscopic Techniques

Introduction

There are more than a thousand products claiming to contain Engineered Nanoparticles (ENP) in products ranging from clothing, cosmetics, and electronics, to biomedical, chemical, energy, environmental, food, materials and optical products. The effects of ENP on environmental and human health are strongly related to their large surface-to-mass ratio and surface properties. Although the influence of natural colloids on the environment is well documented, we have limited understanding of the fate, transport, toxicity and pollutant interactions of ENP. The tools to study these interactions are being developed.

Pollutants-colloid interaction

Many nanoparticles suspended in natural water come in contact with pollutants and proteinaceous materials. The unique properties and behaviors of ENP are strongly influenced by their physical-chemical characteristics, including their high surface area relative to their volume, high interface energy and high surface-to-charge ratio density.

The partitioning and phase distribution of hazardous organic compounds (HOC) can influence the fate and bioavailability of the contaminants in aquatic systems and aquatic microorganisms significantly. There are a wide range of organic and inorganic pollutants that become associated with partitioning of HOC to the particles. This partitioning has been shown to be inversely proportional to log solubility of HOC and the log of particle concentration. Dynamics of nanoparticle-water partitioning can significantly influence the speciation, and hence, understanding the fate, transport and toxicological impact of POPs such as PAHs, PCBs is critical. The fate of organic pollutants in aquatic environment depends largely on their partitioning behavior to nanoparticles and colloids.

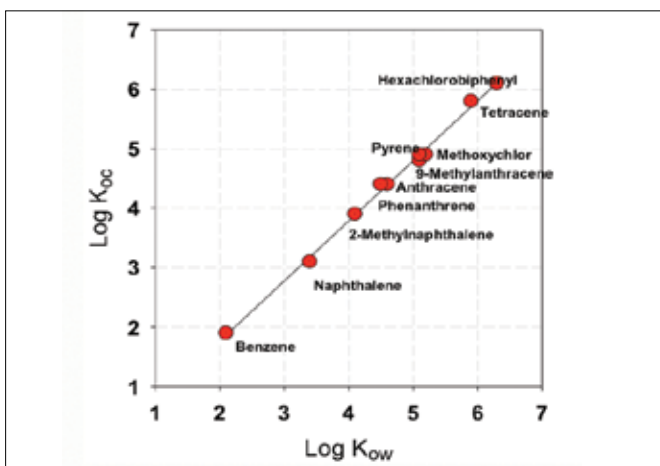


Figure 1. Suspended solid-organic carbon partitioning coefficient versus K_{ow} for polycyclic aromatic hydrocarbons and their derivatives (Karickhoff *et al.*, Water Res., 241 (1979).

Pollutants sorbed on engineered nanoparticles

The sorption of pollutants onto nanoparticles in water phase will be the result of three phase partitioning of pollutants between organic phase, water and suspended solids.

Octanol-Water Partition Coefficient (K_{ow}) This coefficient represents the ratio of the solubility of a compound in octanol (a non-polar solvent) to its solubility in water (a polar solvent). The higher to K_{ow} , the more non-polar the compound. K_d is the ratio of pollutant attached onto the particle and in the water phase.

$$K_{ow} = \frac{C_o}{C_w} \quad K_d = \frac{C_p}{C_w}$$

Where C_o , C_w and C_p are concentration of the pollutant organic compounds in the non-polar organic phase, in an equal weight of water, and concentration pollutants attached on per mass of particles. Ideally, these ratios are equilibrium partitioning of pollutants between organic phase, dissolved in water phase and particulate phases.

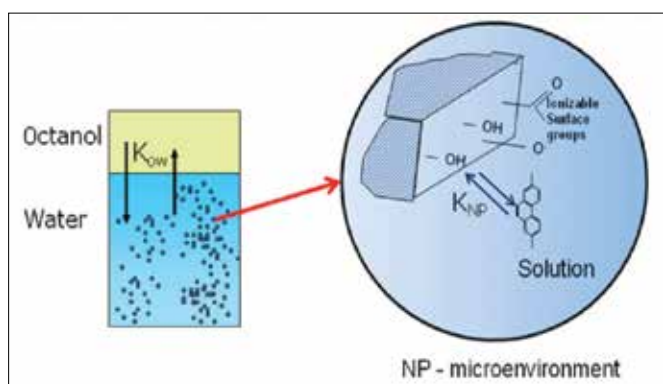


Figure 2. The influence of suspended nanoparticles on octanol-water partitioning of hydrophobic organic pollutants.

The physio-chemical properties relating to the environmental behavior of hydrophobic organic compounds are mainly affected by the aqueous solubility and octanol-water partition coefficient. Aqueous solubility (S_w) is the equilibrium distribution of a solute between water and solute phases. In other words, it is the maximum solute concentration possible at equilibrium, and it can function as a limiting factor in concentration dependent (for example, kinetic) processes. The octanol-water partition coefficient is the ratio of the concentration of a chemical in octanol and in water at equilibrium. Octanol is an organic solvent that is used as a surrogate for natural organic matter. This parameter is used in many environmental studies to help determine the fate of chemicals in the environment, such as predicting the extent to which a contaminant will bioaccumulate in fish. The octanol-water partition coefficient has been correlated to water solubility; therefore, the water solubility of a substance can be used to estimate its octanol-water partition coefficient. The presence of nanoparticles can influence the octanol-water partitioning of hydrophobic organic water contaminants.

Measurement techniques

We selected low molecular weight poly-aromatic hydrocarbons (PAHs) for this study including anthracene, naphthalene and phenanthrene as probe molecules to study the fate and transport of hydrophobic organic pollutants in water streams nanoparticles. The experimental procedure for this study involved the addition of 0-20 mg/L of PAHs in 200 mL of octanol to 900 mL of DI water containing different concentrations of nanoparticles (ranging from 0-20 mg/L) in an Erlenmeyer flask. After stirring the flasks for 5 days the mixture was allowed to settle for 3 hours and then the aqueous and octanol layers were separated. The aqueous suspensions were divided into three portions. One portion was extracted with equal volumes of methylene chloride (MC) and hexane. The mixture was centrifuged and the supernatant organic phase was collected and injected into the Clarus 600 GC from PerkinElmer. The concentrations of PAHs in MC and hexane and water were measured by gas chromatography analysis. The second portion was centrifuged at 10,000 rpm for 30 min. The mixture was decanted and the settled nanoparticles were put in a crucible to dry in an oven at 105 °C for 8 hr. The mass fraction of the adsorbed organics on dried particles was analyzed using a thermal gravimetric analyzer (PerkinElmer) and FT-IR or TOC.

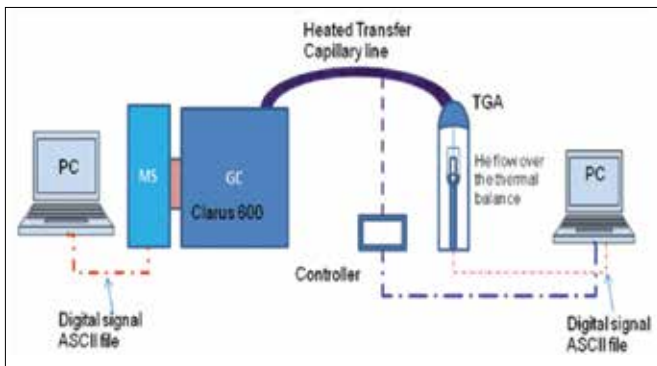


Figure 3. Schematic of PerkinElmer TGA-GC-MS set up with a heated transfer capillary line.

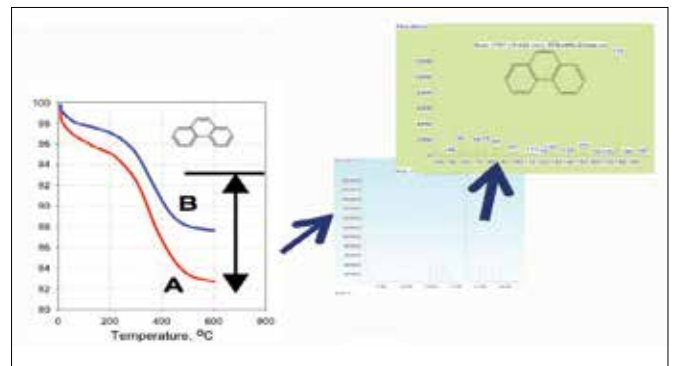


Figure 6. TGA of phenanthrene adsorption on nano-TiO₂ at pH of 10 (curve A) and 6.6 (curve B).

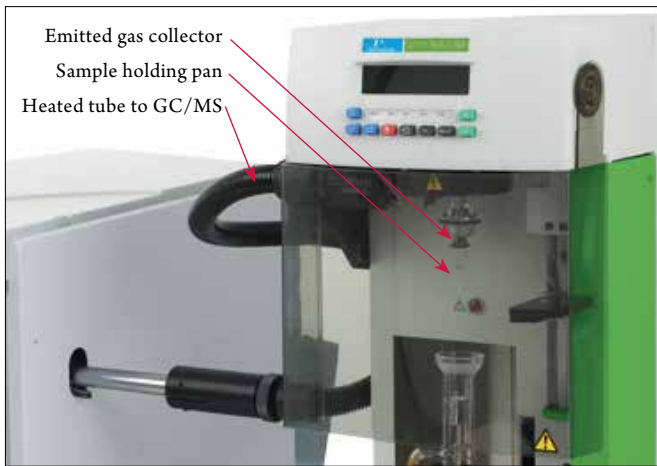


Figure 4. Photograph of PerkinElmer TGA-GC-MS System.

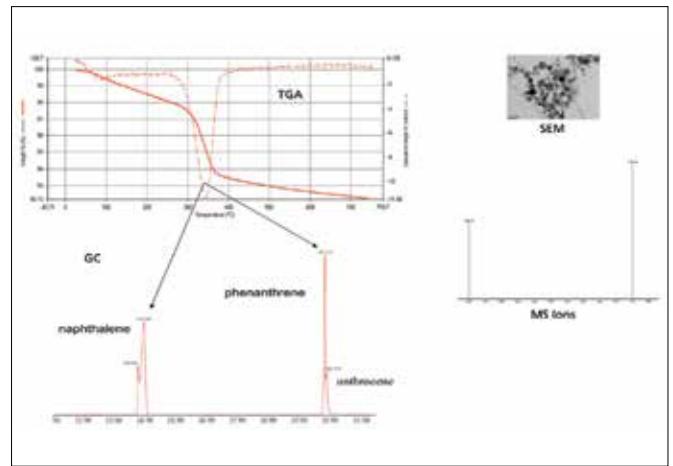


Figure 7. TGA-GC-MS data with SEM image.

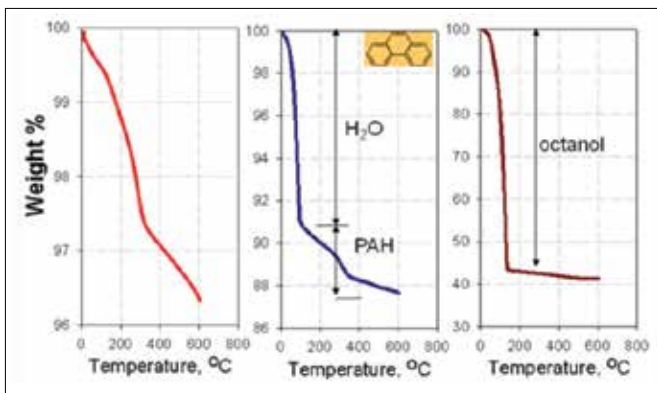


Figure 5. Thermal Analysis of nano-TiO₂, a) conOrganic pollutants adsorbed on nanoparticles: O-W Partitioning.

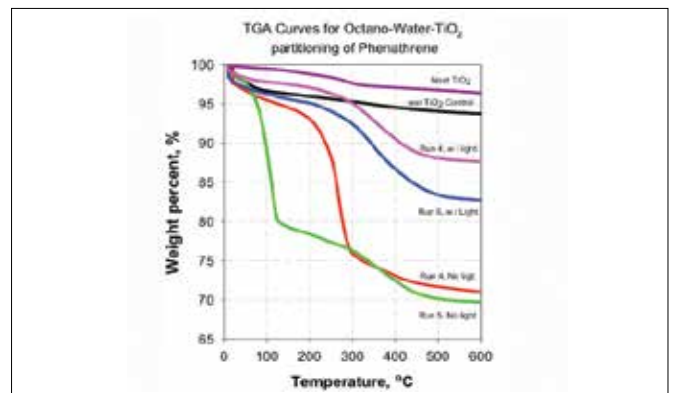


Figure 8. Absence of light made the nanoparticles less hydrophilic and increased the distribution to the organic phase.

Summary

- TGA-GC-MS is a useful technique to study nanoparticle influence on adsorption and partitioning PAHs.
- Presence of nano-TiO₂ increased the partitioning of PAHs to water phase.
- Nanoparticles resulted in increased partitioning of PAHs; six to ten times more than in water-octanol equilibrium conditions.
- Naphthalene and phenanthrene have low water solubility but differing partitioning.
- Partitioning influence increased at higher pH.
- Absence of light made the nanoparticles less hydrophilic and increased the distribution to the organic phase.
- Study suggested that the environmental risk of NP should include their transformation and influence in the transport of other pollutants.

Additional Reading

1. PerkinElmer, Inc. [Nanotechnology and Engineered Nanomaterials – A Primer](http://www.perkinelmer.com/nano), www.perkinelmer.com/nano
2. PerkinElmer, Inc. [Nanomaterials Reference Library](http://www.perkinelmer.com/nano) www.perkinelmer.com/nano

References

1. Bom, D., Andrews, R., Jacques, D., Anthony, J., Chen, B., Meier, M.S., Selegue, J.P., [Thermogravimetric Analysis of the Oxidation of Multiwalled Carbon Nanotubes: Evidence for the Role of Defects Sites in Carbon Nanotube Chemistry](#), *NanoLetters*, 2002, 2, 6, 615-619.
2. Pinault, M., Mayne-L'Hermite, M., Reynaud, C., Beynaud, C., Beyssac, O., Rouzaud, J.N., Clinard, C., [Carbon nanotube produced by aerosol pyrolysis: growth mechanisms and post-annealing effects](#), (2004) 13, 1266-1269.
3. Penn, S.G., He, L. and Natan, M.J., [Nanoparticles for bioanalysis](#). *Current Opinion in Chemical Biology* 2003, 7, 609-615.

Thermogravimetric Analysis – Infrared Spectroscopy



Characterization of Soil Pollution by TG-IR Analysis

There are many scenarios in which soil can become contaminated by hydrocarbon products. Leakage from fuel storage tanks or transfer lines as well as storm water runoff from vehicle washing areas are just two examples. In environmental monitoring or land reclamation, therefore, it is important to test soil for contamination. Total petroleum hydrocarbon (TPH) testing by solvent extraction and infrared spectroscopy is a sensitive method, but has a considerable burden of sample preparation. A gas chromatographic analysis of the extract can provide even greater sensitivity and more detailed compositional information, but further increases the time required for the analysis.

Thermogravimetric analysis coupled to infrared spectroscopy (TG-IR) can provide detailed information about the amount and nature of the pollution, while requiring no sample preparation at all. This application note illustrates the kind of data that can be obtained with a modern TG-IR system.

Experimental

A soil sample was obtained and mixed with diesel fuel at a concentration of about 10% m/m. 17 mg of the soil was transferred to the crucible of a PerkinElmer® TGA 4000, coupled to a PerkinElmer Spectrum™ 100* infrared spectrometer by the TL 8000 transfer line with a 10-cm gas cell. The transfer line and gas cell were heated to 280 °C to avoid any risk of condensation of heavier organic compounds. The purge gas through the TGA was nitrogen at flow rate of 20 mL/min with a balance purge of 40 mL/min. This combined rate of 60 mL/min was kept constant through the transfer line and cell. The temperature was increased from 30 to 800 °C at a constant rate of 20 °C/min. Infrared spectra over the range 4000–600 cm^{-1} were collected every 12 s at 8 cm^{-1} resolution (co-adding four interferometer scans for each spectrum). Pyris™ software was used to control the TGA, while TimeBase™ was used for collection and analysis of the time-resolved IR data.

* The PerkinElmer Frontier FT-IR supersedes the Spectrum 100. The TG-IR interface is compatible with the frontier, and delivers equivalent performance.

Results and Discussion

The weight-loss curve for the soil sample is shown in Figure 1. Broadly, there are three significant, overlapping weight loss events: the first begins just above ambient, the second begins at around 100 °C and continues until 250 °C, and the third begins at around 250 °C and is nearly complete by 600 °C. At 700 °C, approximately 65% of the soil mass remains unburned, and this can be assumed to consist of inorganic material.

The average intensity of the IR absorption is depicted by the Gram-Schmidt thermogram, plotted against the weight and derivative weight curves in Figure 2. The instantaneous concentration of absorbing components in the evolved gas sampled by the IR is proportional to the rate of weight loss (among other factors) and, accordingly, a strong correspondence is seen between the Gram-Schmidt thermogram and the derivative weight curve.

Results from the selected wavenumber regions of the IR measurements are shown in Figure 3 (Page 3), and provide rich information about the processes occurring during the analysis. At temperatures slightly above ambient, an increase in water vapor is seen, indicating that the soil was not completely dry. This accounts for the first weight loss of 5% on the TGA plot. The first peak in the Gram-Schmidt thermogram occurs at about 230 °C and is related to the second weight-loss event. Inspection of the spectrum (Figure 4 - Page 3) reveals that this is due to a mixture of water vapor, aliphatic hydrocarbons, and, from the peak at around 1745 cm^{-1} , an ester. This suggests that the contaminant may be diesel fuel with a significant fraction of biodiesel (fatty acid methyl esters).

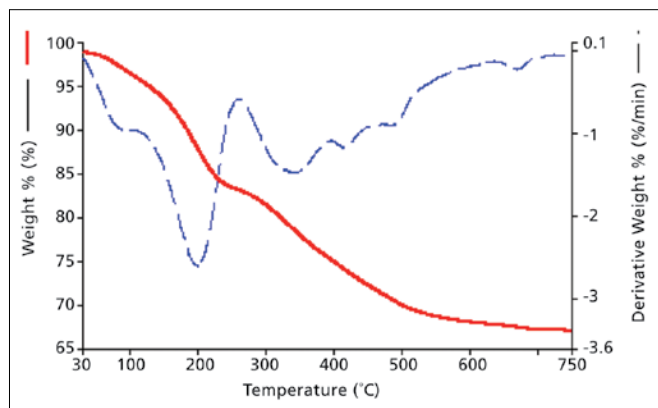


Figure 1. Weight loss (solid red line) and derivative (dashed blue line) for the contaminated soil sample.

The ester peak is overlapped by water-vapor absorption, but there is another selective peak for biodiesel at around 3015 cm^{-1} , corresponding to an alkene C-H stretching mode arising from unsaturation in the fatty-acid chains. Plotting the intensity of this peak as a function of temperature (Figure 3) reveals that the peak occurs slightly later, at around 240 °C. The 10% weight loss seen in this temperature range is in agreement with the known diesel concentration. This indicates that the TGA-IR measurements can provide an estimate of the amount of contamination present, as well as detailed information about the composition.

At higher temperatures, the main gases evolved are CO_2 and H_2O , as organic matter in the soil undergoes combustion. This accounts for the final weight-loss event.

TimeBase also allows the series of spectra to be plotted as a stack or as a surface in a three-dimensional plot, as shown in Figure 5. This gives an excellent overview of the complete dataset, and the evolution of the absorption features with time can be seen at a glance.

A reference diesel/biodiesel blend sample was also analyzed by TG-IR under the same conditions as the soil sample. The results are presented in Figures 6 and 7 (Page 3). The entire sample has evaporated by 300 °C. In Figure 7, it can be seen clearly that the biodiesel evaporation lags behind that of the fossil diesel. There is no water in the diesel standard sample, so the carbonyl absorption can be followed directly. This data gives confidence that a biodiesel/diesel blend is indeed the contaminant present in the soil sample.

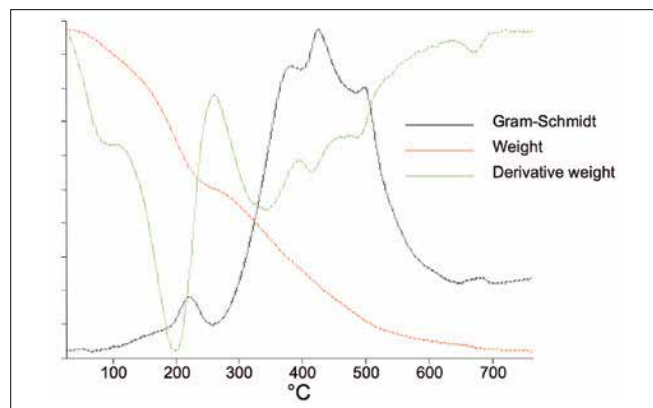


Figure 2. Weight (red), derivative weight (green), and Gram-Schmidt thermogram (black) plots for the contaminated soil sample.

Conclusions

Thermogravimetric analysis gives valuable quantitative information about the sample, but has limited ability to identify materials. Infrared spectroscopic analysis of the evolved gas provides precisely this capability. This note demonstrates that not only is TG-IR capable of determining the quantity of diesel present in soil, but the minor fraction of biodiesel in the fuel could also be detected. For soil analysis, a key advantage of TG-IR over other methods is that no sample preparation or solvent extraction step is required, giving a much faster and more convenient analysis.

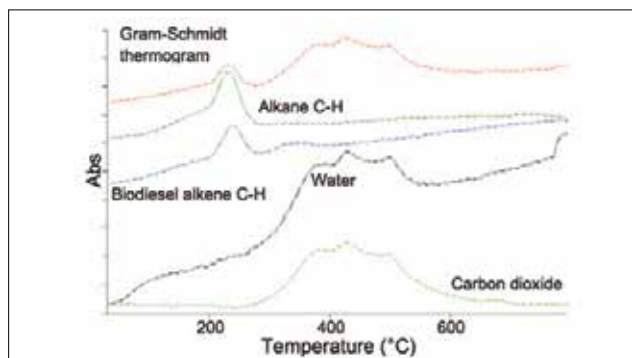


Figure 3. Temperature-based absorbance profiles for the contaminated soil sample. Red: Gram-Schmidt thermogram showing the overall absorption intensity; Dark green: height of the C-H absorption around 2933 cm^{-1} , corresponding to aliphatic hydrocarbons (diesel and biodiesel); Blue: height of the alkene C-H absorption around 3015 cm^{-1} , corresponding to unsaturation in the biodiesel; Black: height of the water absorption between $3800\text{--}3700\text{ cm}^{-1}$; Light green: height of the carbon dioxide peak around 2370 cm^{-1} .

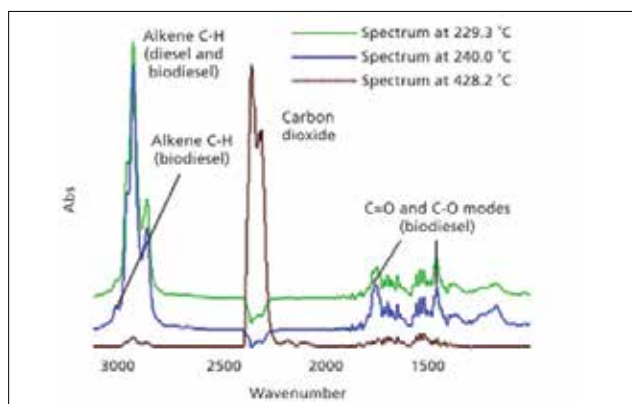


Figure 4. Selected spectra from the TG-IR analysis of the contaminated soil sample.

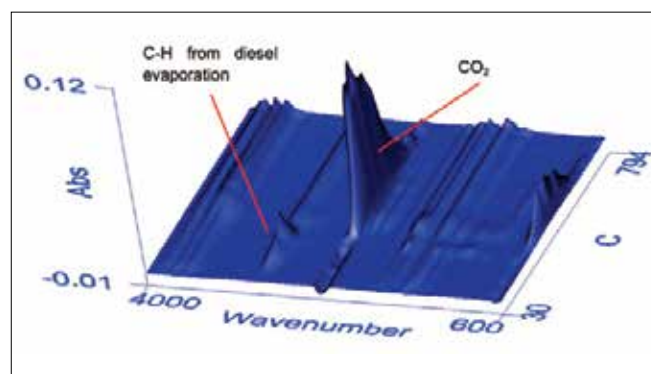


Figure 5. Three-dimensional plot of the time-resolved spectra for the contaminated soil sample.

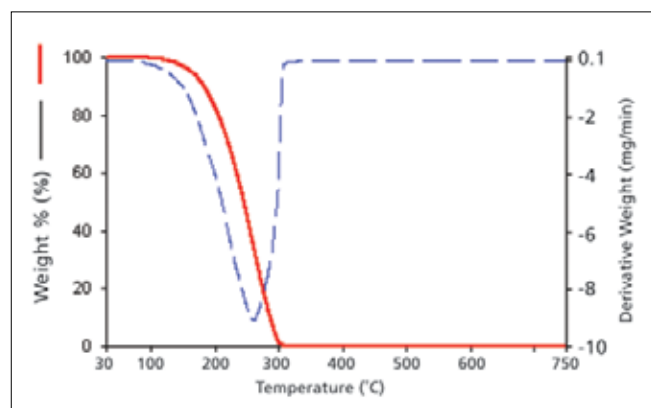


Figure 6. Weight-loss (solid red line) and derivative profile (dashed blue line) for the biodiesel blend standard sample.

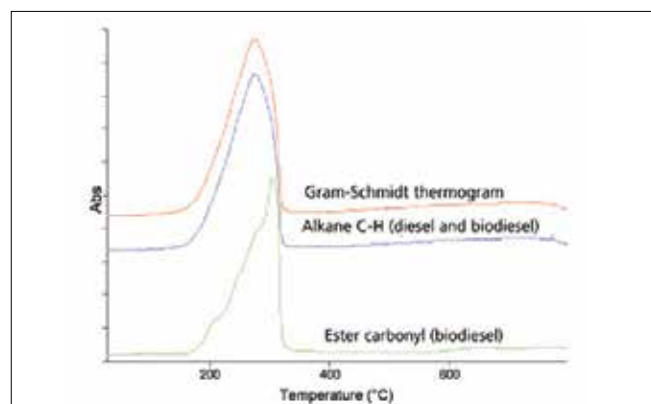


Figure 7. Temperature-based infrared absorption profiles for the biodiesel blend standard sample. Red: Gram-Schmidt thermogram; Blue: height of the C-H absorption around 2933 cm^{-1} ; Green: height of the ester carbonyl absorption around 1745 cm^{-1} .

PerkinElmer, Inc.
940 Winter Street
Waltham, MA 02451 USA
P: (800) 762-4000 or
(+1) 203-925-4602
www.perkinelmer.com



For a complete listing of our global offices, visit www.perkinelmer.com/ContactUs

Copyright ©2017, PerkinElmer, Inc. All rights reserved. PerkinElmer® is a registered trademark of PerkinElmer, Inc. All other trademarks are the property of their respective owners.